Supporting Information

Synthesis and Characterization of Heptacoordinated Molybdenum(II) Complexes Supported with 2,6-Bis(pyrazol-3-yl)pyridine (bpp) Ligands

Arno Estival,[a] Luis E. Blancarte,[b] Loïc Pinto,[a] Romane Pointis,[a] Nathan Galas,[a] Alix Sournia-Saquet,[a] Laure Vendier,[a] Rosa Santillan,[c] Norberto Farfán,[b] Jean-Baptiste Sortais,[a] Mary Grellier,[a] Antoine Simonneau[a]*

[a] LCC-CNRS, Université de Toulouse, CNRS, UPS, 205 route de Narbonne, BP44099, F-31077 Toulouse cedex 4, France.
[b] Facultad de Química, Departamento de Química Orgánica, Universidad Nacional Autónoma de México, 04510 CDMX, México
[c] Departamento de Química, Centro de Investigación y de Estudios Avanzados del IPN, México D.F. Apdo. Postal 14–740, 07000, Mexico

Table of Contents

1. NMR spectra

1.1. Compounds 4a, 5a and 6a

1.1.1. Complex 4a

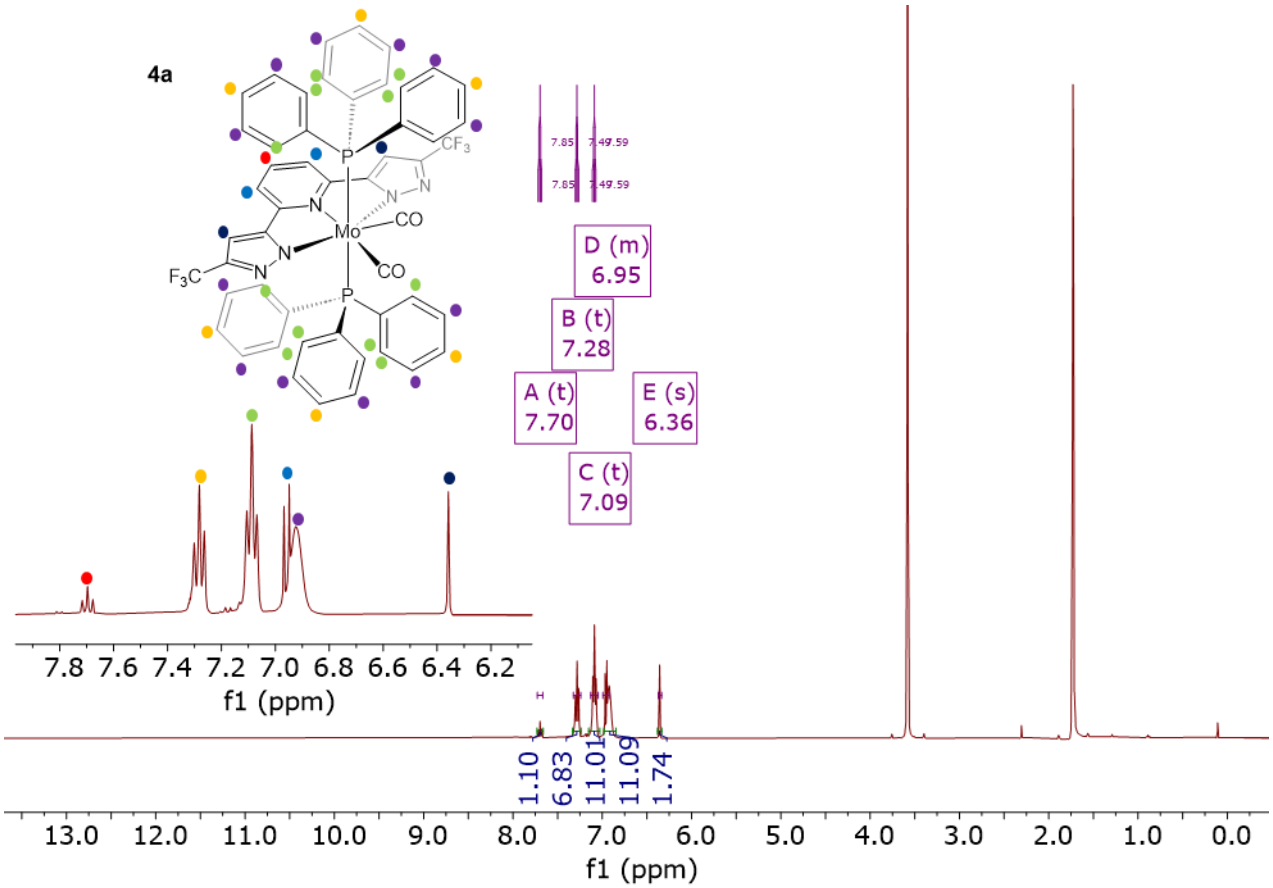

Figure S1. ^{1}H NMR (400 MHz, THF-d_8) of compound **4a:** δ 7.70 (t, J = 7.9 Hz, 1H), 7.28 (t, J = 7.5 Hz, 6H), 7.09 (t, J = 7.6 Hz, 12H), 6.99 – 6.92 (m, 13H overlapping), 6.36 (s, 2H).

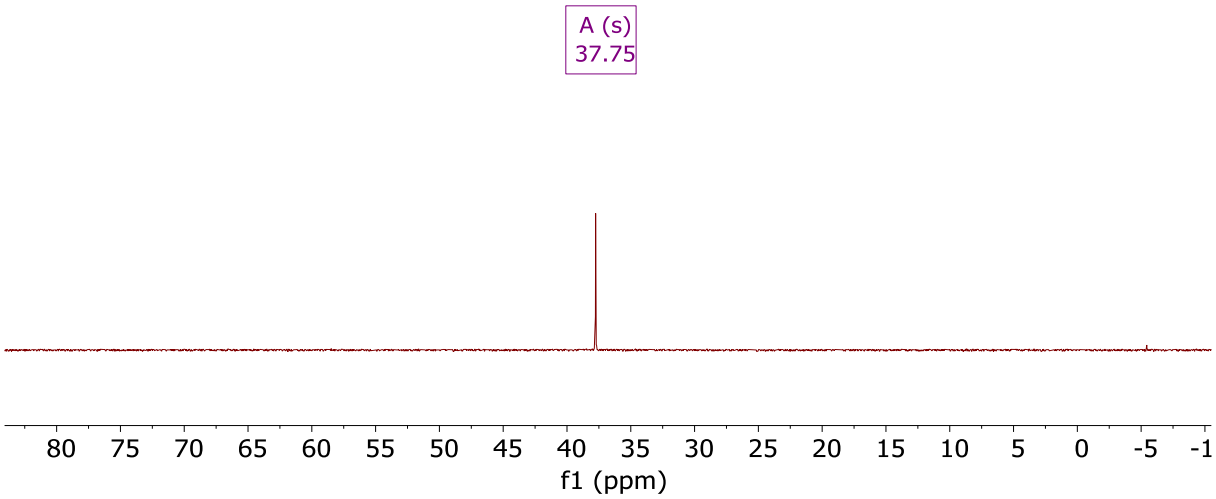

Figure S2. $^{31}P\{H\}$ NMR (162 MHz, THF-d_8) of compound **4a:** δ 37.75 (s, 2P).

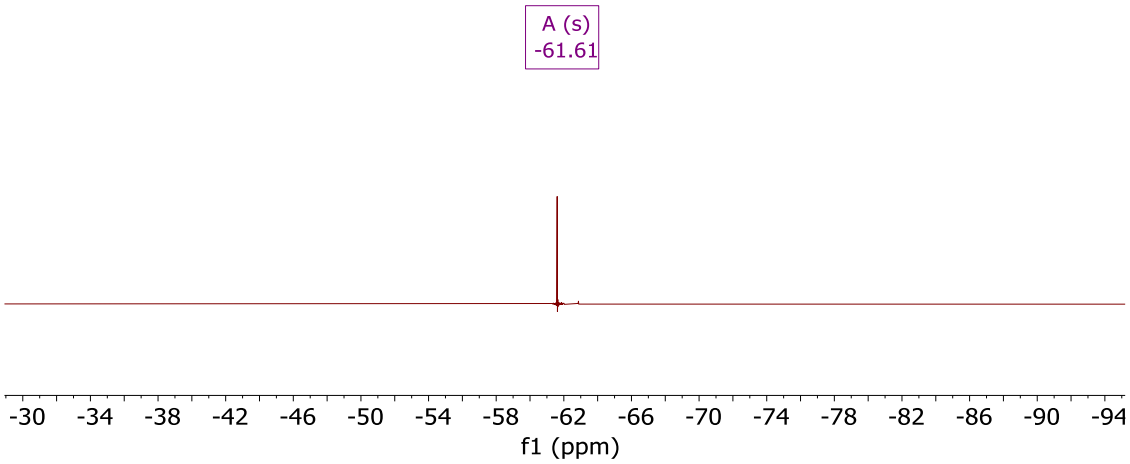

Figure S3. ^{19}F NMR (377 MHz, THF-d_8) of compound **4a:** δ -61.61.

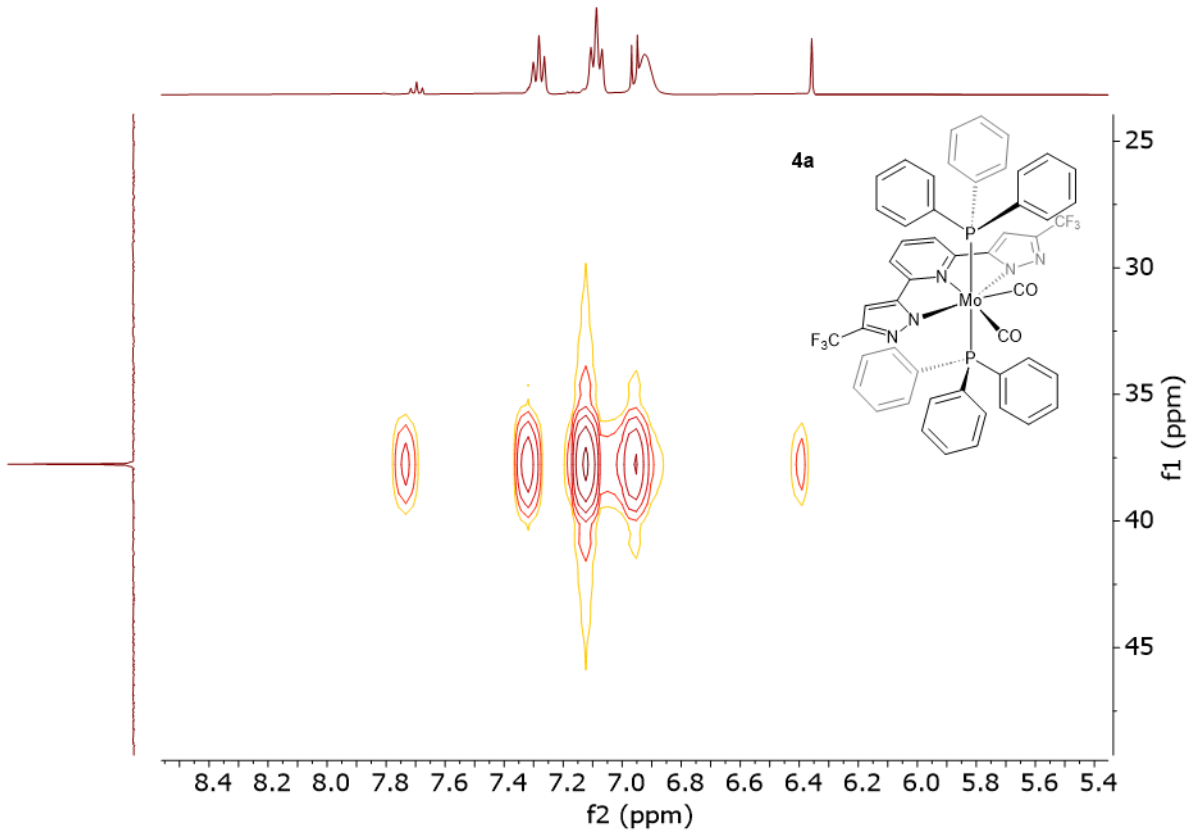

Figure S4. 2D NMR ^{31}P HMQC (400MHz, THF-d_8) of compound **4a.**

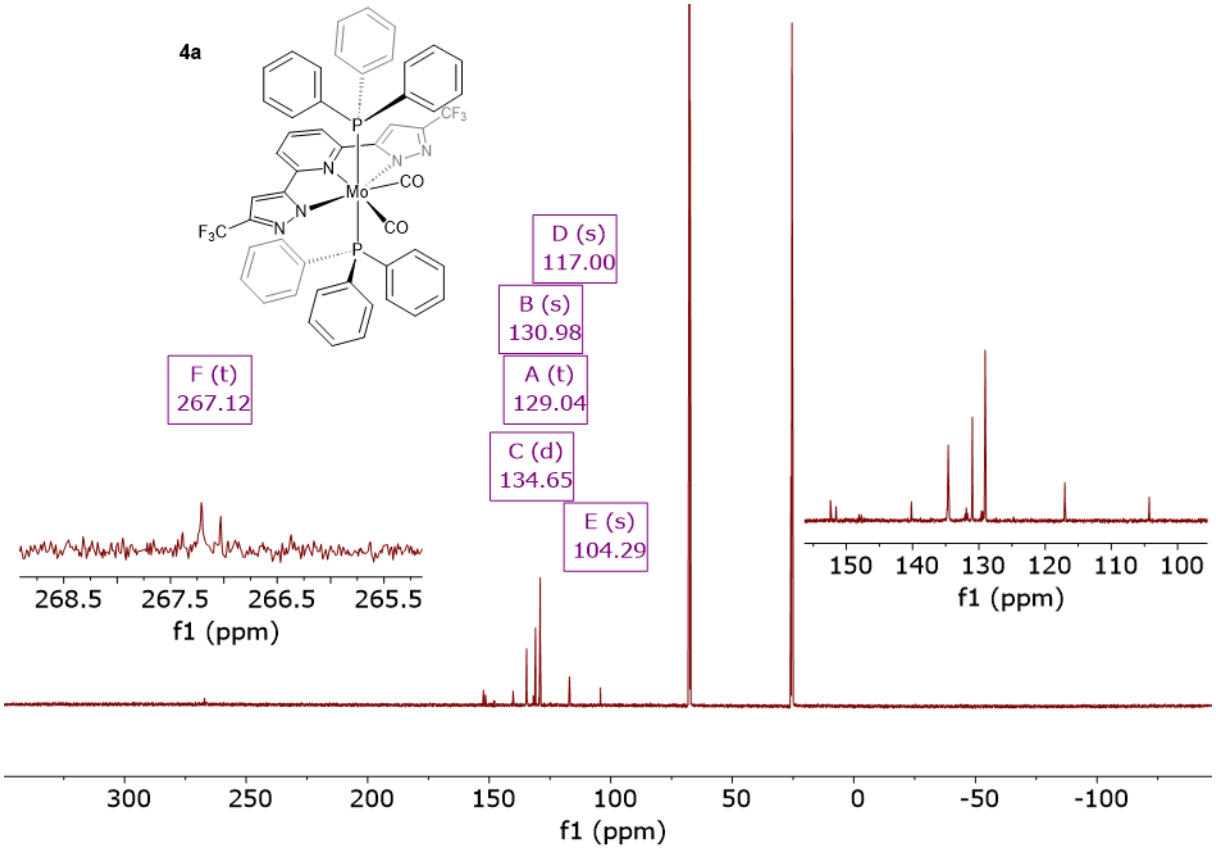

Figure S5. $^{13}C\{^{1}H\}$ NMR (101 MHz, THF-d_8) **4a:** δ 267.12 (t, J = 18.2 Hz), 134.65 (d, J = 6.0 Hz), 130.98, 129.04 (t, J = 4.6 Hz), 117.00, 104.29.

1.1.2. Complex 5a

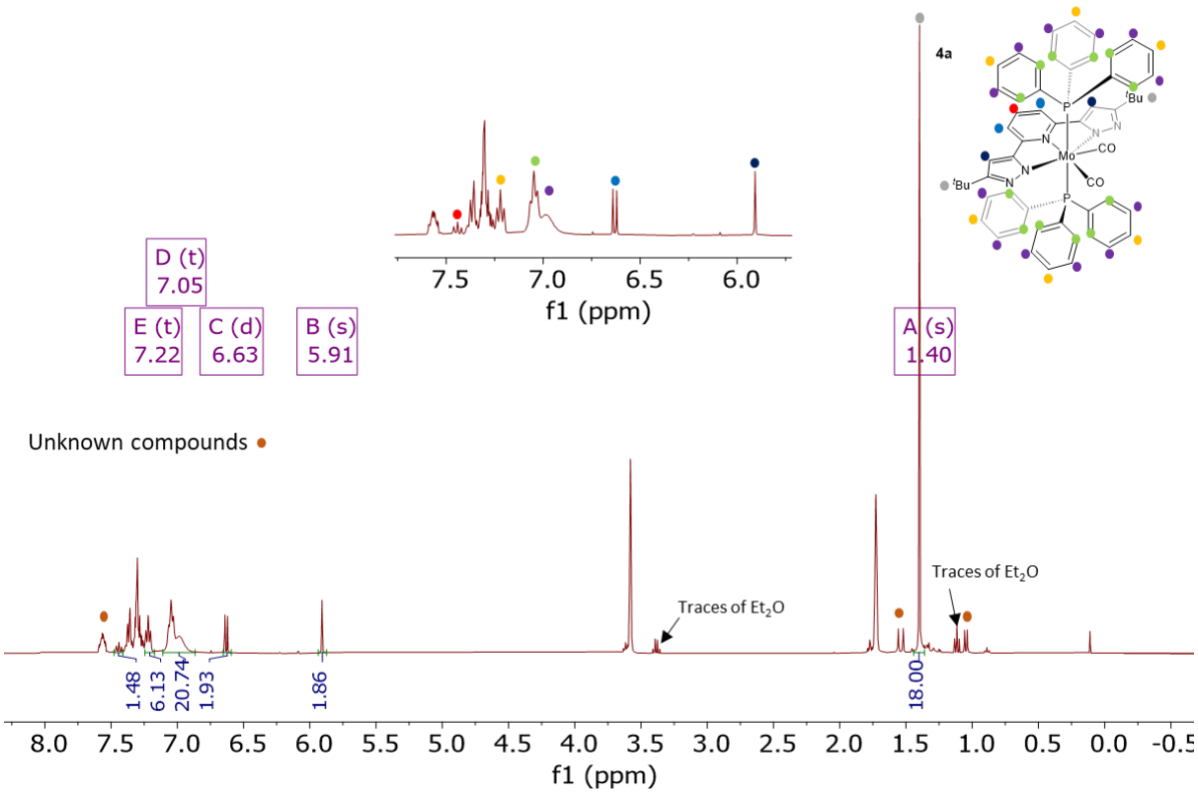

Figure S6. ^{1}H NMR (400 MHz, THF-d_8) of compound **5a:** δ 7.22 (t, *J* = 7.3 Hz, 1H), 7.05 (t overlapping, *J* = 7.5 Hz), 6.63 (d, *J* = 7.8 Hz, 2H), 5.91 (s, *J* = 0.8 Hz, 2H), 1.40 (s, 18H).

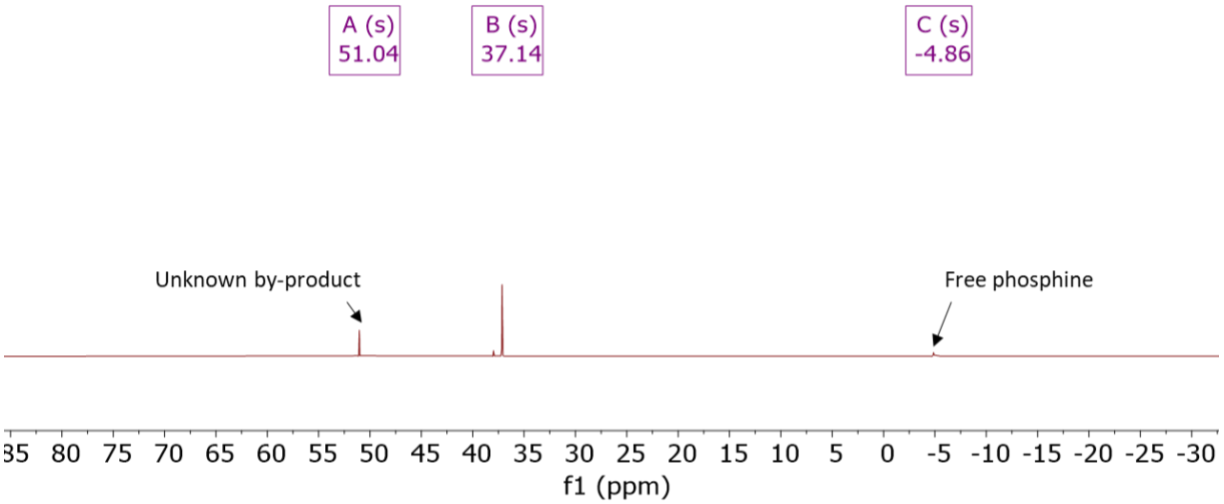

Figure S7. $^{31}P\{^{1}H\}$ NMR (162 MHz, THF-d_8) of compound **5a:** δ 37.14 (s, 2P).

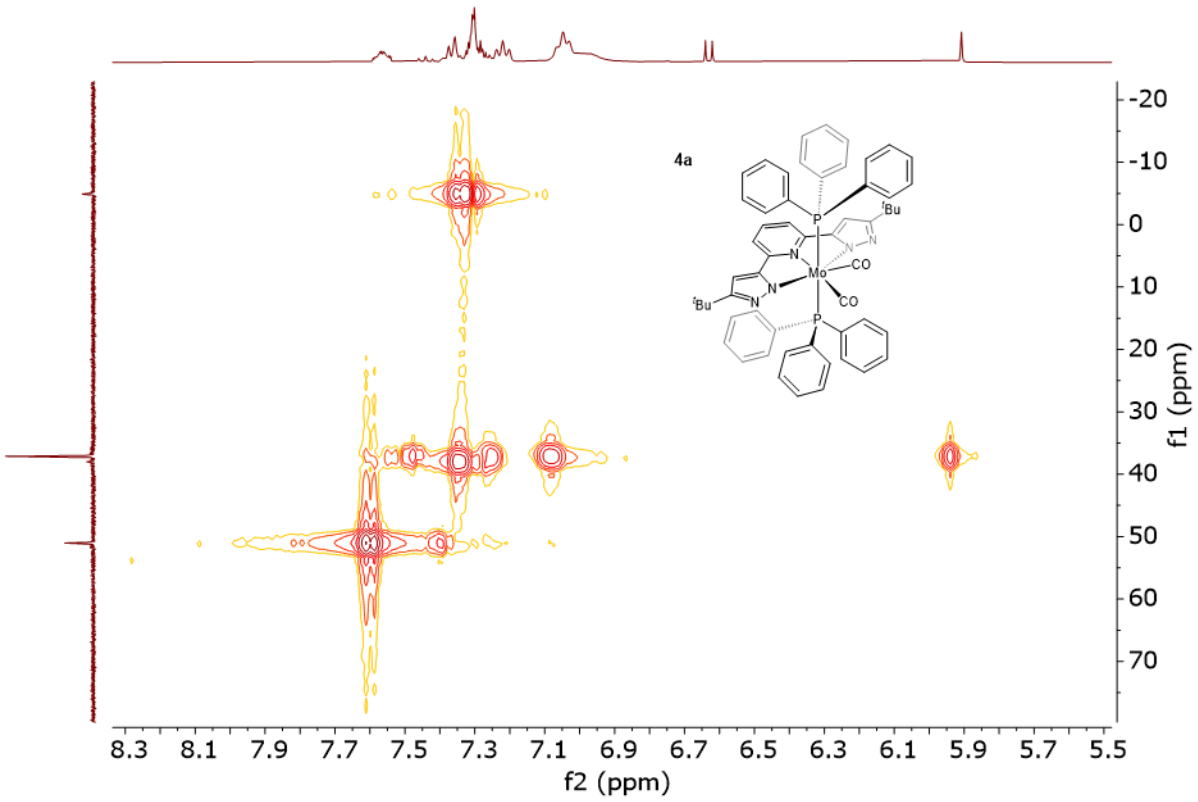

Figure S8. 2D NMR ^{31}P HMQC (400MHz, THF-d_8) of compound **5a**.

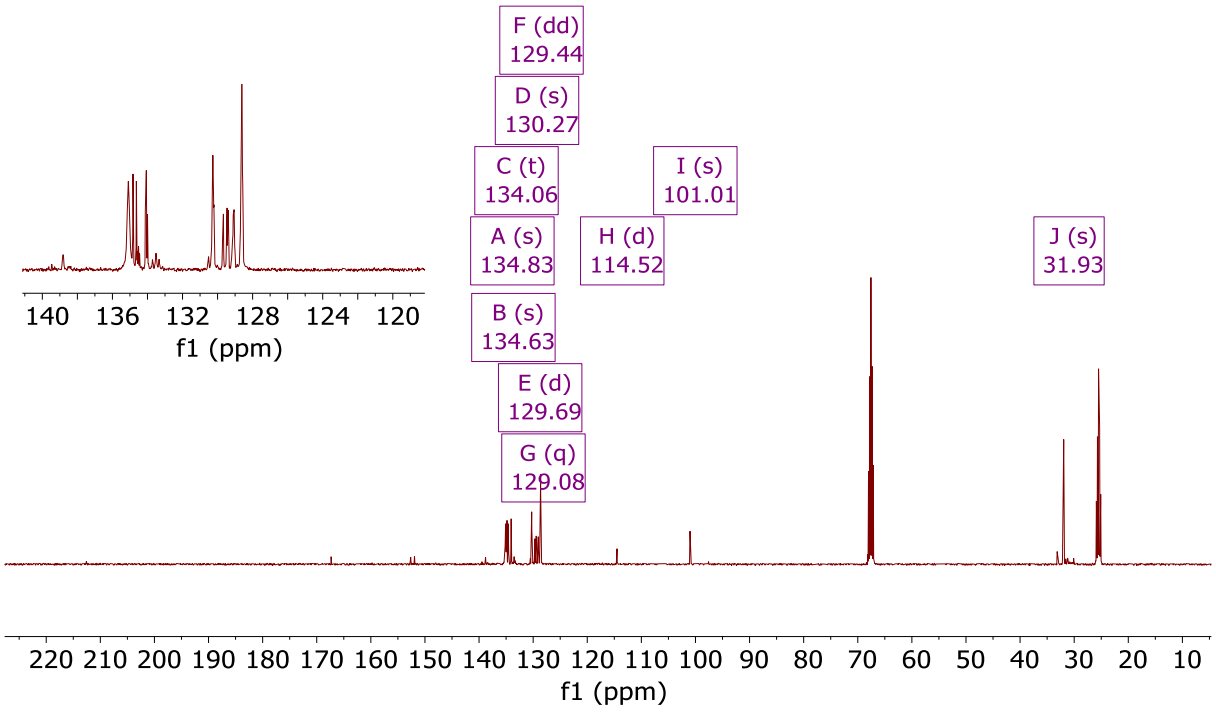

Figure S9. $^{13}C\{^{1}H\}$ NMR (101 MHz, THF-d_8) of compound **5a**: δ 134.83, 134.63, 134.06 (t, *J* = 6.2 Hz), 130.27, 129.69 (d, *J* = 3.8 Hz), 129.44 (dd, *J* = 7.2, 2.7 Hz), 129.08 (q, *J* = 4.1 Hz), 114.52 (d, *J* = 4.3 Hz), 101.01, 31.93.

1.1.3. Complex 6a

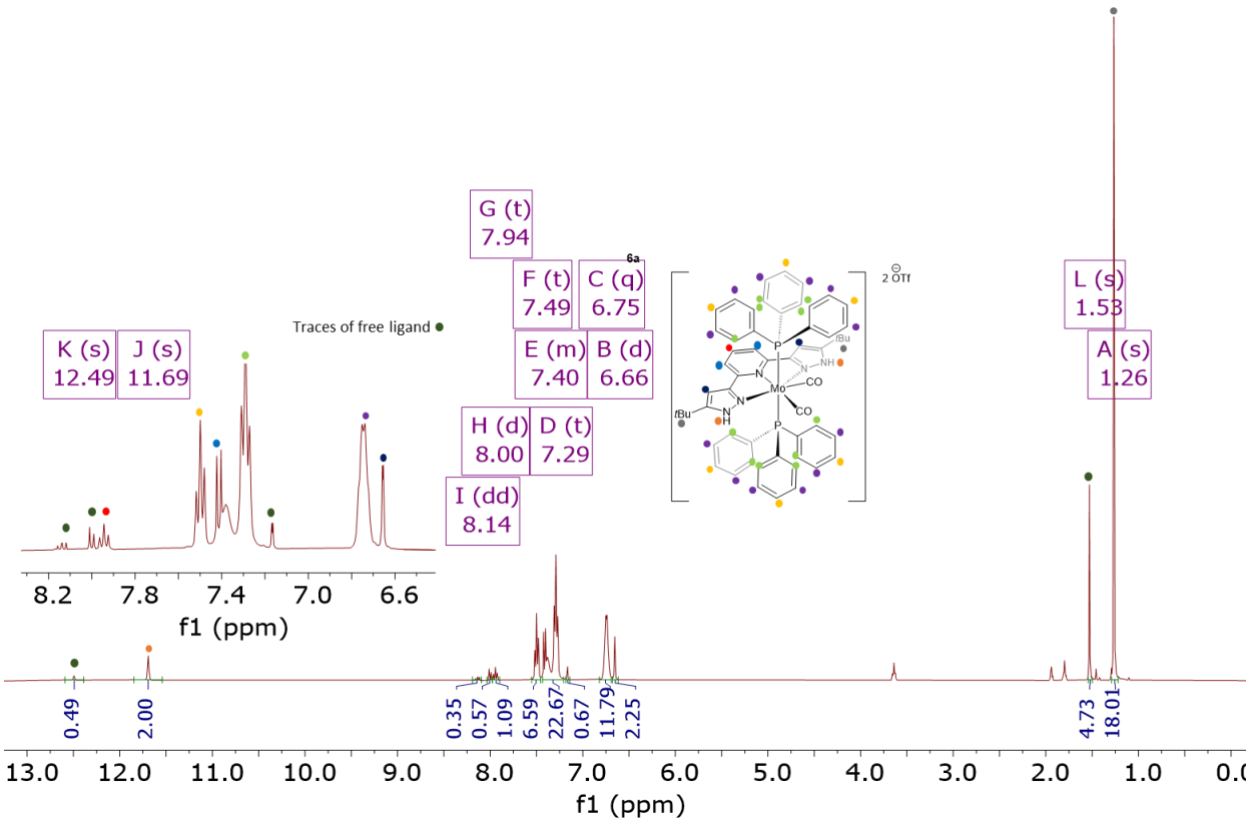

Figure S10. ^{1}H NMR (400 MHz, CD_3CN) of compound **6a**: δ 11.69 (s, 2H), 7.94 (t, 1H), 7.49 (t, 6H), 7.45 – 7.36 (m, 2H), 7.29 (t, *J* = 7.8 Hz, 2H), 6.75 (q, *J* = 6.7, 6.3 Hz, 12H), 1.26 (s, 18H).

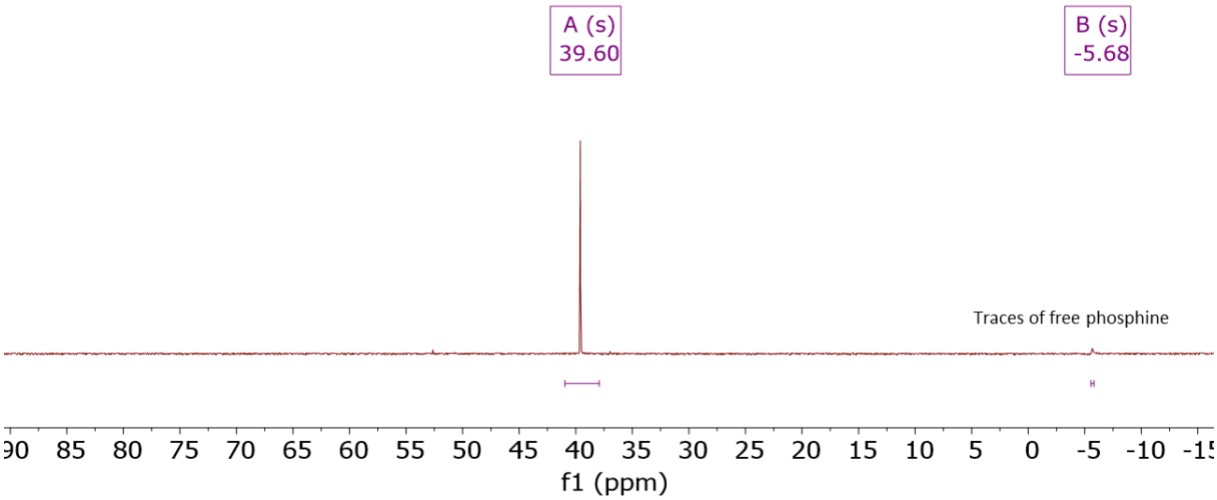

Figure S11. $^{31}P\{^{1}H\}$ NMR of compound **6a** (162 MHz, CD_3CN) δ 39.60.

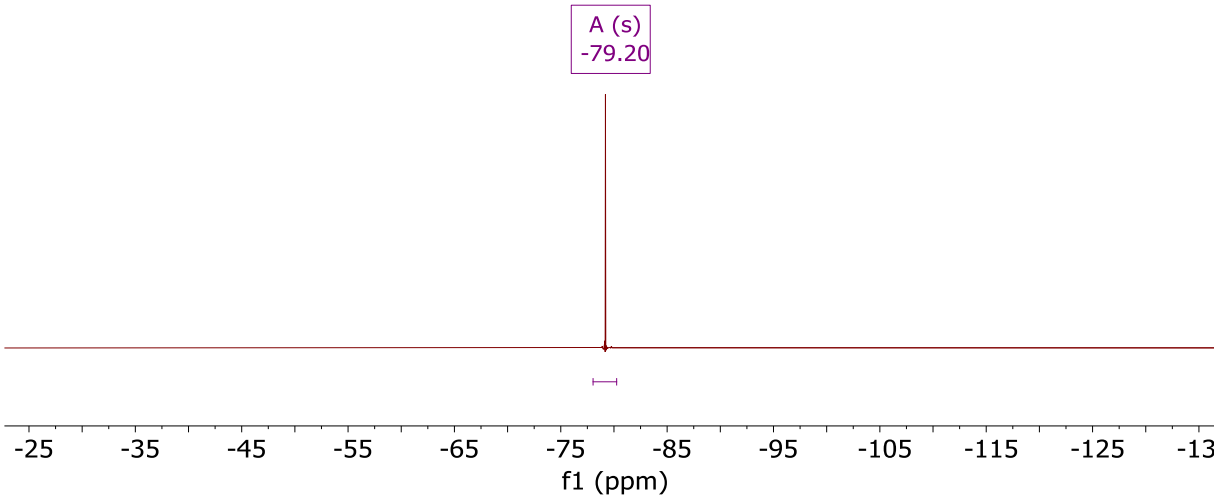

Figure S12. ^{19}F NMR of compound **6a** (377 MHz, CD_3CN) δ -79.20.

1.2. Compounds 4b, 5b and 6b.

1.2.1. Complex 4b

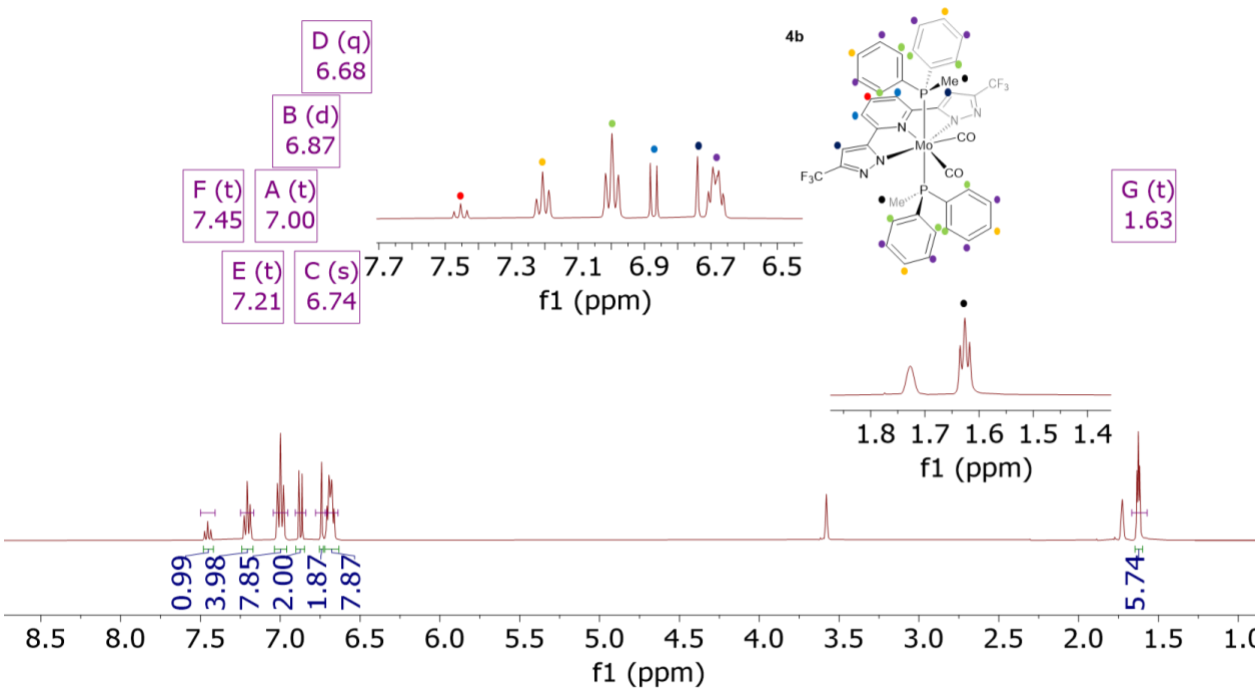

Figure S13. ^{1}H NMR (40 MHz, THF-d_8) of compound **4b**: δ 7.45 (t, 1H), 7.21 (t, J = 7.4 Hz, 4H), 7.00 (t, 8H), 6.87 (d, J = 7.9 Hz, 2H), 6.74 (s, 2H), 6.68 (q, 8H), 1.63 (t, J = 3.5 Hz, 6H).

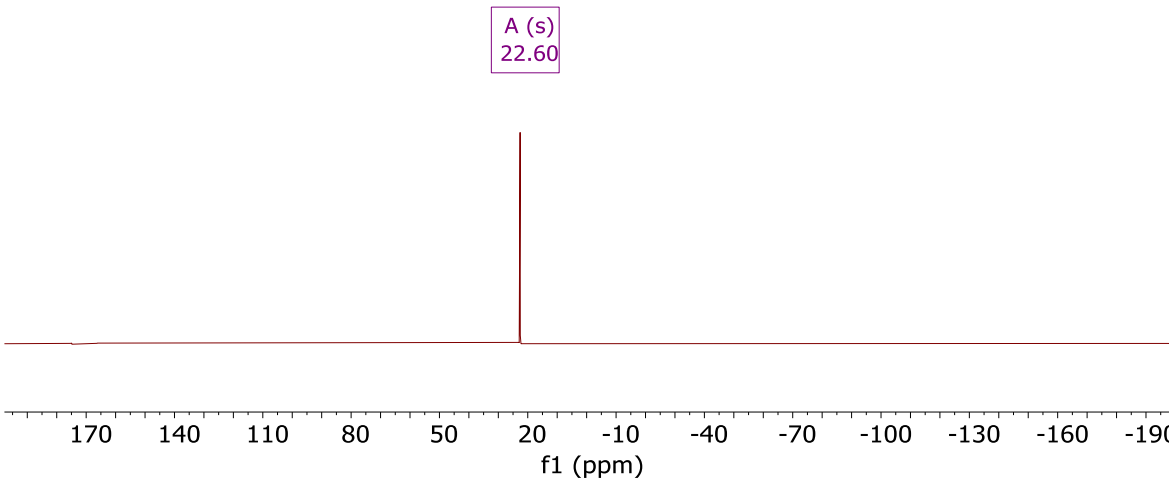

Figure S14 : $^{31}P\{H\}$ NMR (162 MHz, THF-d_8) of compound **4b**: δ 22.60 (s).

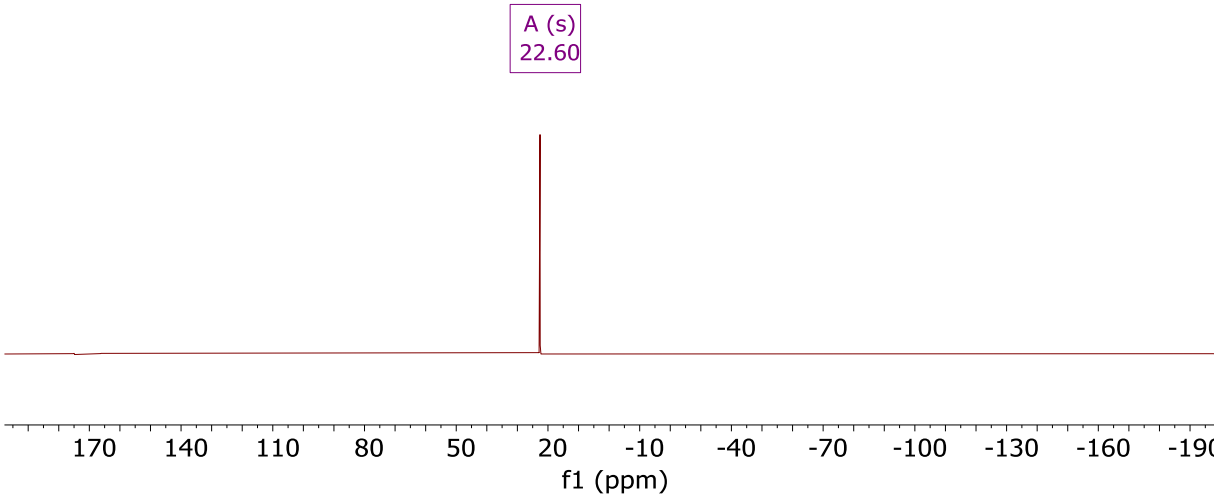

Figure S15. ^{19}F NMR (377 MHz, THF-d_8) of compound **4b**: δ -61.55 (s, 6F).

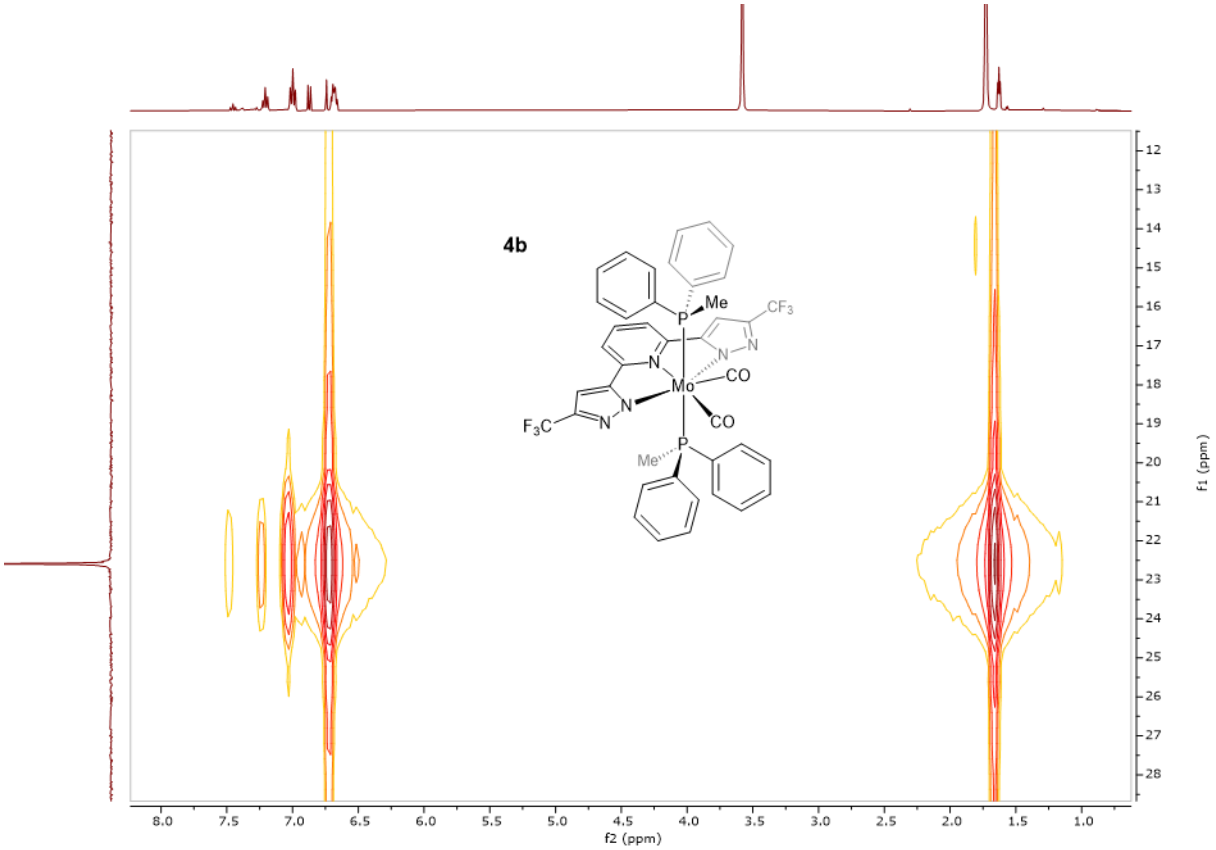

Figure S16. 2D NMR ^{31}P HMQC (400MHz, THF) of compound **4b**

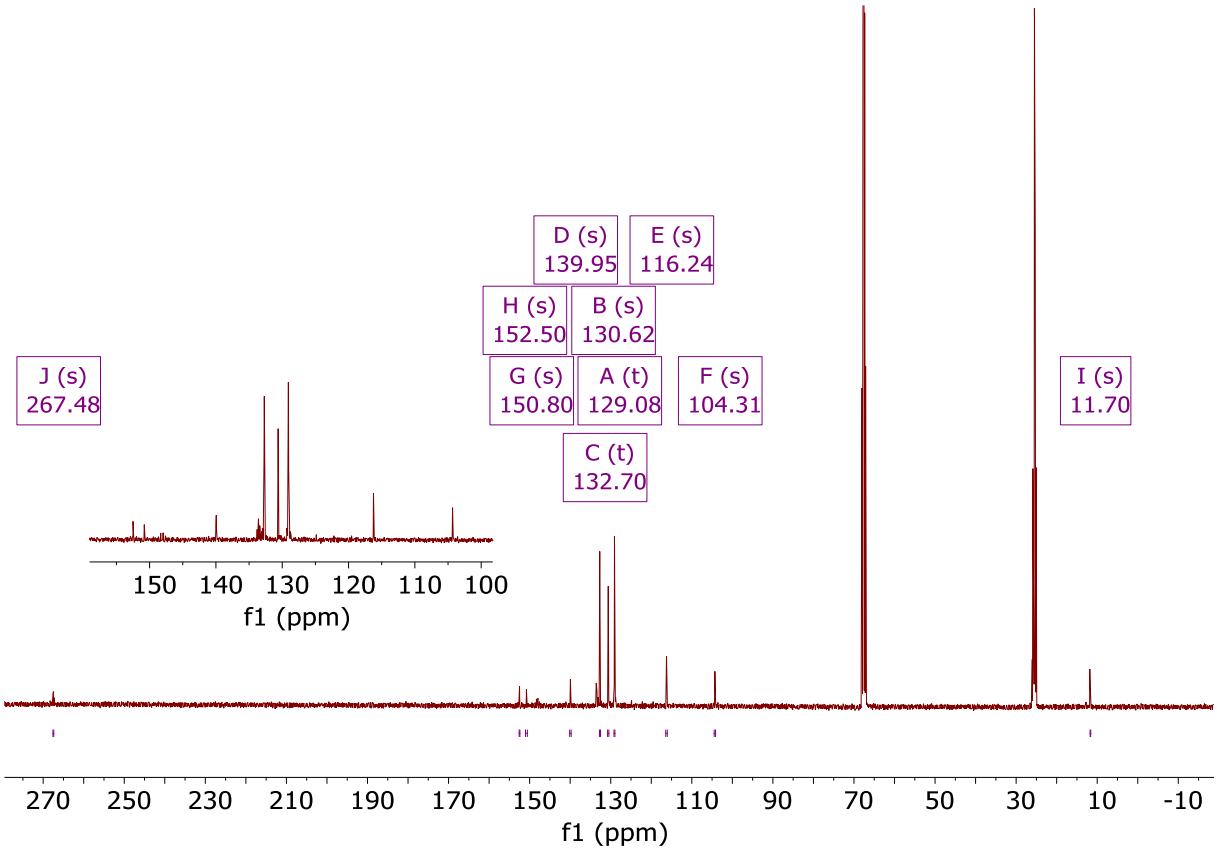

Figure S17. $^{13}C\{^{1}H\}$ NMR (101 MHz, THF) of compound **4b**: δ 267.48, 152.50, 150.80, 139.95, 132.70 (t, *J* = 5.5 Hz), 130.62, 129.08 (t, *J* = 4.6 Hz), 116.24, 104.31, 11.70.

1.2.2. Complex 5b

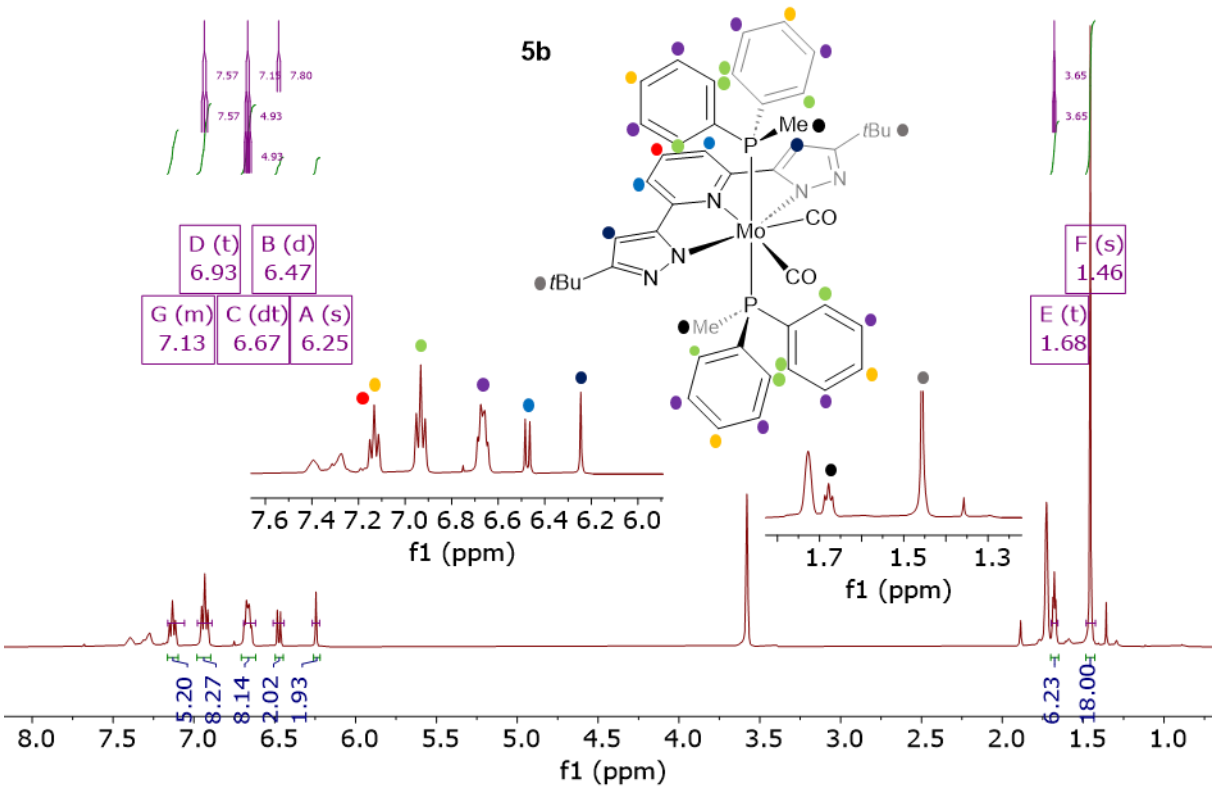

Figure S18. ^{1}H NMR (400 MHz, THF-d_8) of compound **5b:** δ 7.11 (t, 4H), 6.93 (t, J = 7.6 Hz, 8H), 6.67 (dt, J= 7.1, 4.9 Hz, 8H), 6.47 (d, J = 7.8 Hz, 2H), 6.25 (s, 2H), 1.68 (t, J = 3.6 Hz, 6H), 1.46 (s, 18H).

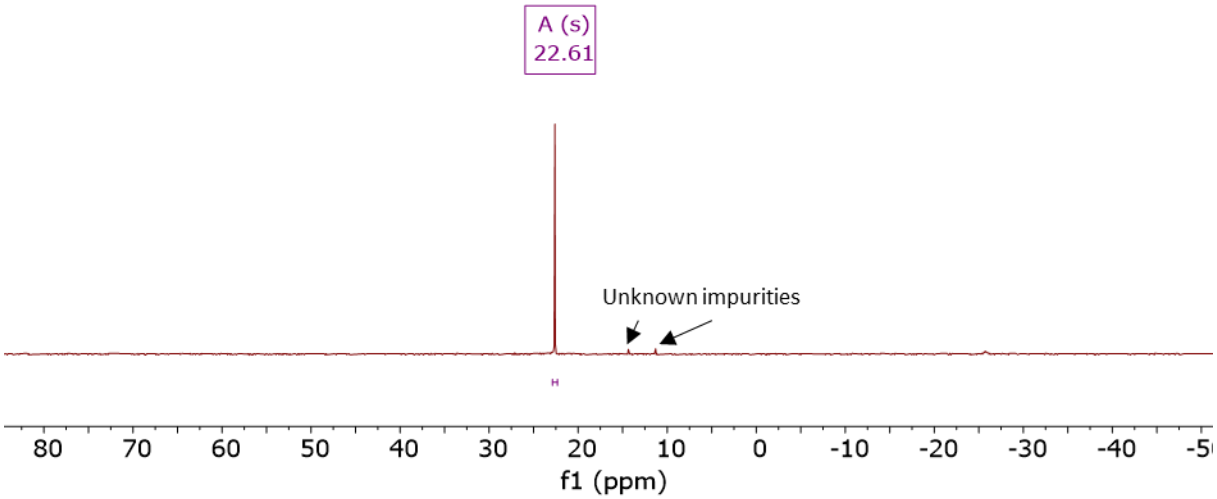

Figure S19. ^{31}P NMR (400 MHz, THF-d_8) of compound **5b**: δ 22.61 (s).

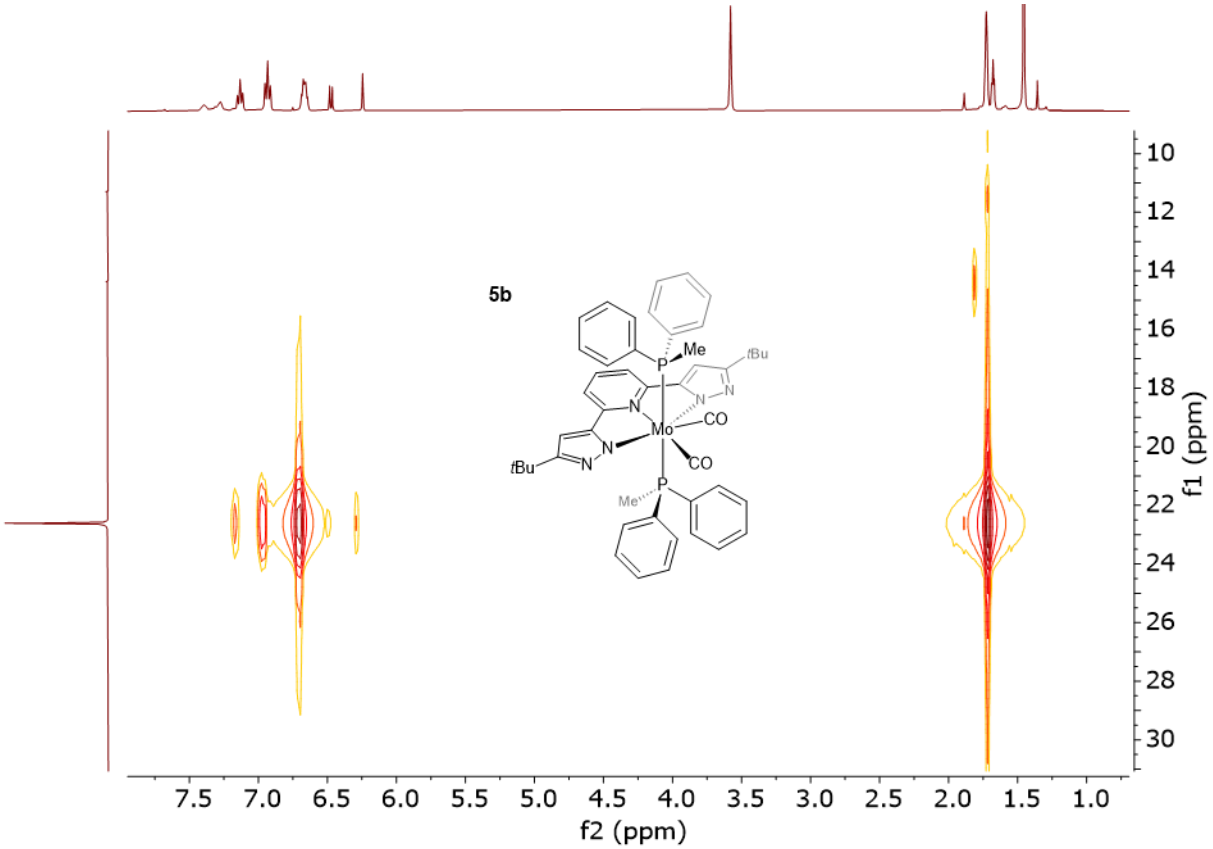

Figure S20. 2D NMR ^{31}P HMQC (400 MHz, THF-d_8) of compound **5b.**

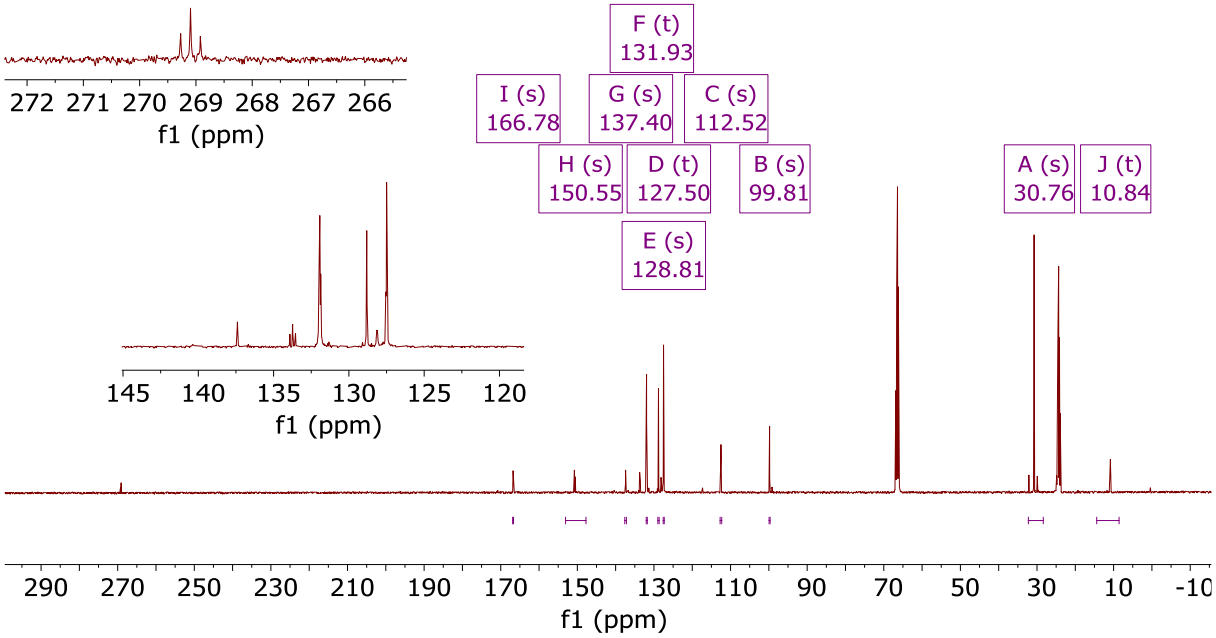

Figure S21. ^{13}C NMR (400 MHz, THF-d_8) of compound **5b**: δ 269 (t, *J* = 17,7 Hz), 166.78, 150.55, 137.40, 131.93 (t, *J* = 5.6 Hz), 128.81, 127.50 (t, *J* = 4.6 Hz), 112.52, 99.81, 30.76., 10.84.

1.2.3. Complex 6b

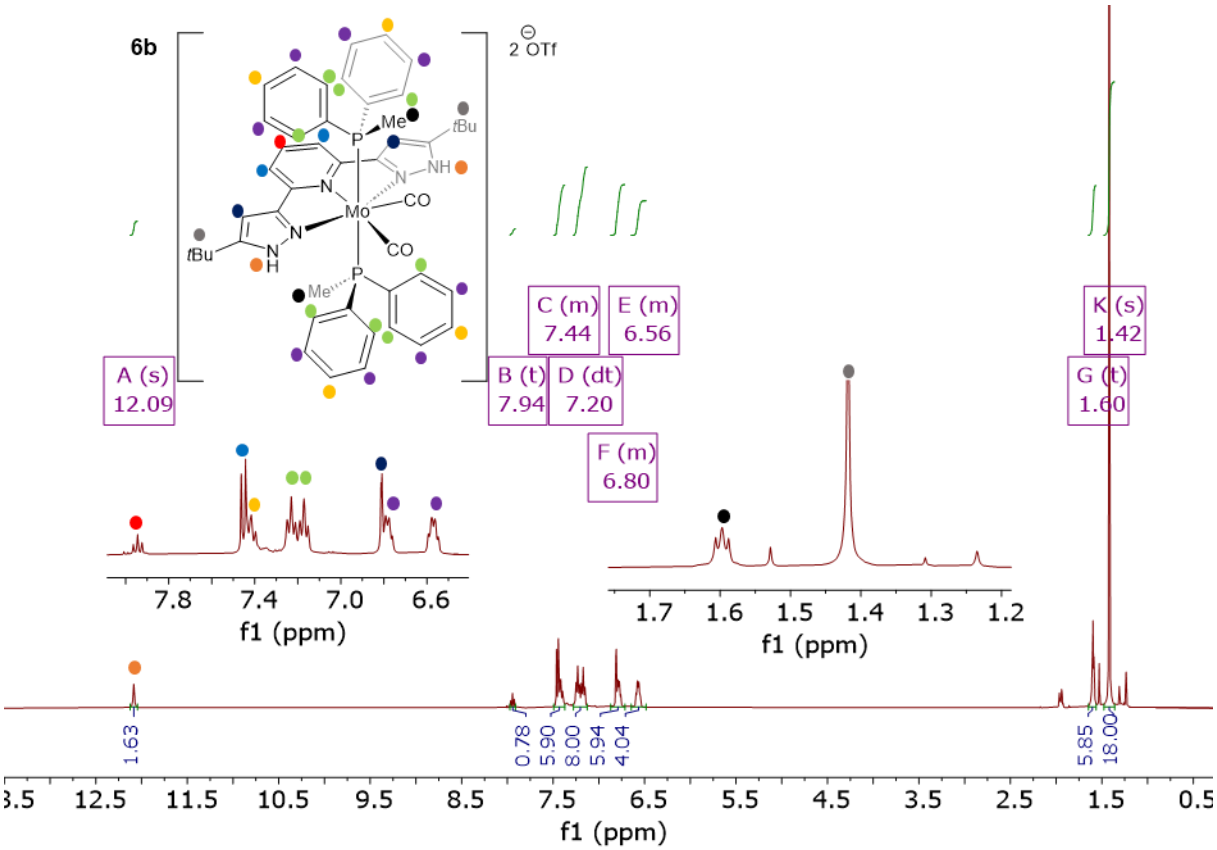

Figure S22. ^{1}H NMR (400 MHz, CD_3CN) of compound **6b**: δ 12.09 (s, 2H), 7.94 (t, J = 7.9, 1.2 Hz, 1H), 7.50 – 7.38 (m, 6H), 7.20 (dt, J = 23.4, 7.6 Hz, 9H), 6.84 – 6.74 (m, 6H), 6.62 – 6.52 (m, 4H), 1.60 (t, J = 3.7 Hz, 6H), 1.42 (s, 18H).

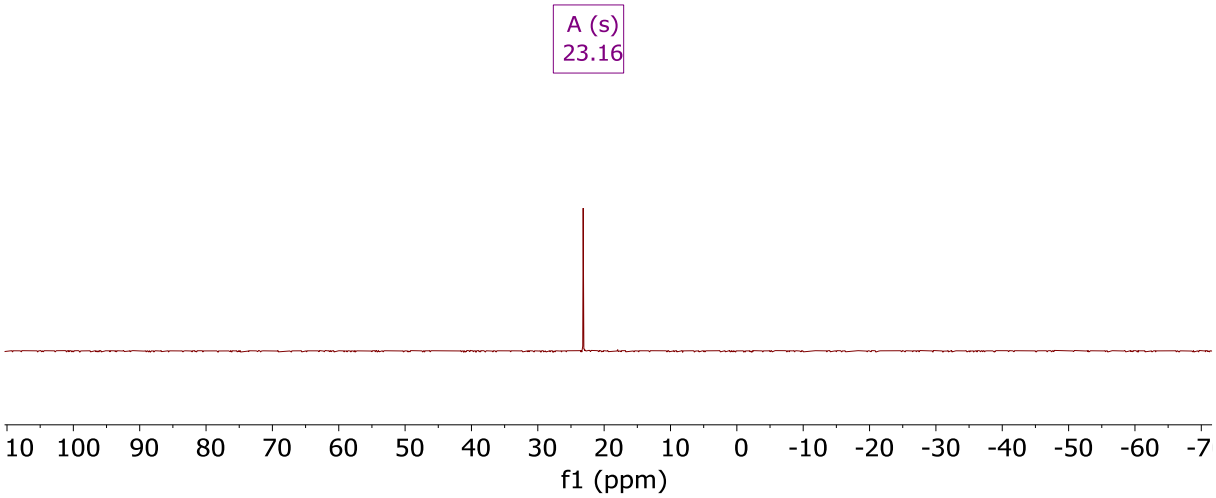

Figure S23. $^{31}P\{^{1}H\}$ NMR (162 MHz, CD_3CN) of compound **6b**: δ 23.16 (s).

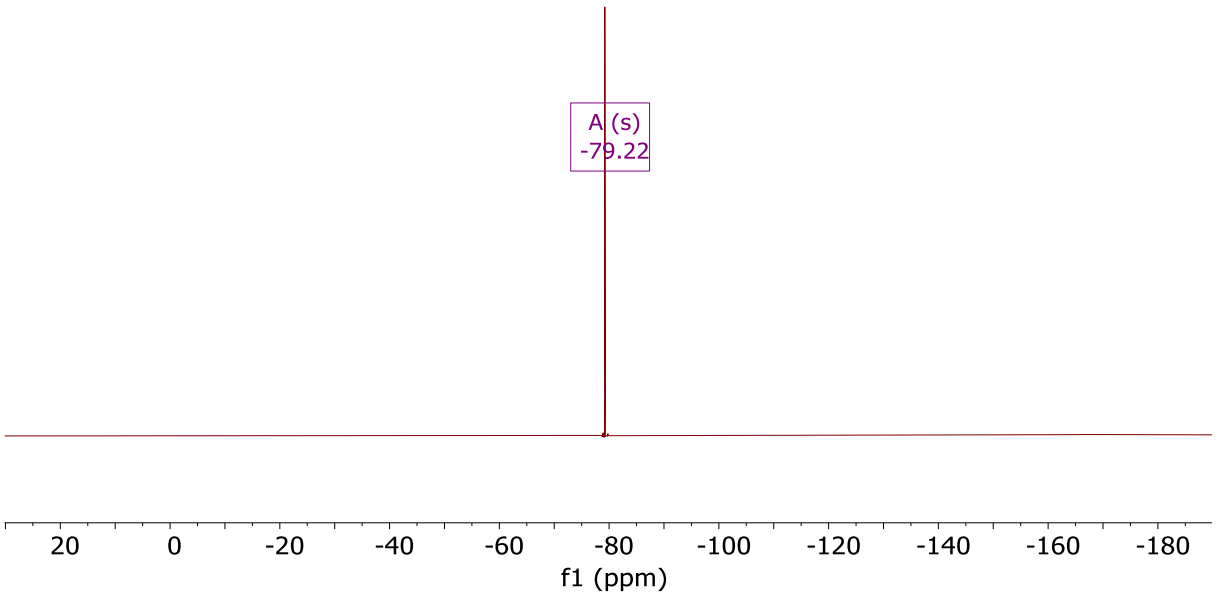

Figure S24. ^{19}F NMR (377 MHz, CD_3CN) of compound **6b**: δ -79.22 (s).

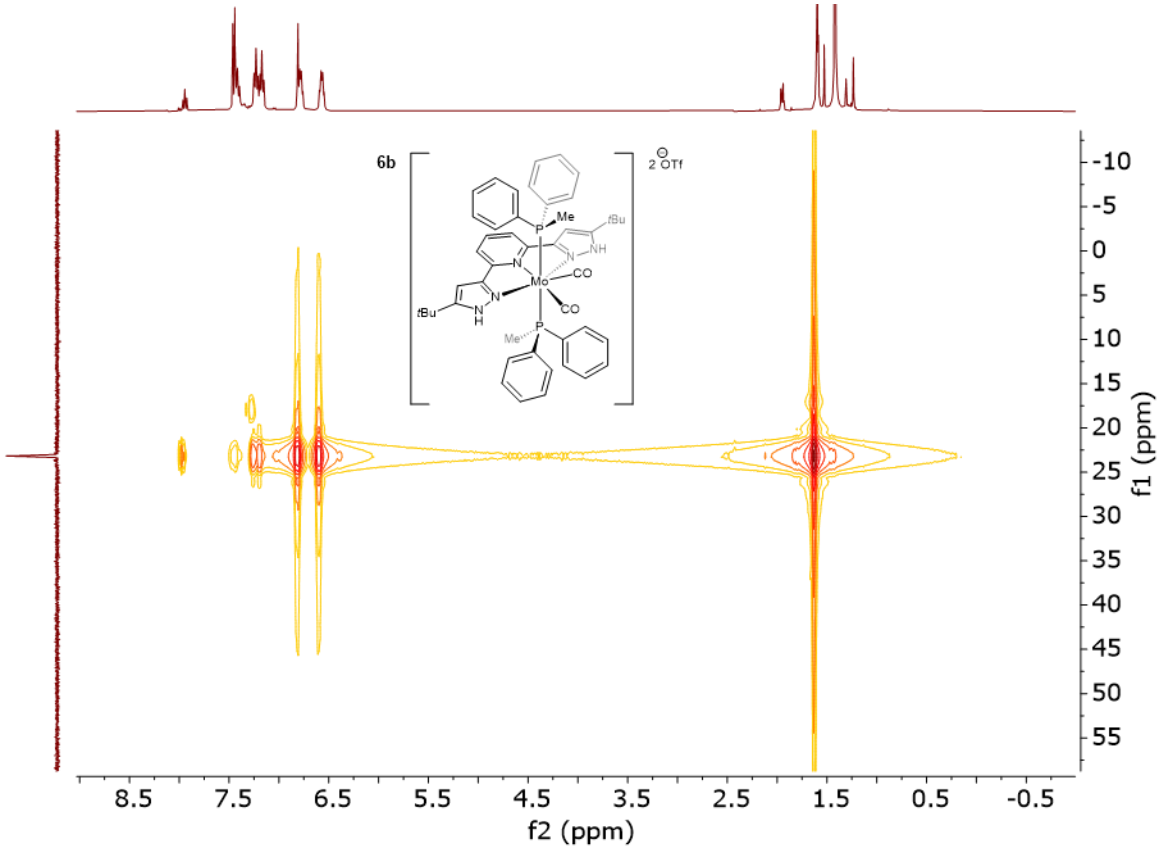

Figure S25. 2D NMR ^{31}P HMQC (162 MHz, CD_3CN) of compound **6b**.

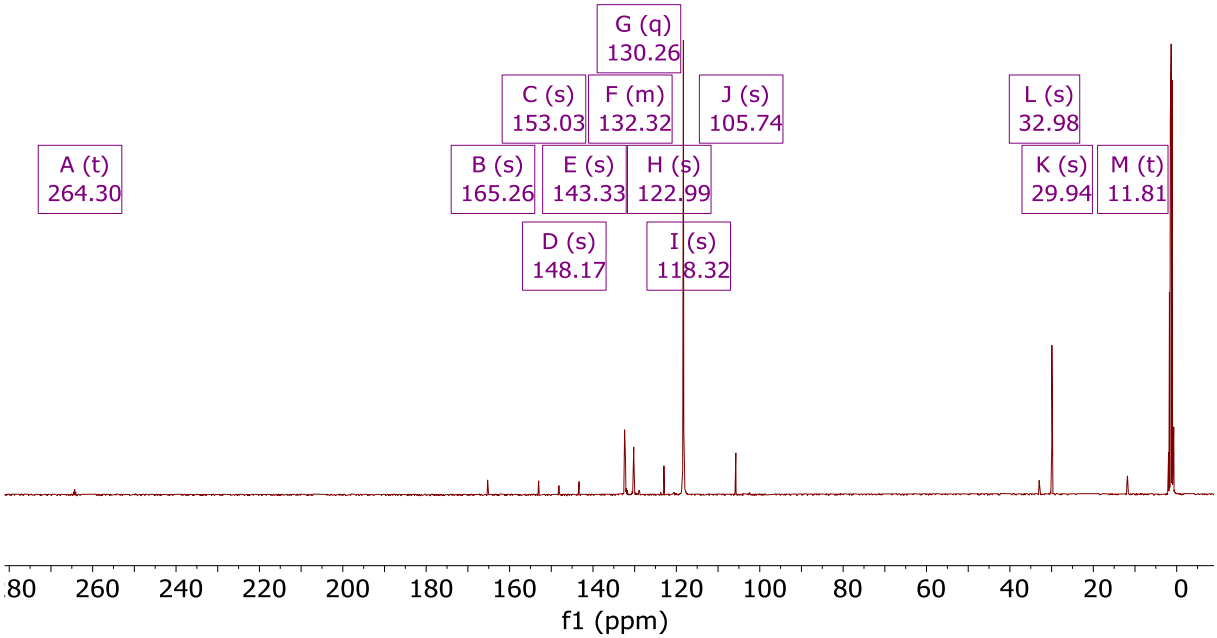

Figure S26. $^{13}C\{^{1}H\}$ NMR (101 MHz, CD_3CN) of compound **6b:** δ 264.30 (t, J = 20.9 Hz), 165.26, 153.03, 148.17, 143.33, 132.77 – 132.13 (m), 130.26 (q, J = 5.4 Hz), 122.99, 118.32, 105.74, 32.98, 29.94, 11.81 (t, J = 14.8 Hz).

1.3. Compounds 4c, 5c and 6c.

1.3.1. Complex 4c

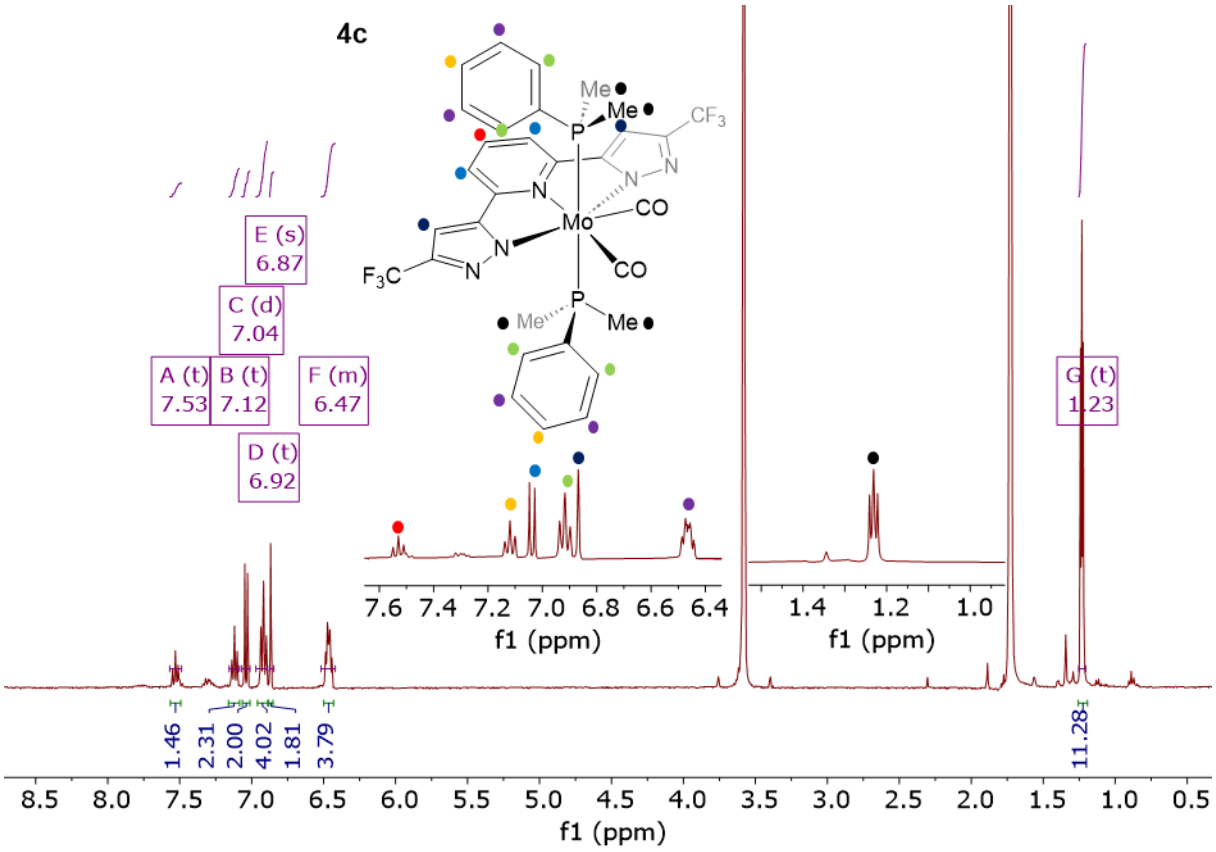

Figure S27. ^{1}H NMR (400 MHz, THF-d_8) of compound **4c**: δ 7.53 (t, *J* = 7.8 Hz, 1H), 7.12 (t, *J* = 7.4 Hz, 2H), 7.04 (d, *J* = 7.8 Hz, 2H), 6.92 (t, *J* = 7.6 Hz, 4H), 6.87 (s, 2H), 6.52 – 6.42 (m, 4H), 1.23 (t, 12H).

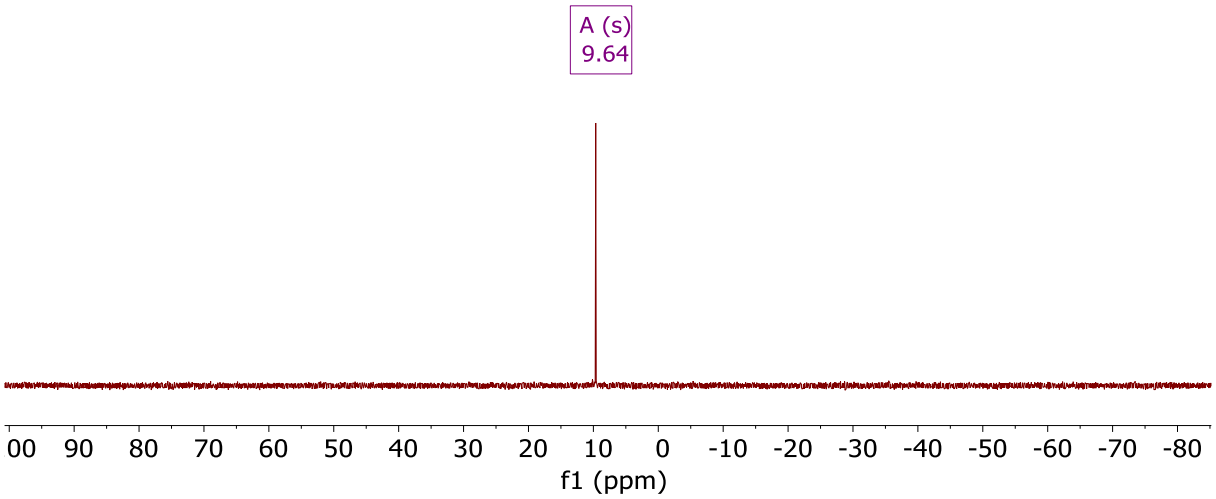

Figure S28. $^{31}P\{^{1}H\}$ NMR (162 MHz, THF-d_8) of compound **4c**: δ 9.64 (s).

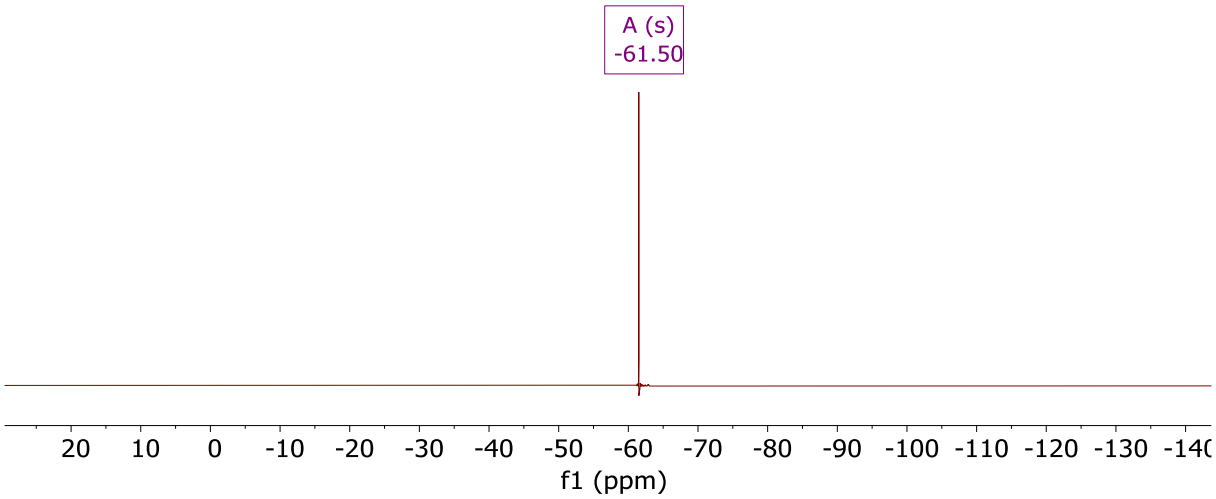

Figure S29. ^{19}F NMR (377 MHz, THF) of compound **4c**: δ -61.50 (s).

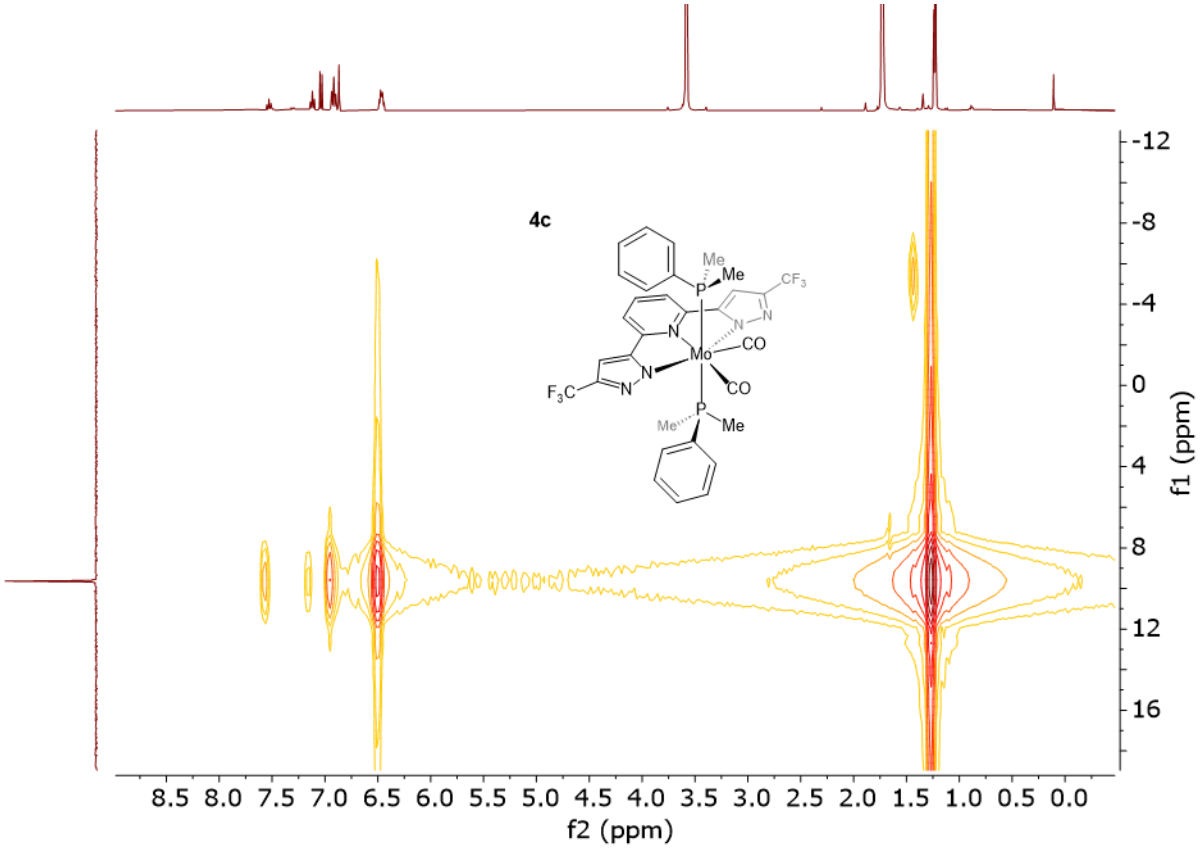

Figure S30. 2D NMR ^{31}P HMQC (162MHz, THF-d_8) of compound **4c.**

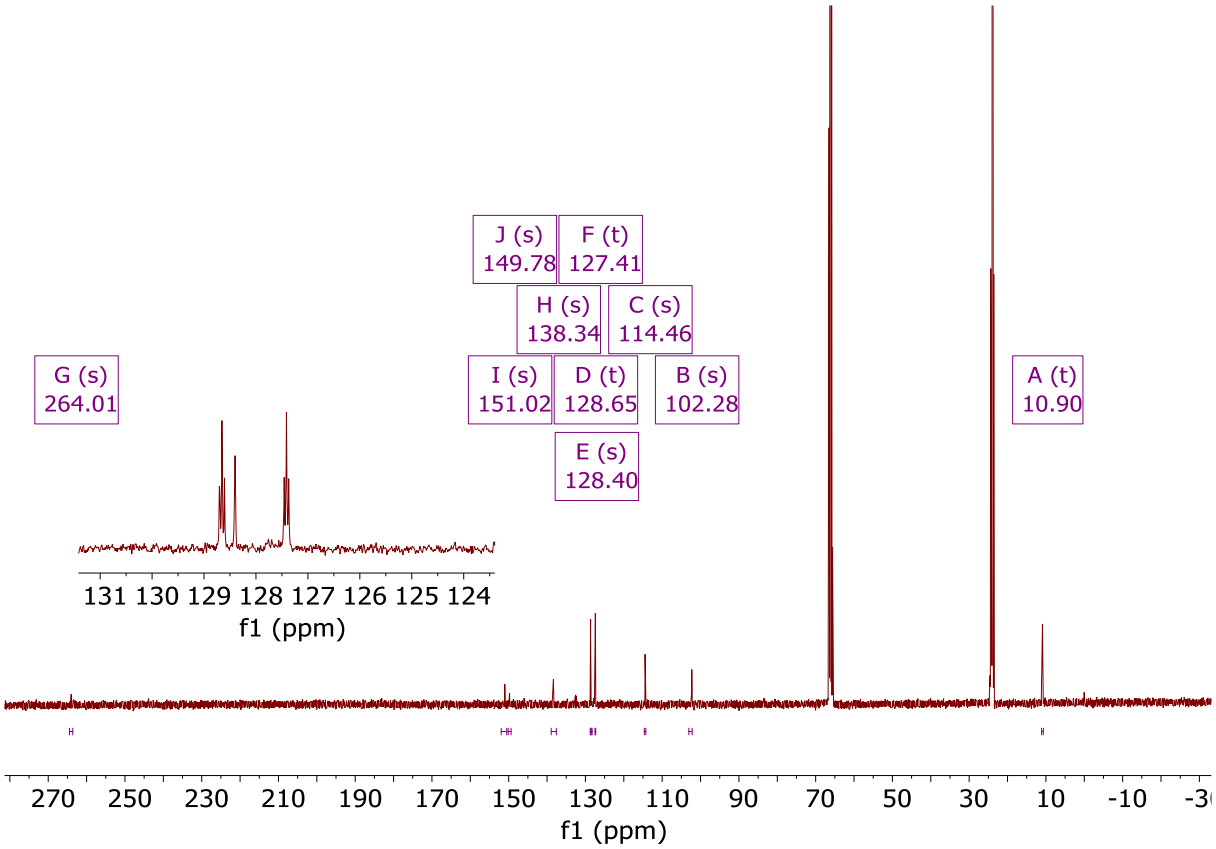

Figure S31. $^{13}C\{^{1}H\}$ NMR (400 MHz, THF-d_8) of compound **4c**: δ 264.01, 151.02, 149.78, 138.34, 128.65 (t, J = 4.9 Hz), 128.40, 127.41 (t, J = 4.4 Hz), 114.46, 102.28, 10.90 (t, J = 13.1 Hz).

1.3.2. Complex 5c

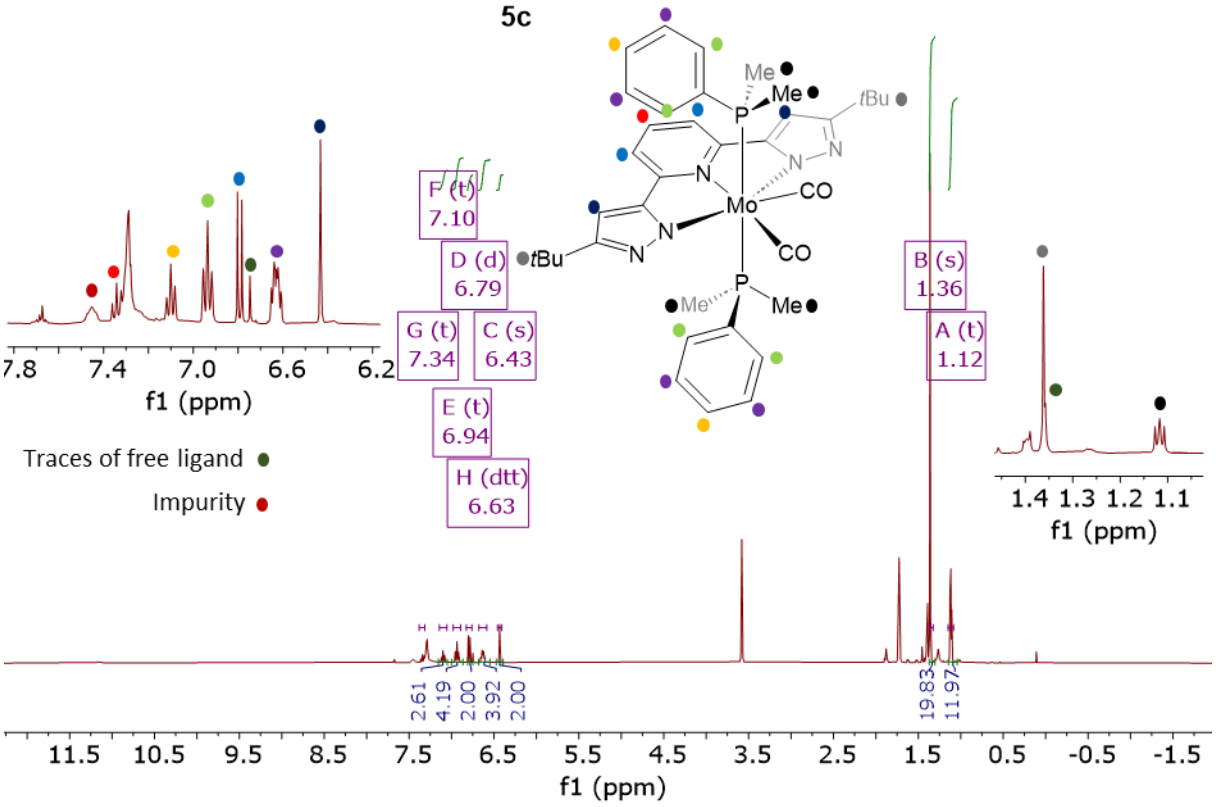

Figure S32. ^{1}H NMR (400 MHz, THF-d_8) of compound **5c:** δ 7.34 (t, 1H), 7.10 (t, *J* = 7.5, 5.9, 1.8, 0.9 Hz, 2H), 6.94 (t, *J* = 8.7, 7.6, 1.2 Hz, 4H), 6.79 (d, *J* = 7.8 Hz, 2H), 6.63 (dtt, *J* = 8.4, 5.0, 1.5 Hz, 4H), 6.43 (s, 2H), 1.36 (s, 19H), 1.12 (t, 12H).

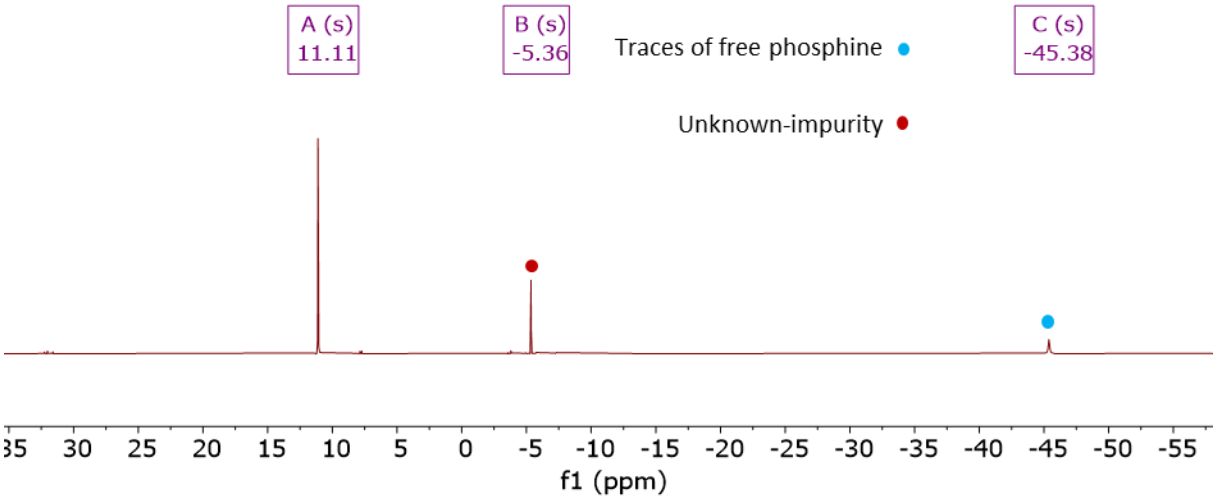

Figure S33. $^{31}P\{H\}$ NMR (162 MHz, THF-d_8) of compound **5c:** δ 11.11.

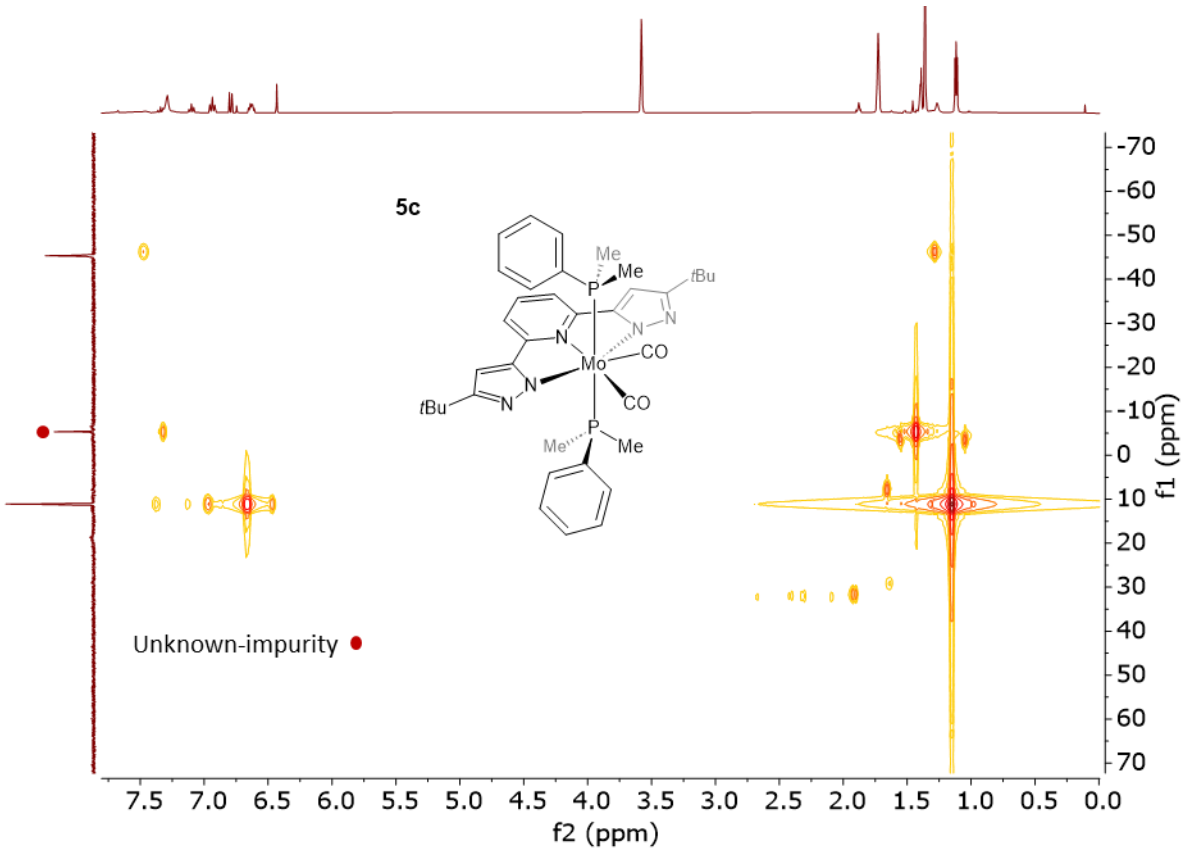

Figure S34. 2D NMR ^{31}P HMQC (162MHz, THF-d_8) of compound **5c**

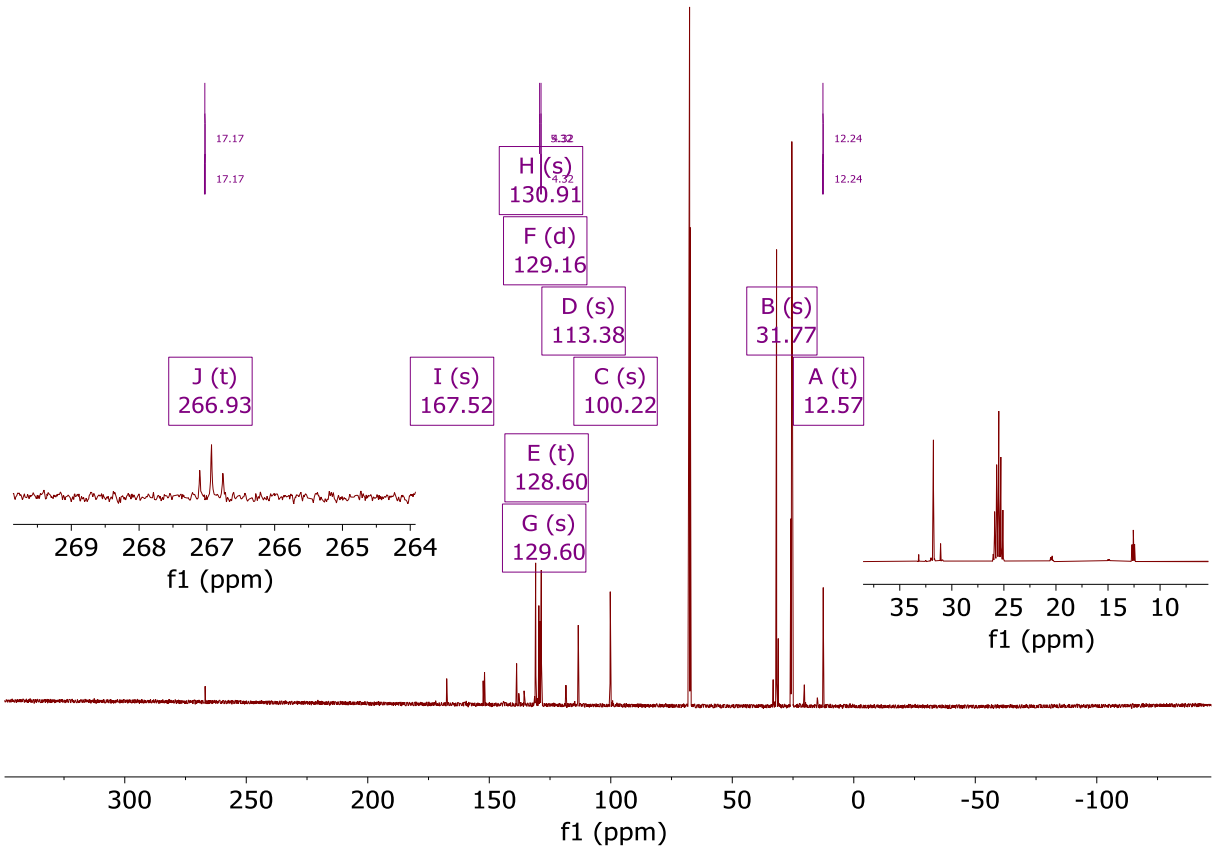

Figure S35. $^{13}C\{^{1}H\}$ NMR (101 MHz, THF-d_8) of compound **5c:** δ 266.93 (t, *J* = 17.2 Hz), 167.52, 130.91, 129.60, 129.16 (d, *J* = 5.3 Hz), 128.60 (t, *J* = 4.3 Hz), 113.38, 100.22, 31.77, 12.57 (t, *J* = 12.2 Hz).

1.3.3. Complex 6c

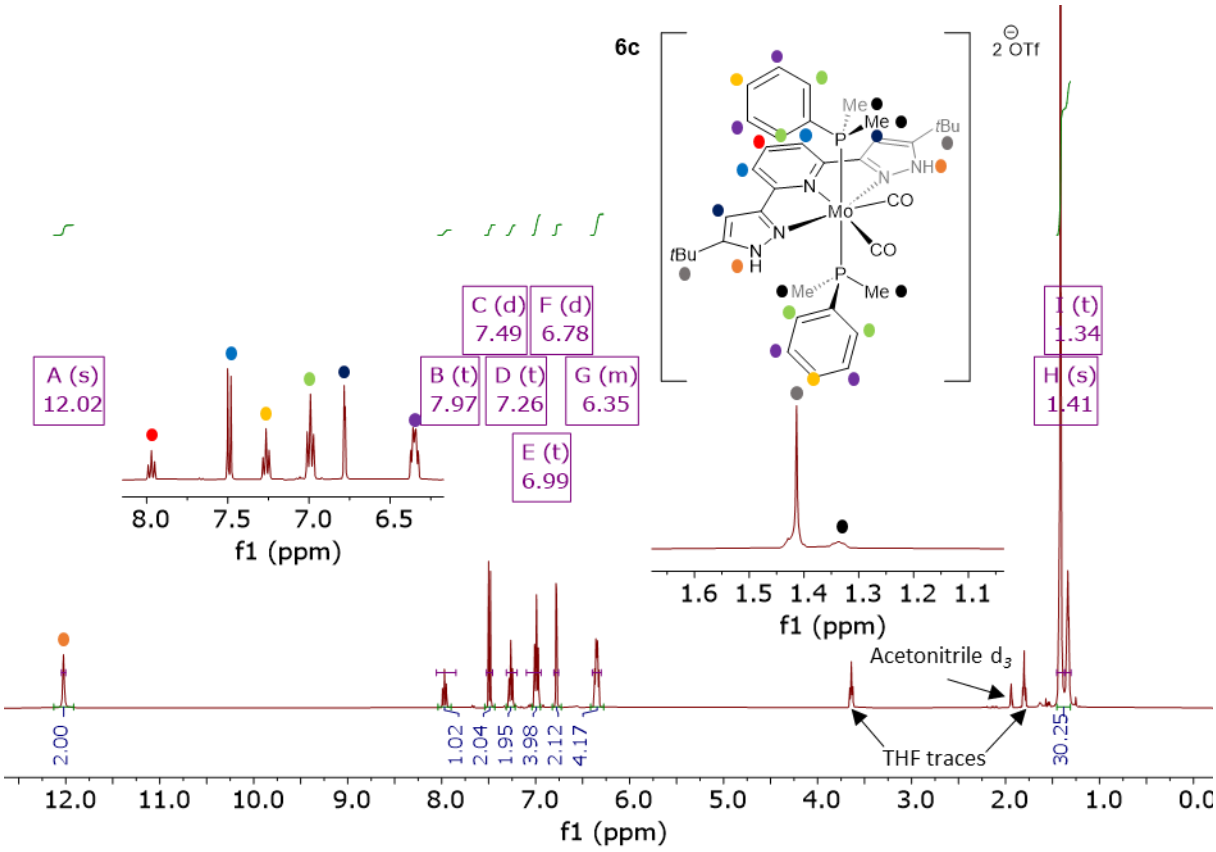

Figure S36. ^{1}H NMR (400 MHz, CD_3CN) of compound **6c**: δ 12.02 (s, 2H), 7.97 (t, 1H), 7.49 (d, *J* = 8.0 Hz, 2H), 7.26 (t, 2H), 6.99 (t, *J* = 8.7, 7.5, 1.3 Hz, 4H), 6.78 (d, *J* = 2.0 Hz, 2H), 6.40 – 6.30 (m, 4H), 1.41 (s, 18H), 1.34 (t, *J* = 4.4 Hz, 12H).

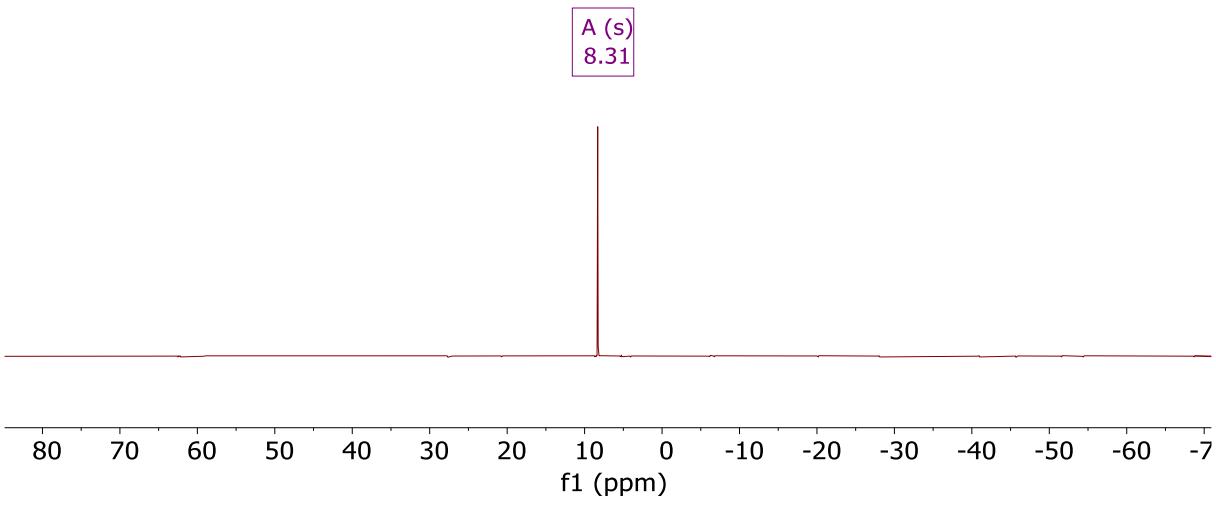

Figure S37. $^{31}P\{^{1}H\}$ NMR (162 MHz, CD_3CN) of compound **6c**: δ 8.31 (s).

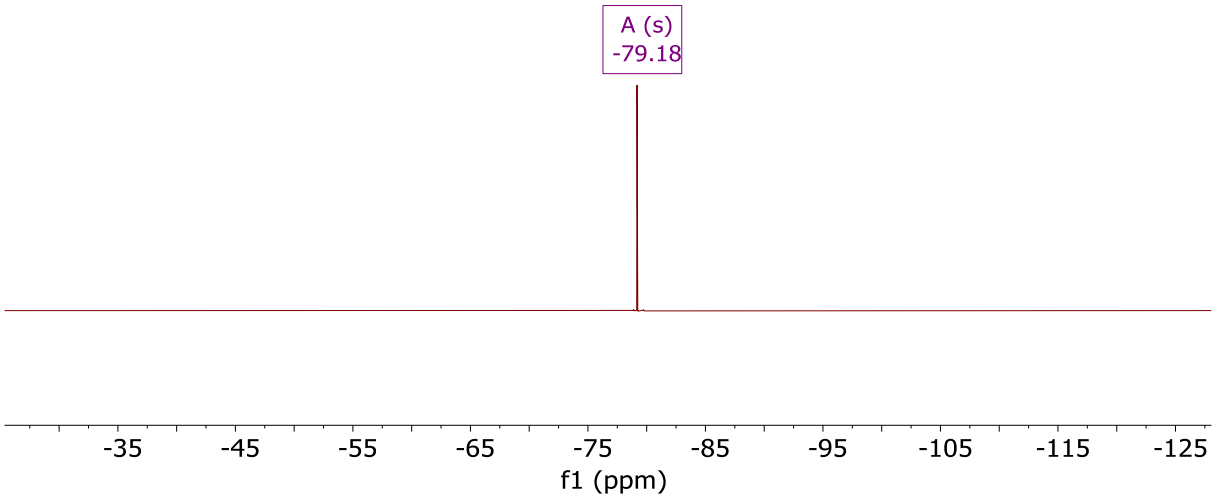

Figure S38. ^{19}F NMR (377 MHz, CD_3CN) of compound **6c**: δ -79.18 (s).

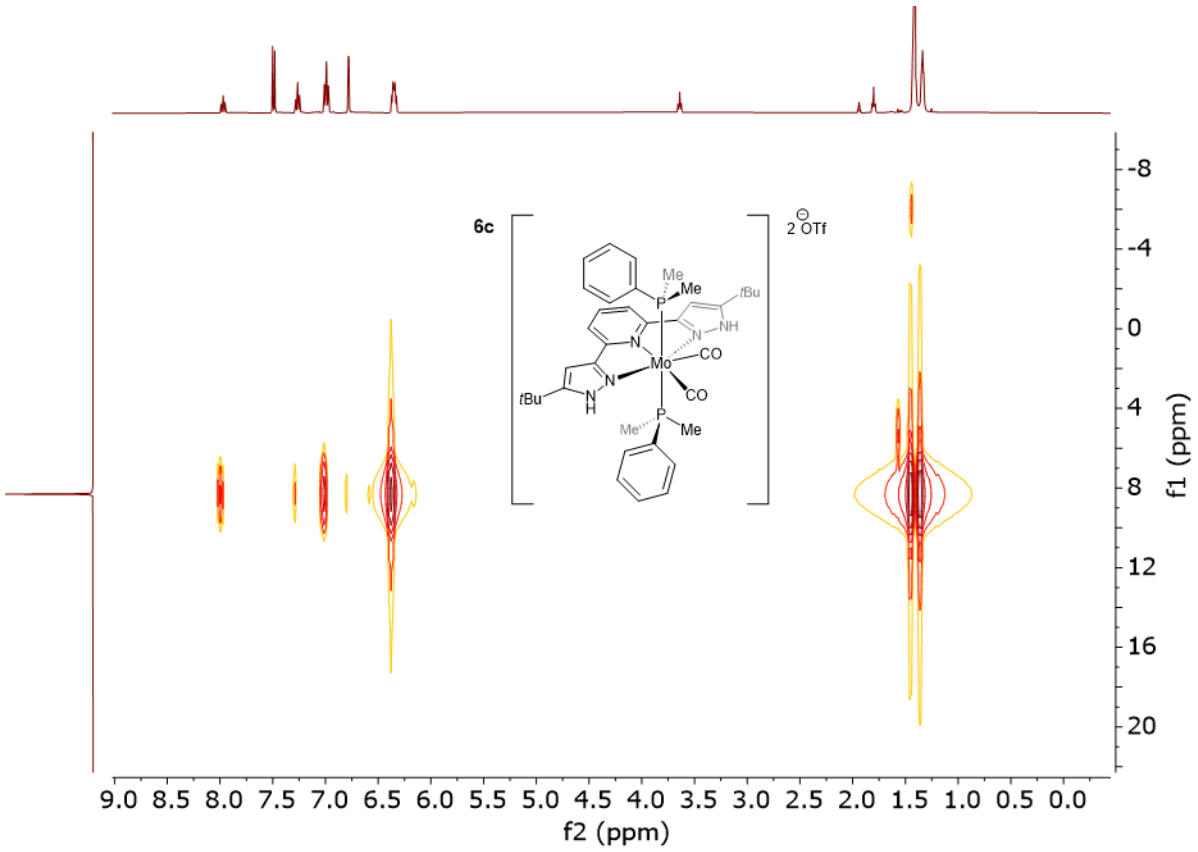

Figure S39. 2D NMR ^{31}P HMQC (400MHz, CD_3CN) of compound **6c**.

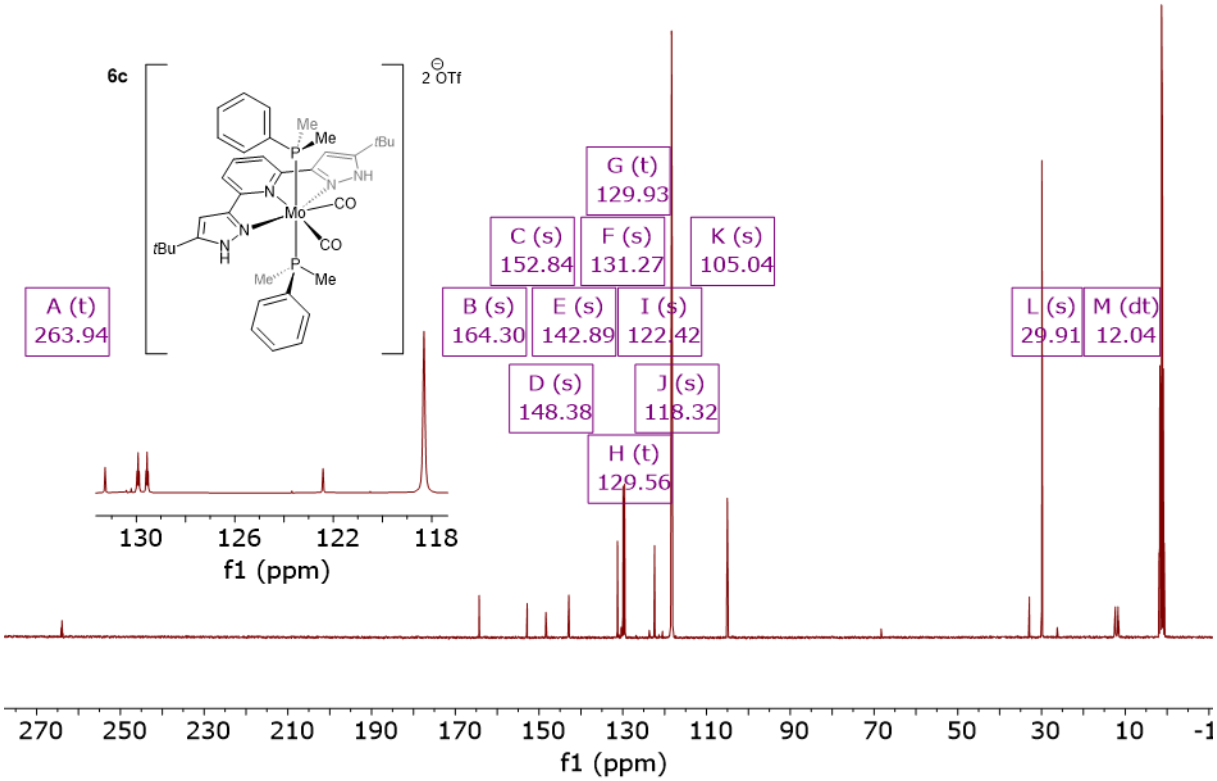

Figure S40. $^{13}C\{^{1}H\}$ NMR (101 MHz, CD_3CN) of compound **6c:** δ 263.94 (t, J = 20.1 Hz), 164.30, 152.84, 148.38, 142.89, 131.27, 129.93 (t, J = 4.6 Hz), 129.56 (t, J = 4.6 Hz), 122.42, 118.32, 105.04, 29.91.

2. IR spectra

2.1. Compounds 4a, 5a and 6a.

2.1.1. Complex 4a

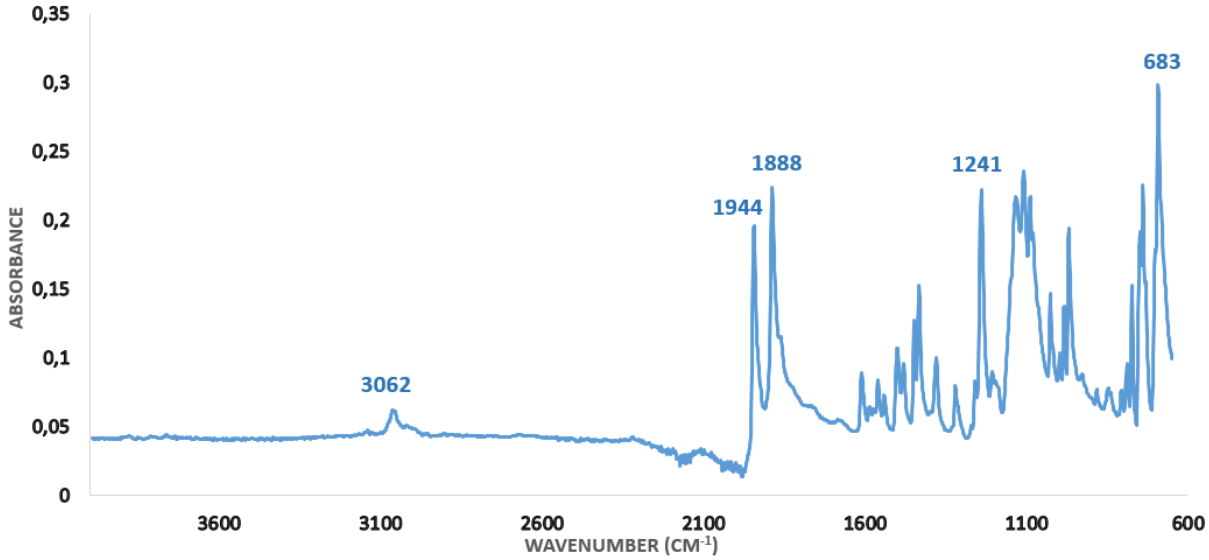

Figure S41. ATR spectrum (298K, under nitrogen) of compound **4a.**

2.1.2. Complex 5a

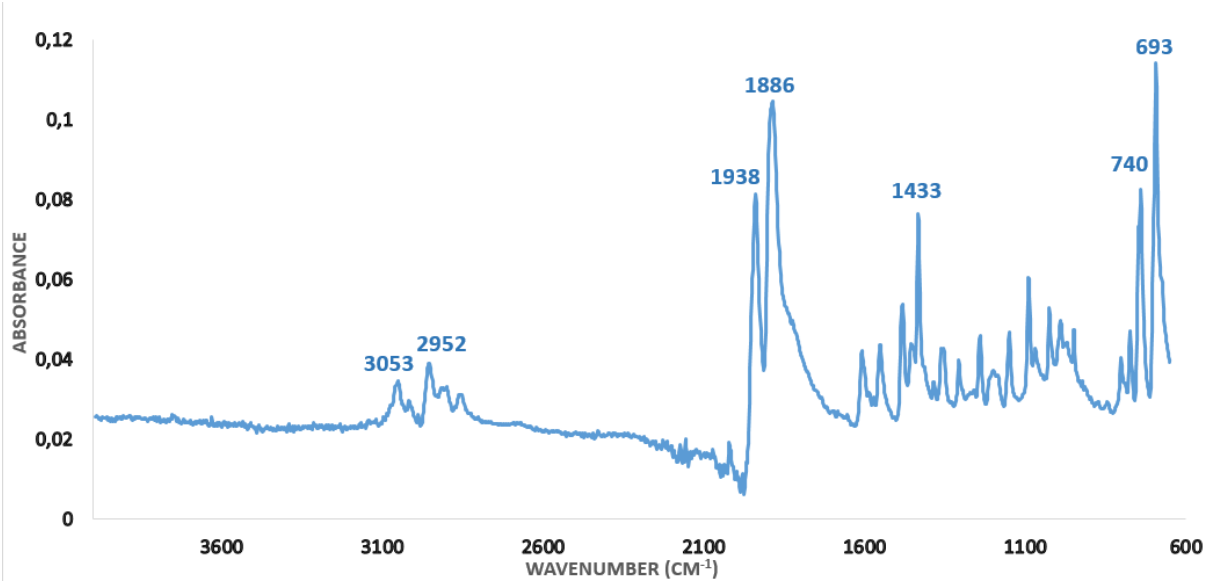

Figure S42. ATR spectrum (298K, under nitrogen) of compound **5a.**

2.1.3. Complex 6a

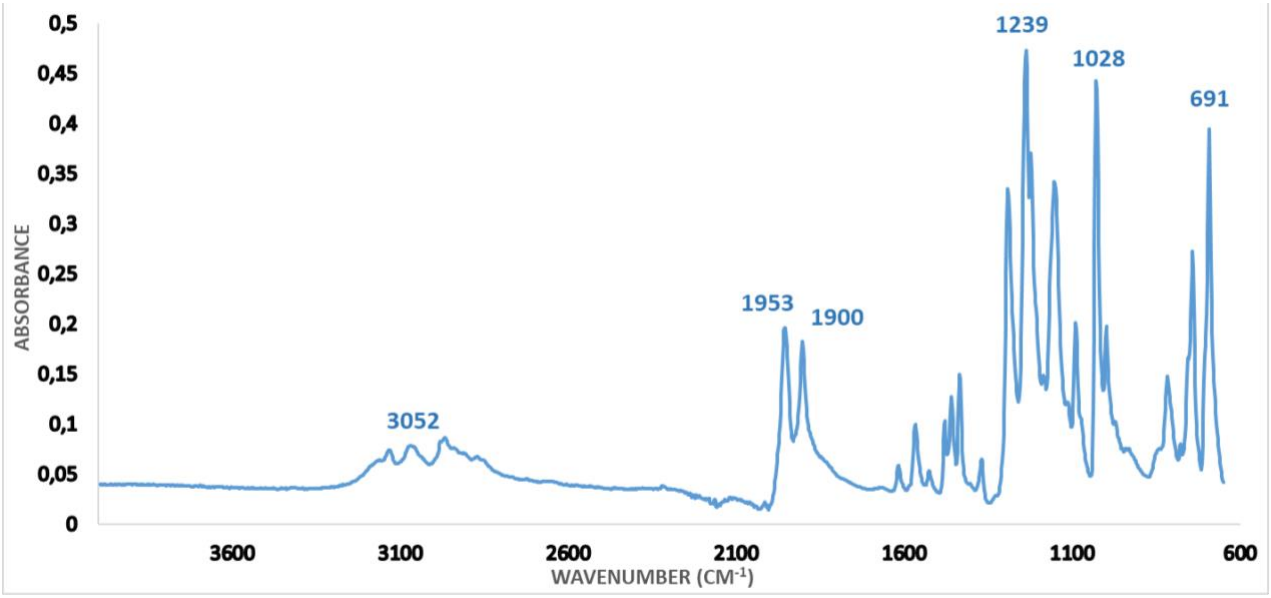

Figure S43. ATR spectrum (298K, under nitrogen) of compound **6a.**

2.2. Series 4b, 5b and 6b.

2.2.1. Complex 4b

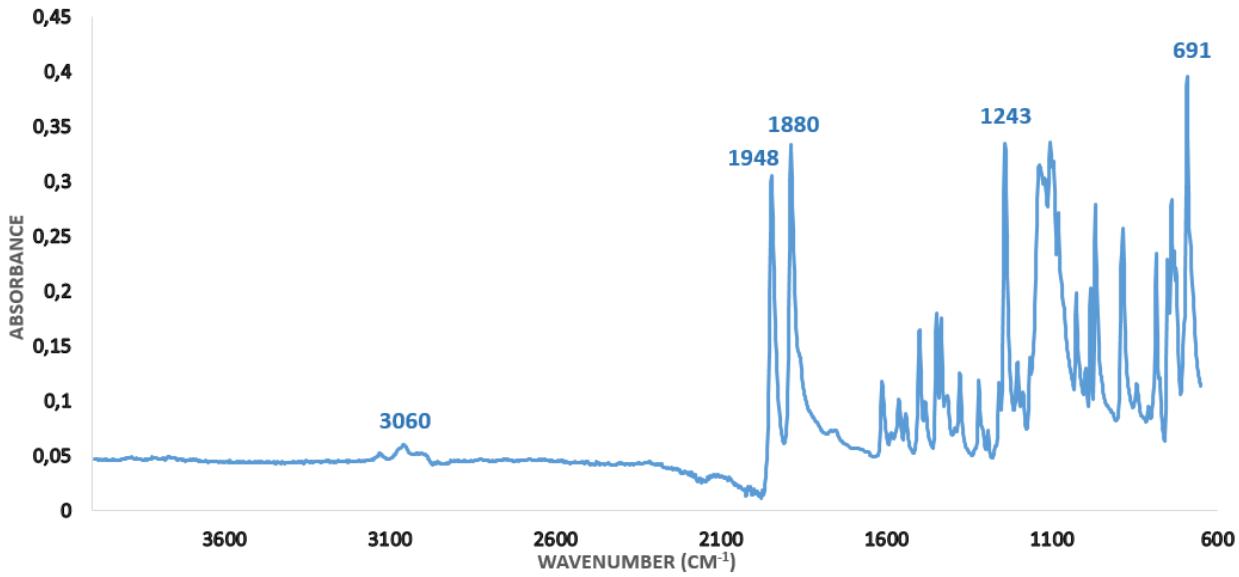

Figure S44. ATR spectrum (298K, under nitrogen) of compound **4b.**

2.2.2. Complex 5b

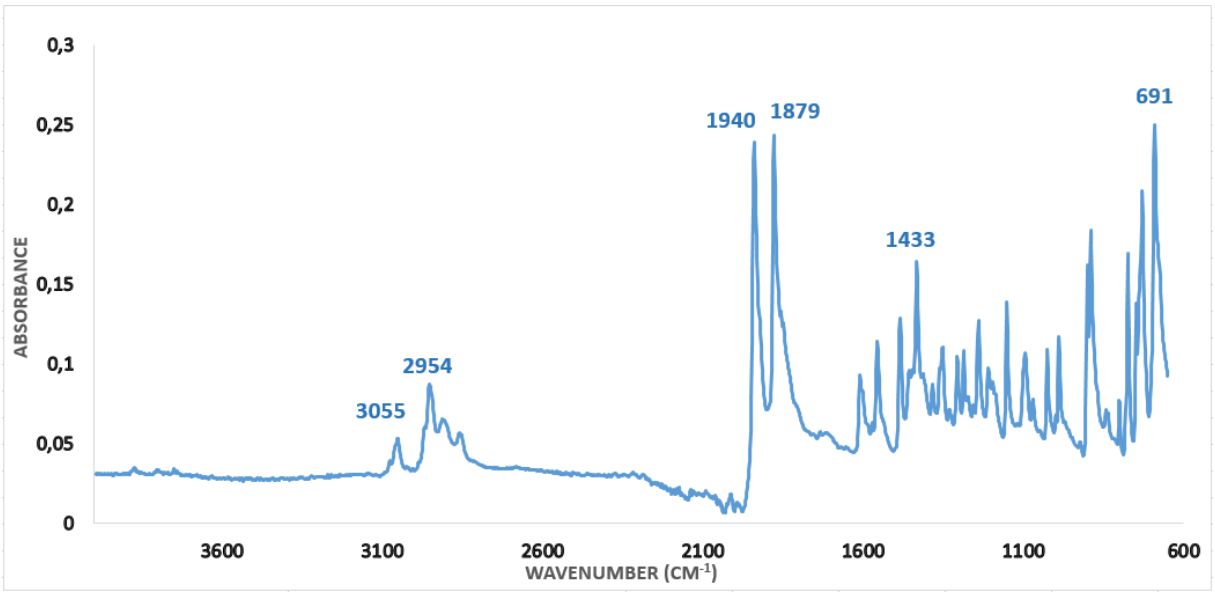

Figure S45. ATR spectrum (298K, under nitrogen) of compound **5b.**

2.2.3. Complex 6b

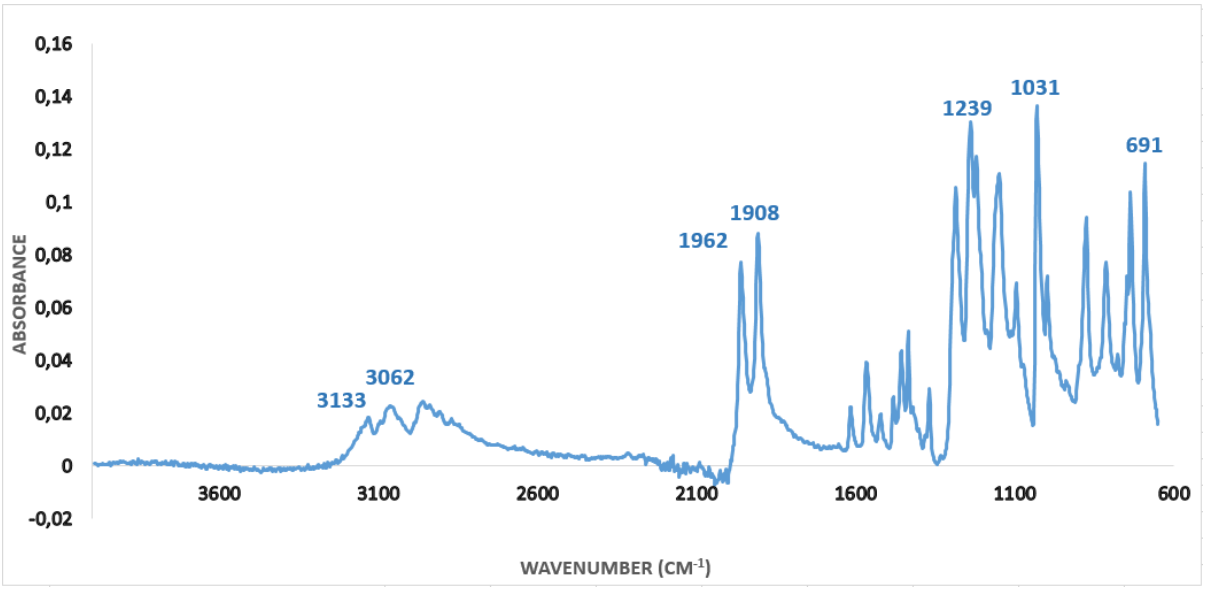

Figure S46. ATR spectrum (298K, under nitrogen) of compound **6b.**

2.3. Compounds 4c, 5c and 6c.

2.3.1. Complex 4c

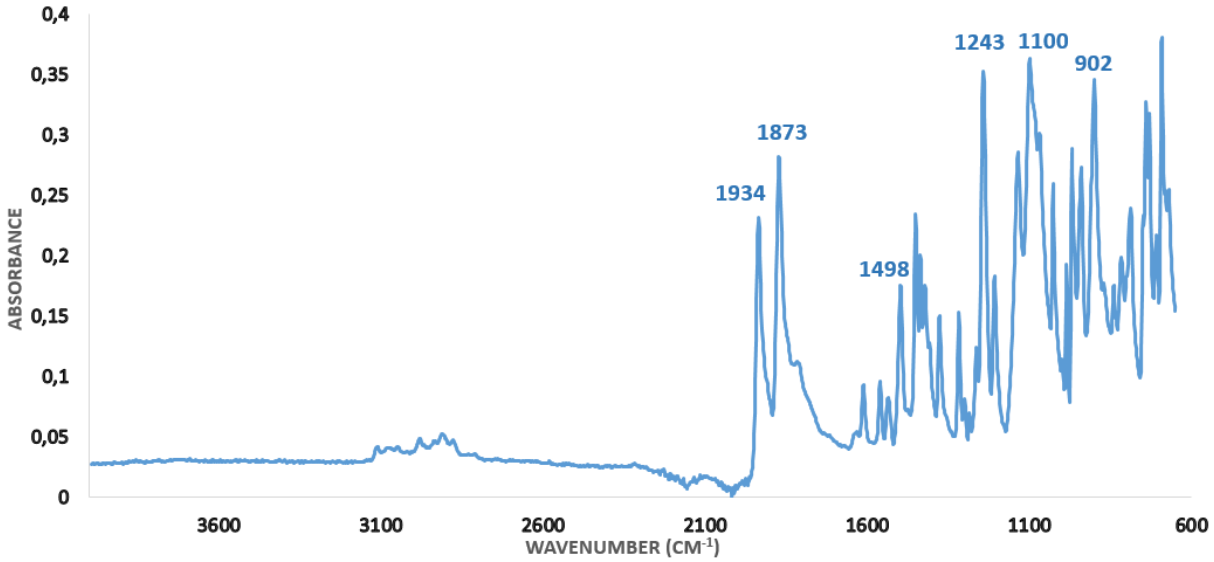

Figure S47. ATR spectrum (298K, under nitrogen) of compound **4c**.

2.3.2. Complex 5c

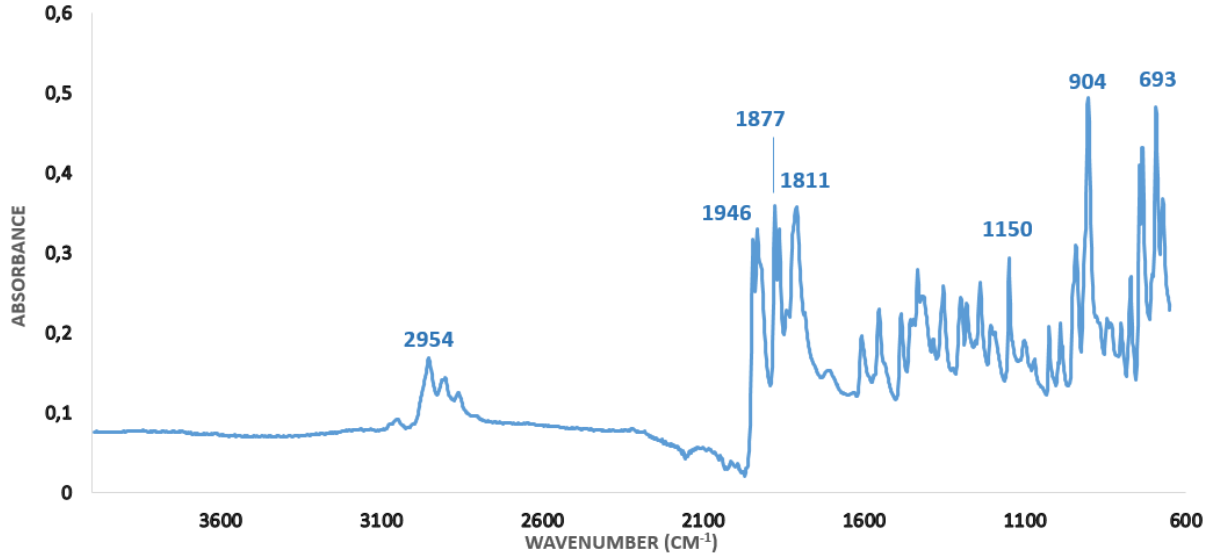

Figure S48. ATR spectrum (298K, under nitrogen) of compound **5c.**

2.3.3. Complex 6c

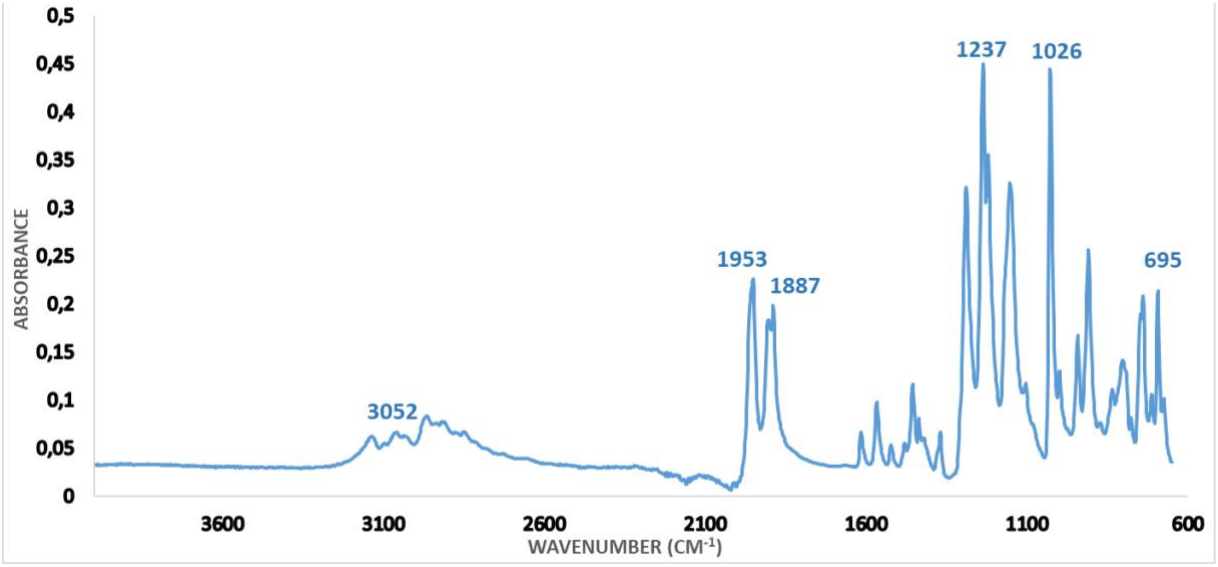

Figure S49. ATR spectrum (298K, under nitrogen) of compound **6c.**

3. UV-Visible spectra

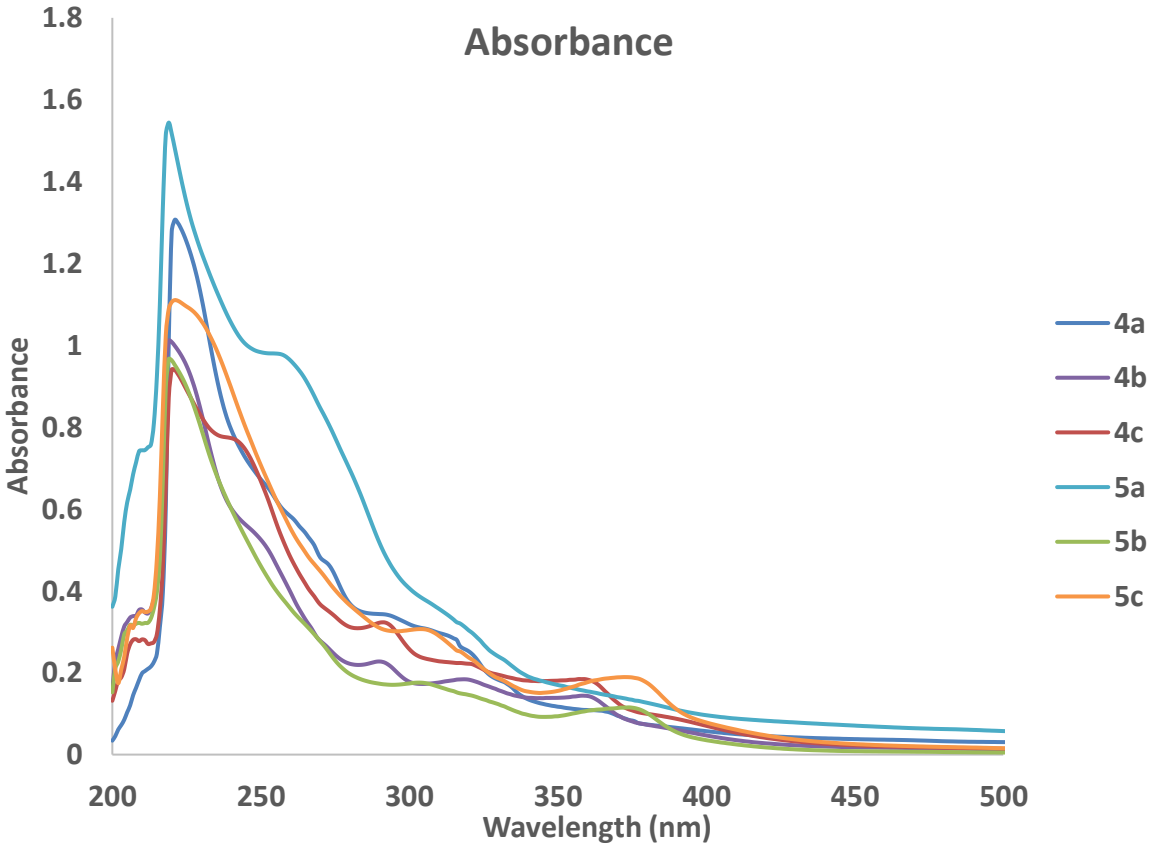

Figure S50. UV-Visible spectrum (298K, under air) of the heptacoordinated Mo complexes (**4a-c** and **5a-c**) stacked and centered in the UV range.

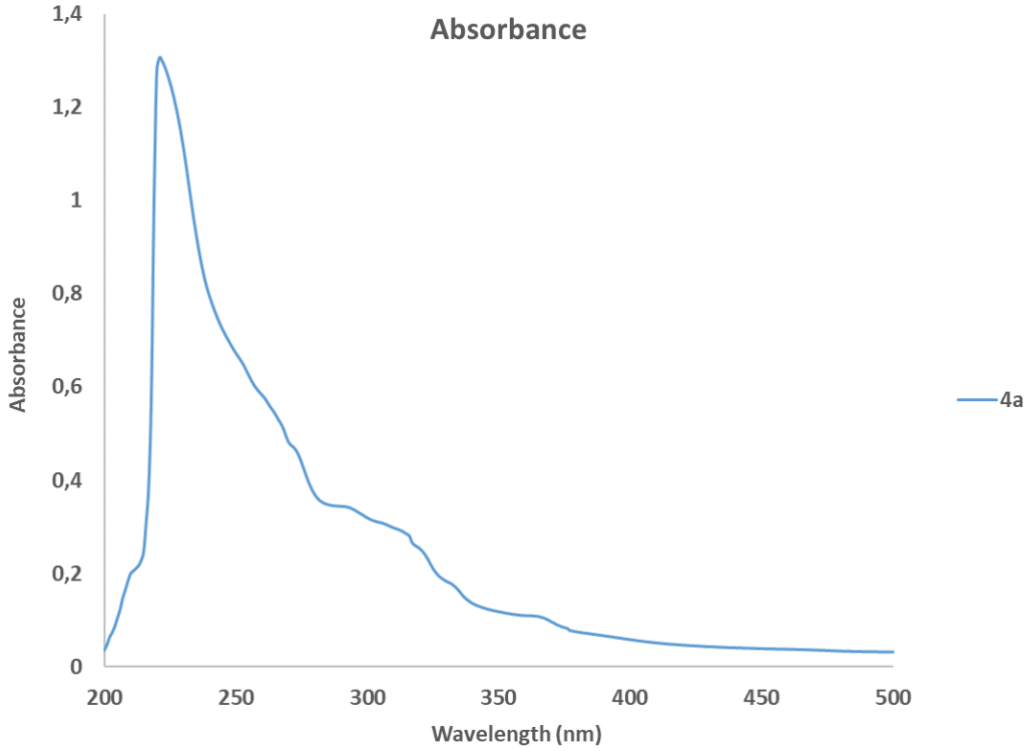

Figure S51. UV-Visible spectrum (298K, under air) of **4a**. λ_{max} = 221 nm ; ε = 26726 L·mol^{-1}·cm^{-1}, with A = 1.3061 and C = 4.8875·10^{-5} mol.L^{-1}.

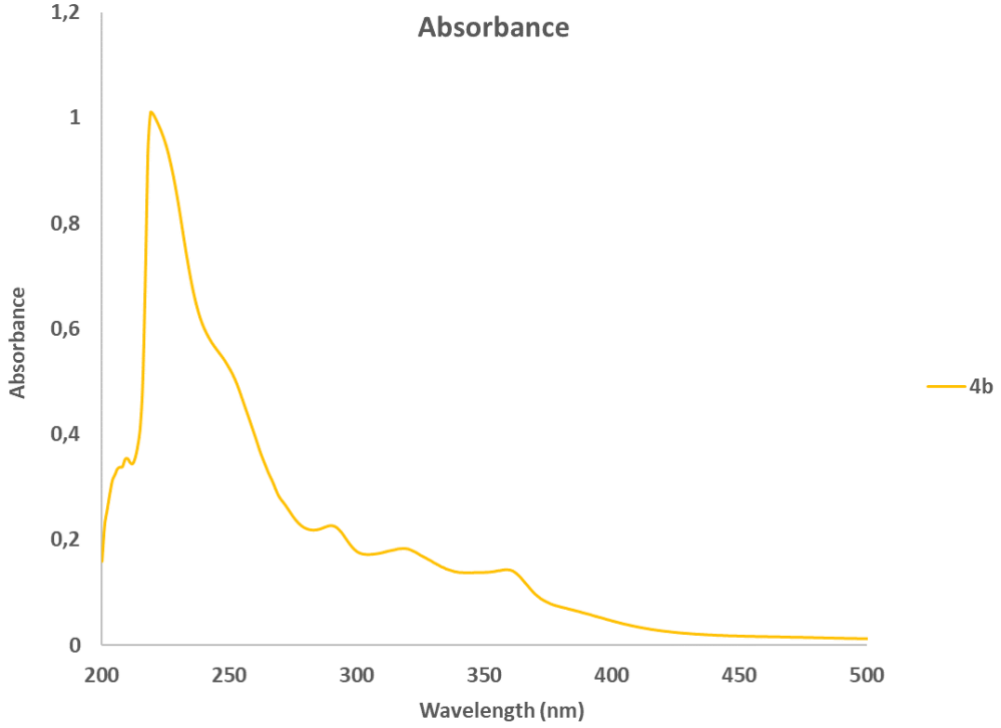

Figure 52 : UV-Visible spectrum (298K, under air) of **4b**. λ_{max} = 220 nm. ε = 18181 L·mol^{-1}·cm^{-1}, with A = 1.01123 and C = 5.5617·10^{-5} mol·L^{-1}.

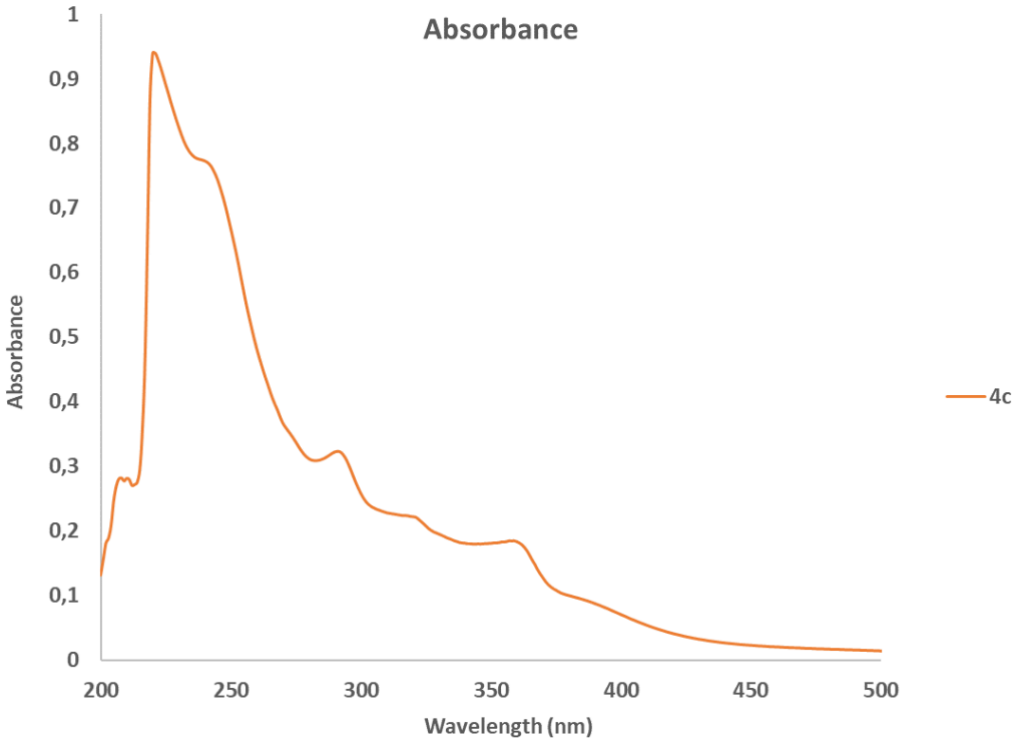

Figure S53. UV-Visible spectrum (298K, under air) of **4c**. λ_{max} = 220 nm. ε = 14577 $L \cdot mol^{-1} \cdot cm^{-1}$, with A = 0.9405 and C = $6.4516 \cdot 10^{-5}$ $mol \cdot L^{-1}$.

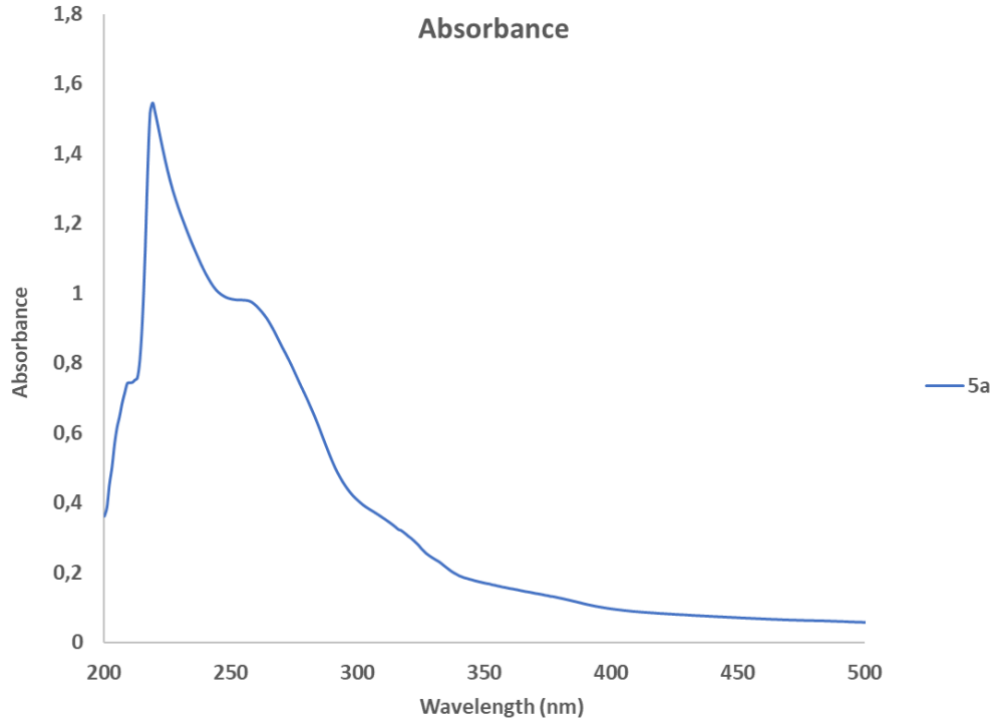

Figure S54. UV-Visible spectrum (298K, under air) of **5a**. λ_{max} = 219 nm. ε = 30851 $L \cdot mol^{-1} \cdot cm^{-1}$, with A = 1.5441 and C = $5.005 \cdot 10^{-5}$ $mol \cdot L^{-1}$.

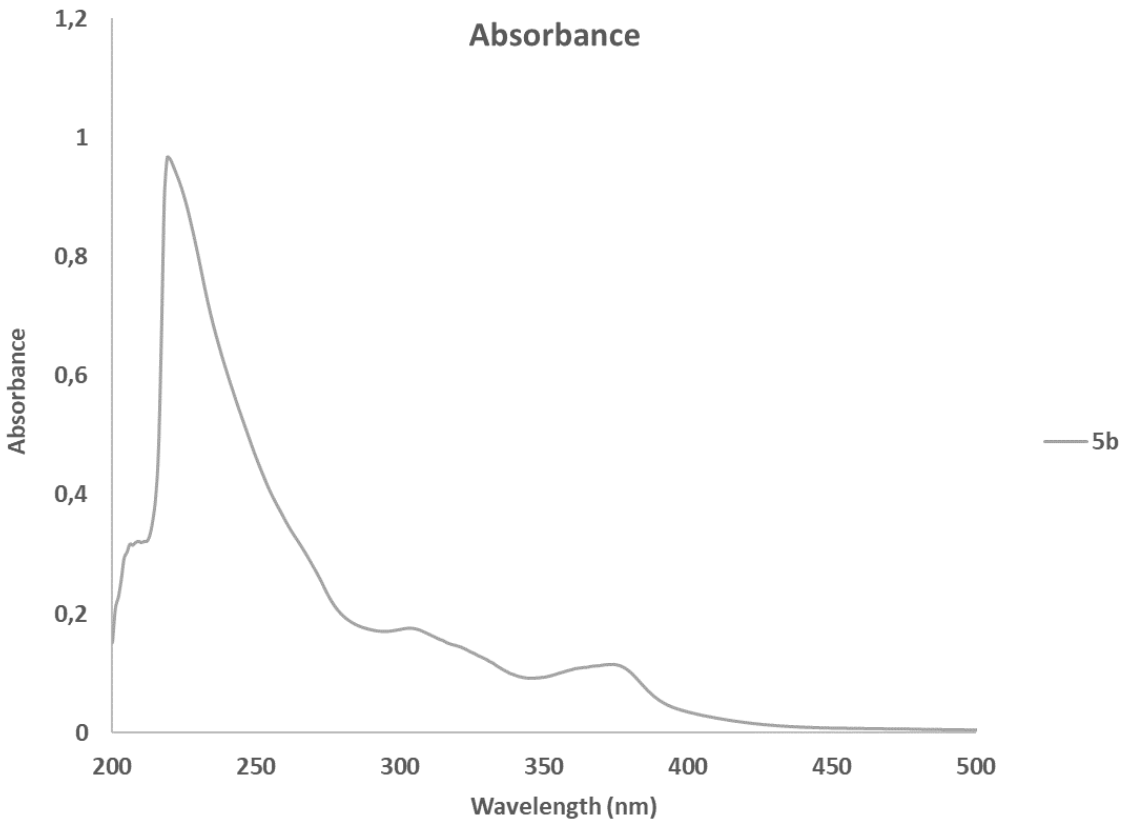

Figure S55. UV-Visible spectrum (298K, under air) of **5b**. λ_{max} = 220 nm. ε = 16910 L·mol^{-1}·cm^{-1}, with A = 0.9663 and C = 5.7142·10^{-5} mol·L^{-1}.

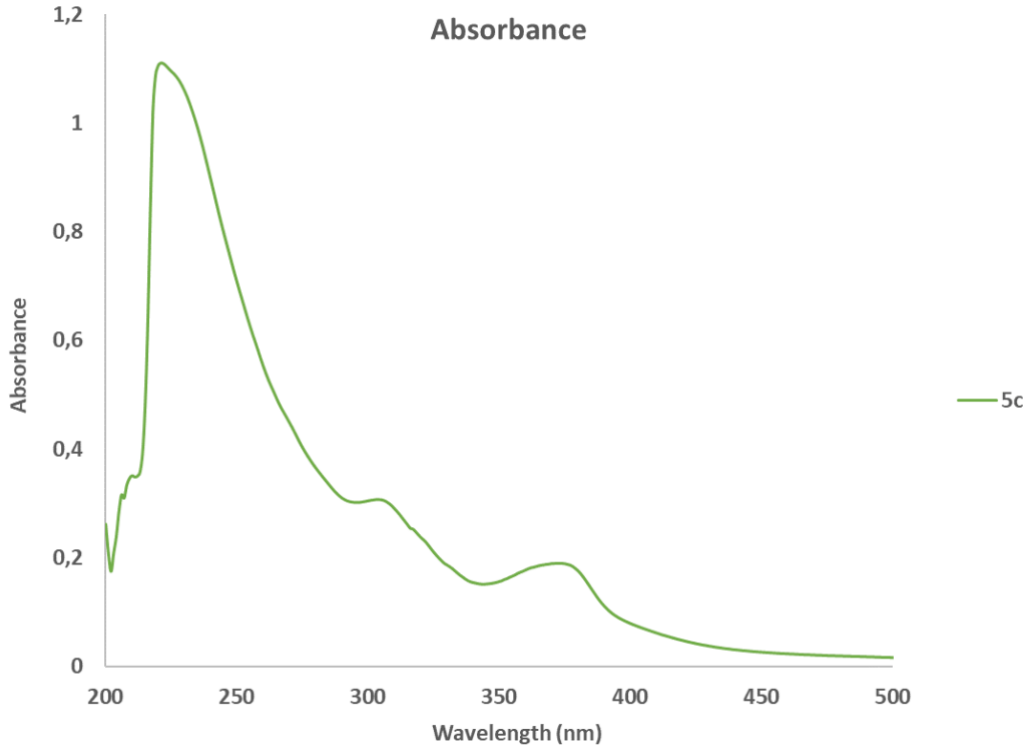

Figure S56. UV-Visible spectrum (298K, under air) of **5c**. λ_{max} = 221 nm. ε = 16672 $L \cdot mol^{-1} \cdot cm^{-1}$, with A = 1.110 and C = $6.6577 \cdot 10^{-5}$ $mol \cdot L^{-1}$.

4. Crystallographic data

Data for compounds **4a, 4b, 4c, 5b, 5c** and **6b** were collected at low temperature (100 K) on a XtaLAB Synergy, Dualflex, HyPix diffractometer using a Cu-Kα radiation (λ = 1.54184 Å) micro-source and equipped with an Oxford Cryosystems Cryostream Cooler Device. The structures have been solved using the new dual-space algorithm program SHELXT,[1] and refined by means of least-squares procedures using either SHELXL-2018[1] program included in the software package WinGX[2] version 1.639 (complexes **4b** and **5b**), or with the aid of the program CRYSTALS[3] (complexes **4a**, **4c**, **5c** and **6b**). The Atomic Scattering Factors were taken from International Tables for X-Ray Crystallography.[4] Hydrogen atoms were placed geometrically and refined using a riding model. All non-hydrogen atoms were anisotropically refined.
It was not possible to resolve diffuse electron-density residuals (enclosed solvent molecule) for the structure **6b**. Treatment with the 'SQUEEZE facility from PLATON'[5] resulted in a smooth refinement. Since a few low order reflections are missing from the data set, the electron count will be underestimated. Thus, the values given for D(calc), F(000) and the molecular weight are only valid for the ordered part of the structure.ms were anisotropically refined.
Drawing of molecules in the following figures were performed with the program Mercury[6] with 25% probability displacement ellipsoids for non-hydrogen atoms. The crystal structures have been deposited at the Cambridge Crystallographic Data Centre and allocated the deposition numbers 2403147-2403152.

4.1. XRD data for compound 4a

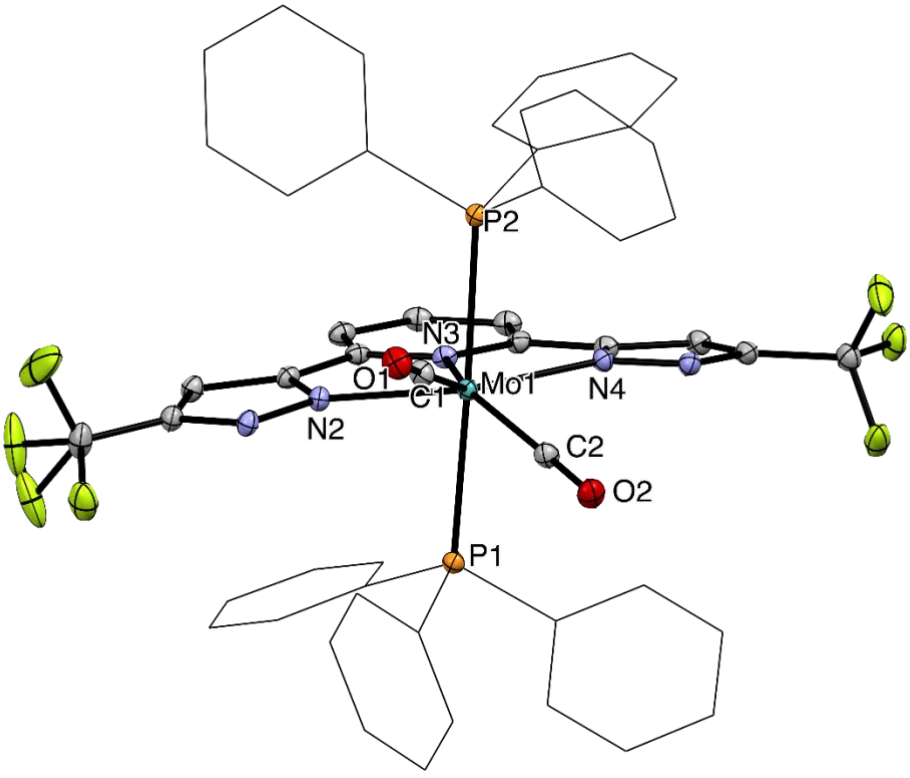

Figure S57. Solid-state structure of **4a** [Mo(L^{CF_3})(PPh_3)$_2$(CO)$_2$]. Ellipsoids are represented with 25% probability level. Hydrogen atoms have been omitted for clarity and phosphorus substituents appear as wireframe. Space group and selected bond distances (Å): $P2_1/n$; Mo-N2 2.177(2), Mo-N3 2.206(2), Mo-N4 2.182(2), Mo-P1 2.5711(6), Mo-P2 2.5442(6), Mo-C1 1.991(2), Mo-C2 1.986(2), C1-O1 1.137(3), C2-O2 1.149(3). One of the CF_3 groups of **4a** presents disorder.

Crystal data

$C_{51}H_{35}F_6MoN_5O_2P_2$	$F(000)$ = 2072
M_r = 1021.75	D_x = 1.508 Mg m^{-3}
Monoclinic, $P2_1/n$	
Hall symbol: -P 2yn	Cu $K\alpha$ radiation, λ = 1.54184 Å
a = 13.61346 (7) Å	Cell parameters from 70105 reflections
b = 19.90355 (10) Å	θ = 3.8–79.7°
c = 16.96940 (8) Å	μ = 3.68 mm^{-1}
β = 101.8476 (5)°	T = 100 K
V = 4500.01 (4) Å^3	Block, red
Z = 4	0.20 × 0.15 × 0.08 mm

Data collection

XtaLAB Synergy, Dualflex, HyPix diffractometer	9775 independent reflections
Radiation source: micro-focus sealed X-ray tube, PhotonJet (Cu) X-ray Source	9404 reflections with $I > 2.0\sigma(I)$
Mirror monochromator	R_{int} = 0.047
Detector resolution: 10.0000 pixels mm^{-1}	θ_{max} = 80.5°, θ_{min} = 3.5°
ϕ & ω scans	h = −16 17
Absorption correction: multi-scan CrysAlisPro 1.171.42.102a (Rigaku OD, 2023)	k = −20 25
T_{min} = 0.43, T_{max} = 0.74	l = −21 21
106885 measured reflections	

Refinement

Refinement on F^2	
Least-squares matrix: full	Hydrogen site location: difference Fourier map
$R[F^2 > 2\sigma(F^2)]$ = 0.041	H-atom parameters not refined
$wR(F^2)$ = 0.118	Method = Modified Sheldrick $w = 1/[\sigma^2(F^2) + (0.08P)^2 + 6.17P]$, where $P = (\max(F_o^2,0) + 2F_c^2)/3$
S = 0.99	$(\Delta/\sigma)_{max}$ = 0.002
9775 reflections	$\Delta\rho_{max}$ = 0.86 e Å^{-3}
613 parameters	$\Delta\rho_{min}$ = −1.45 e Å^{-3}
7 restraints	Extinction correction: None

4.2. XRD data for compound 4b

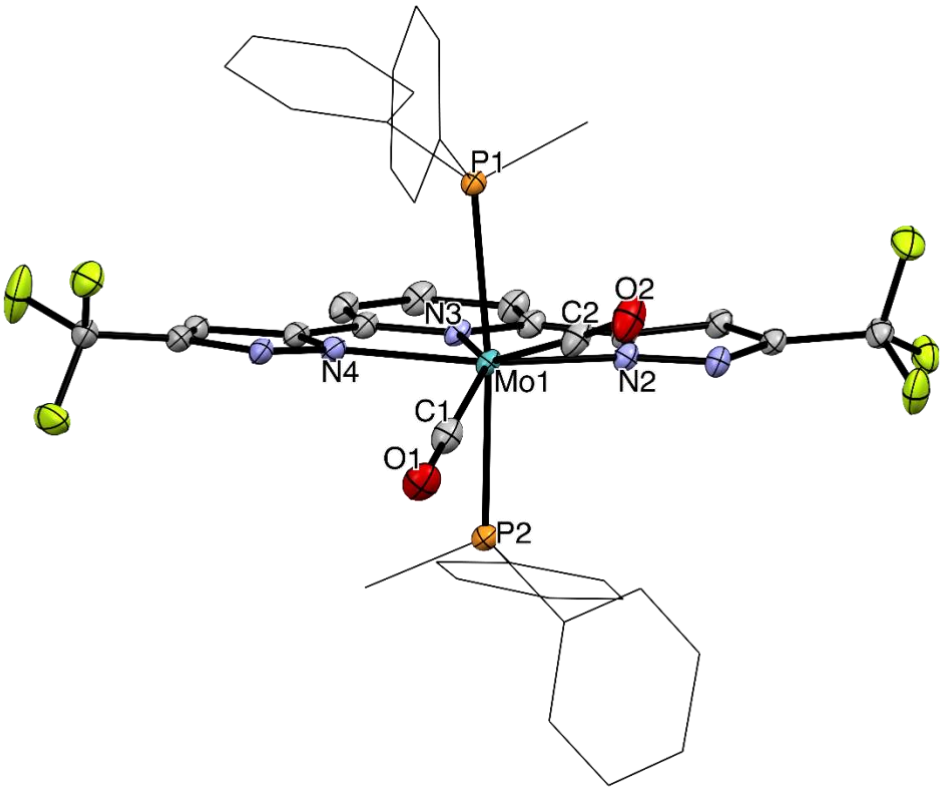

Figure S58. Solid-state structure of **4b** [Mo(L^{CF_3})(PPh_2Me)$_2$(CO)$_2$]. Ellipsoids are represented with 25% probability level. Hydrogen atoms have been omitted for clarity and phosphorus substituents appear as wireframe. Space group and selected bond distances (Å): $P2_1/n$; Mo-N2 2.171(2), Mo-N3 2.200(2), Mo-N4 2.162(2), Mo-P1 2.5131(8), Mo-P2 2.5226(8), Mo-C1 1.974(3), Mo-C2 1.979(3), C1-O1 1.159(3), C2-O2 1.168(4).

Crystal data

$C_{41}H_{31}F_6MoN_5O_2P_2$	$F(000)$ = 1816
M_r = 897.59	D_x = 1.554 Mg m^{-3}
Monoclinic, $P2_1/n$	
Hall symbol: -P 2yn	Cu $K\alpha$ radiation, λ = 1.54184 Å
a = 13.8694 (2) Å	Cell parameters from 38057 reflections
b = 17.5030 (2) Å	θ = 3.7–79.5°
c = 16.2883 (2) Å	μ = 4.22 mm^{-1}
β = 103.927 (1)°	T = 100 K
V = 3837.85 (9) Å^3	Parallelepiped, orange
Z = 4	0.10 × 0.05 × 0.02 mm

Data collection

XtaLAB Synergy, Dualflex, HyPix diffractometer	7276 independent reflections
Radiation source: micro-focus sealed X-ray tube, PhotonJet (Cu) X-ray Source	6704 reflections with $I > 2\sigma(I)$
Mirror monochromator	R_{int} = 0.048
Detector resolution: 10.0000 pixels mm^{-1}	θ_{max} = 70.1°, θ_{min} = 3.8°
	h = −15 16
Absorption correction: multi-scan CrysAlisPro 1.171.41.120a (Rigaku Oxford Diffraction, 2021) Empirical absorption correction using spherical harmonics, implemented in SCALE3 ABSPACK scaling algorithm.	k = −20 21
T_{min} = 0.817, T_{max} = 1.000	l = −19 19
64919 measured reflections	

Refinement

Refinement on F^2	
Least-squares matrix: full	Hydrogen site location: inferred from neighbouring sites
$R[F^2 > 2\sigma(F^2)]$ = 0.035	H-atom parameters constrained
$wR(F^2)$ = 0.092	$w = 1/[\sigma^2(F_o^2) + (0.0512P)^2 + 4.1491P]$ where $P = (F_o^2 + 2F_c^2)/3$
S = 1.03	$(\Delta/\sigma)_{max}$ = 0.002
7276 reflections	$\Delta\rho_{max}$ = 0.71 e Å^{-3}
516 parameters	$\Delta\rho_{min}$ = −0.87 e Å^{-3}
0 restraints	Extinction correction: none

4.3. XRD data for compound 5b

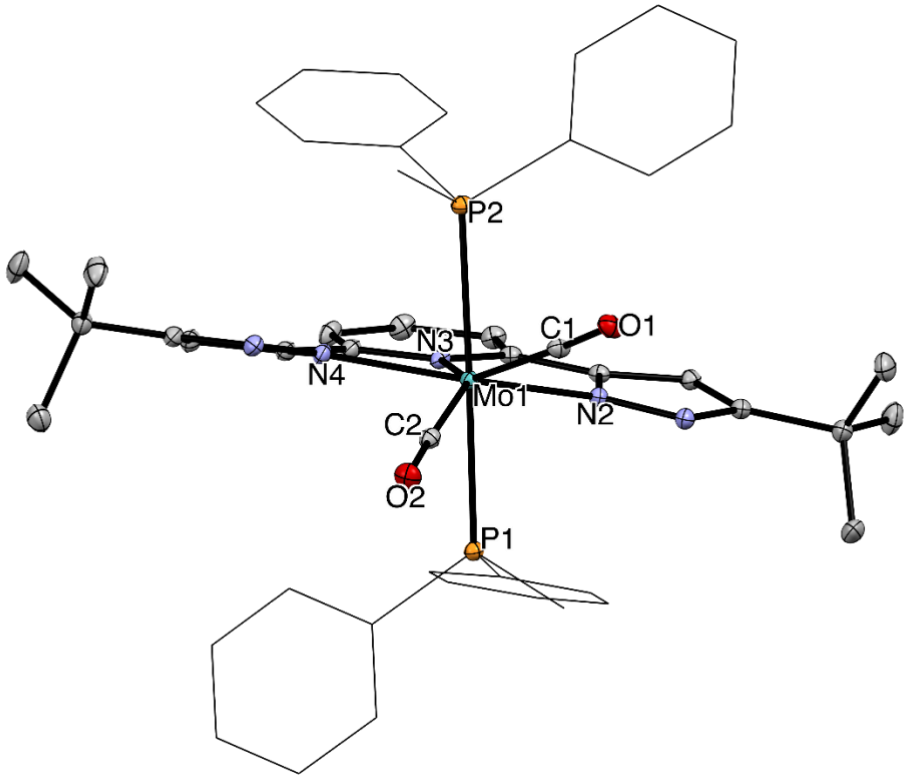

Figure S59. Solid-state structure of **5b** [Mo(L^{tBu})(PPh_2Me)$_2$(CO)$_2$]. Ellipsoids are represented with 25% probability level. Hydrogen atoms have been omitted for clarity and phosphorus substituents appear as wireframe. Two molecules are present in the asymmetric unit of this crystal (Z' = 2), only one is represented. Space group and selected bond distances (Å): Pbca; Mo-N2 2.173(1), Mo-N3 2.190(1), Mo-N4 2.168(1), Mo-P1 2.5218(7), Mo-P2 2.5372(7), Mo-C1 1.963(2), Mo-C2 1.980(2), C1-O1 1.152(2), C2-O2 1.147(2).

Crystal data

$C_{47}H_{49}MoN_5O_2P_2$	$F(000)$ = 3632
M_r = 873.83	D_x = 1.357 Mg m^{-3}
Orthorhombic, *Pbca*	Cu $K\alpha$ radiation, λ = 1.54184 Å
Hall symbol: -P 2ac 2ab	Cell parameters from 92810 reflections
a = 12.7581 (1) Å	θ = 3.0–79.8°
b = 22.8235 (2) Å	μ = 3.56 mm^{-1}
c = 29.3695 (2) Å	T = 100 K
V = 8551.94 (12) Å^3	Bloc, red
Z = 8	0.12 × 0.08 × 0.04 mm

Data collection

XtaLAB Synergy, Dualflex, HyPix diffractometer	9313 independent reflections
Radiation source: micro-focus sealed X-ray tube, PhotonJet (Cu) X-ray Source	8980 reflections with $I > 2\sigma(I)$
Mirror monochromator	R_{int} = 0.045

Detector resolution: 10.0000 pixels mm^{-1}	θ_{max} = 80.1°, θ_{min} = 3.0°
	h = −14 16
Absorption correction: multi-scan CrysAlisPro 1.171.41.120a (Rigaku Oxford Diffraction, 2021) Empirical absorption correction using spherical harmonics, implemented in SCALE3 ABSPACK scaling algorithm.	*k* = −29 29
T_{min} = 0.822, T_{max} = 1.000	*l* = −32 37
147625 measured reflections	

Refinement

Refinement on F^2	
Least-squares matrix: full	Hydrogen site location: inferred from neighbouring sites
$R[F^2 > 2\sigma(F^2)]$ = 0.028	H-atom parameters constrained
$wR(F^2)$ = 0.077	$w = 1/[\sigma^2(F_o^2) + (0.0431P)^2 + 5.656P]$ where $P = (F_o^2 + 2F_c^2)/3$
S = 1.08	$(\Delta/\sigma)_{max}$ = 0.003
9313 reflections	$\Delta\rho_{max}$ = 0.43 e Å^{-3}
522 parameters	$\Delta\rho_{min}$ = −0.69 e Å^{-3}
0 restraints	Extinction correction: none

4.4. XRD data for compound 6b

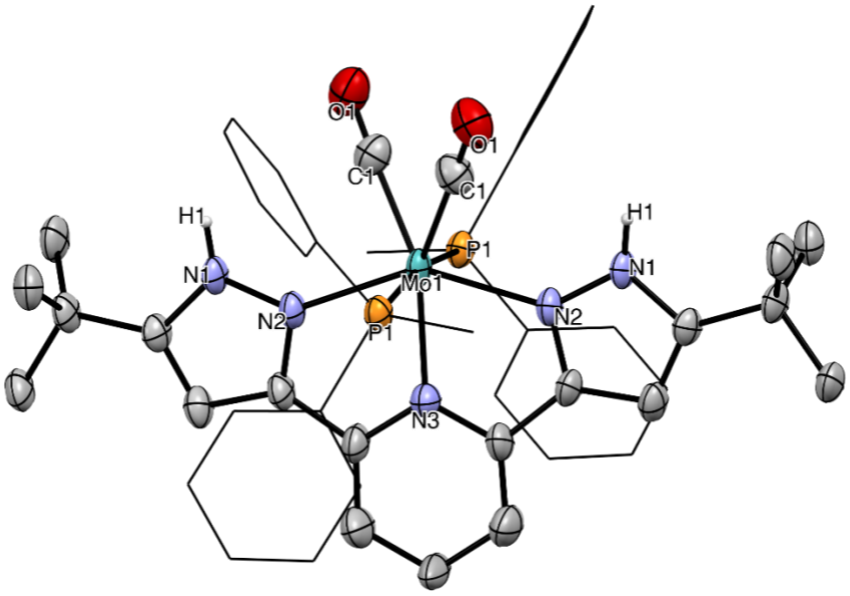

Figure S60. Solid-state structure of **6b** [(Mo(H_2L^{tBu})(PPh_2Me)$_2$(CO)$_2$)$^{2+}$ (2 OTf^-)]. Solid-state structure of **4b** [Mo(L^{CF_3})(PPh_2Me)$_2$(CO)$_2$]. Ellipsoids are represented with 25% probability level. Hydrogen atoms have been omitted for clarity (except the N(pyrazol)-H bonds) and phosphorus substituents appear as wireframe. The metrics are not usable because of the non-sufficient quality of the crystal.

Crystal data

$C_{47}H_{51}MoN_5O_2P_2 \cdot 2(CF_3O_3S)$	
M_r = 1173.98	D_x = 1.361 Mg m^{-3}
Monoclinic, *C*2/*c*	
Hall symbol: -C 2yc	Cu *K*α radiation, λ = 1.54184 Å
a = 22.4003 (7) Å	Cell parameters from 22700 reflections
b = 10.8477 (5) Å	θ = 3.8–74.6°
c = 23.697 (1) Å	μ = 3.70 mm^{-1}
β = 95.741 (3)°	*T* = 100 K
V = 5729.3 (4) Å^3	Parallelepiped, yellow
Z = 4	0.20 × 0.07 × 0.03 mm
F(000) = 2408	

Data collection

XtaLAB Synergy, Dualflex, HyPix diffractometer	5995 independent reflections
Radiation source: micro-focus sealed X-ray tube, PhotonJet (Cu) X-ray Source	3335 reflections with $I > 2.0\sigma(I)$
Mirror monochromator	R_{int} = 0.151
Detector resolution: 10.0000 pixels mm^{-1}	θ_{max} = 57.6°, θ_{min} = 3.8°
ϕ & ω scans	*h* = −28 25
Absorption correction: multi-scan CrysAlisPro 1.171.42.102a (Rigaku OD, 2023)	*k* = −13 13
T_{min} = 0.46, T_{max} = 0.89	*l* = −29 30
81801 measured reflections	

Refinement

Refinement on F^2	
Least-squares matrix: full	Hydrogen site location: difference Fourier map
$R[F^2 > 2\sigma(F^2)]$ = 0.103	H atoms treated by a mixture of independent and constrained refinement
$wR(F^2)$ = 0.312	Method = Modified Sheldrick $w = 1/[\sigma^2(F^2) + (0.2P)^2 + 0.0P]$, where $P = (\max(F_o^2,0) + 2F_c^2)/3$
S = 1.42	$(\Delta/\sigma)_{max}$ = 0.001
3919 reflections	$\Delta\rho_{max}$ = 2.37 e Å^{-3}
335 parameters	$\Delta\rho_{min}$ = −0.89 e Å^{-3}
4 restraints	Extinction correction: None

4.5. XRD data for compound 4c

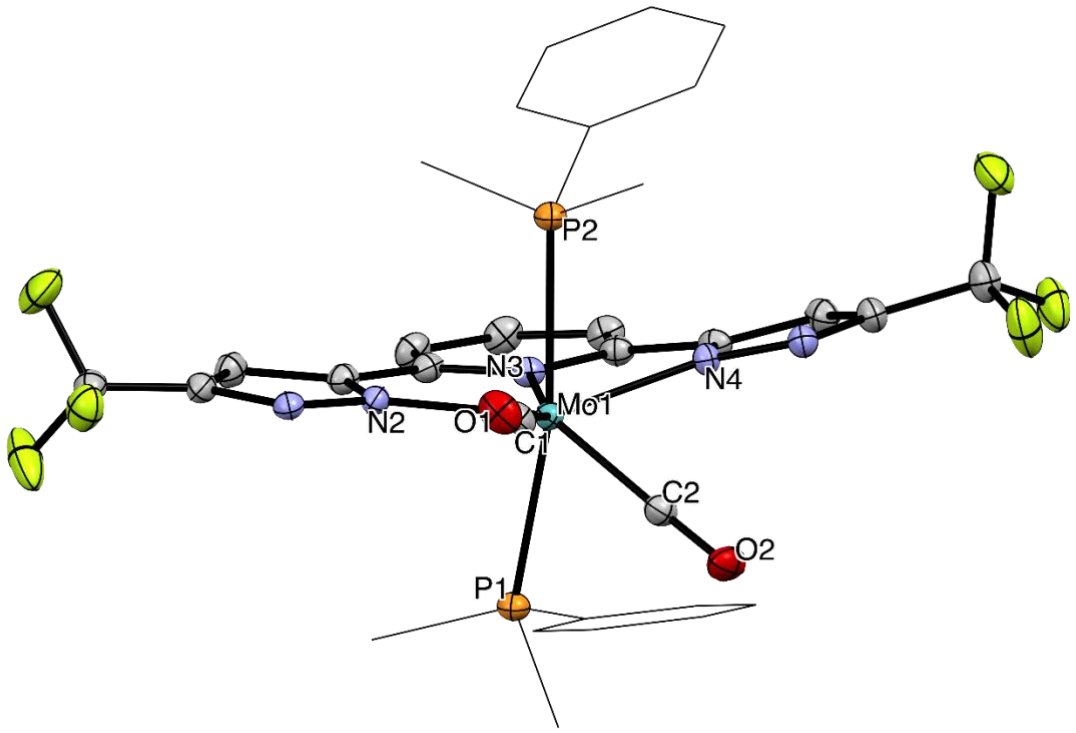

Figure S61. Solide-state structure of **4c** [Mo(L^{CF_3})($PPhMe_2$)$_2$(CO)$_2$]. Ellipsoids are represented with 25% probability level. Hydrogen atoms have been omitted for clarity and phosphorus substituents appear as wireframe. Space group and selected bond distances (Å): $P2_1/c$; Mo-N2 2.178(2), Mo-N3 2.192(2), Mo-N4 2.180(2), Mo-P1 2.5540(7), Mo-P2 2.5190(7), Mo-C1 1.970(3), Mo-C2 1.971(3), C1-O1 1.144(4), C2-O2 1.151(4)

Crystal data

$C_{31}H_{27}F_6MoN_5O_2P_2 \cdot C_4H_8O$	$F(000)$ = 1720
M_r = 845.57	D_x = 1.521 Mg m^{-3}
Monoclinic, $P2_1/c$	
Hall symbol: -P 2ybc	Cu $K\alpha$ radiation, λ = 1.54184 Å
a = 18.27310 (11) Å	Cell parameters from 38640 reflections
b = 10.97842 (8) Å	θ = 4.6–78.9°
c = 18.42521 (12) Å	μ = 4.36 mm^{-1}
β = 92.3005 (6)°	T = 100 K
V = 3693.30 (4) Å^3	Platelet, yellow
Z = 4	0.15 × 0.10 × 0.02 mm

Data collection

XtaLAB Synergy, Dualflex, HyPix diffractometer	7972 independent reflections
Radiation source: micro-focus sealed X-ray tube, PhotonJet (Cu) X-ray Source	7295 reflections with $I > 2.0\sigma(I)$
Mirror monochromator	R_{int} = 0.059

Detector resolution: 10.0000 pixels mm^{-1}	θ_{max} = 80.5°, θ_{min} = 4.7°
ω/2θ scans	*h* = −23 23
Absorption correction: multi-scan CrysAlisPro 1.171.42.102a (Rigaku OD, 2023)	*k* = −13 10
T_{min} = 0.50, T_{max} = 0.92	*l* = −22 23
70434 measured reflections	

Refinement

Refinement on F^2	
Least-squares matrix: full	Hydrogen site location: difference Fourier map
$R[F^2 > 2\sigma(F^2)]$ = 0.041	H-atom parameters not refined
$wR(F^2)$ = 0.120	Method = Modified Sheldrick $w = 1/[\sigma^2(F^2) + (0.09P)^2 + 3.76P]$, where $P = (\max(F_o^2,0) + 2F_c^2)/3$
S = 0.95	$(\Delta/\sigma)_{max}$ = 0.001
7972 reflections	$\Delta\rho_{max}$ = 0.65 e $Å^{-3}$
469 parameters	$\Delta\rho_{min}$ = −1.09 e $Å^{-3}$
0 restraints	Extinction correction: None

4.6. XRD data for compound 5c

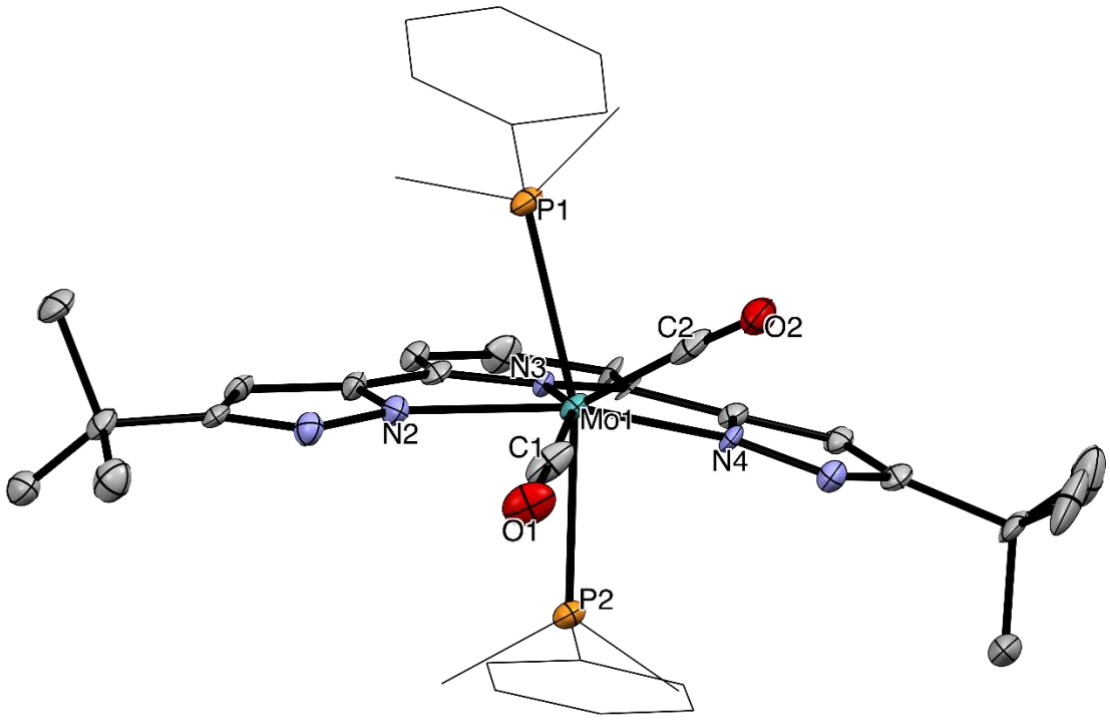

Figure S62. Solide-state structure of **5c** [Mo(L^{tBu})($PPhMe_2$)$_2$(CO)$_2$]. Ellipsoids are represented with 25% probability level. Hydrogen atoms have been omitted for clarity and phosphorus substituents appear as wireframe. The metrics are not usable because of the non-sufficient quality of the crystal.

Crystal data

$C_{74}H_{90}Mo_2N_{10}O_4P_4$	$F(000)$ = 1560
M_r = 1499.37	
Triclinic, P-1	D_x = 1.376 Mg m^{-3}
Hall symbol: - P 1	M
a = 11.4341 (9) Å	Cu $K\alpha$ radiation, λ = 1.54184 Å
b = 14.8708 (5) Å	Cell parameters from 9552 reflections
c = 21.8140 (4) Å	θ = 4.0–72.9°
α = 90.044 (2)°	μ = 4.11 mm^{-1}
β = 102.445 (5)°	T = 100 K
γ = 92.558 (6)°	Platelet, yellow
V = 3618.2 (3) Å^3	0.10 × 0.06 × 0.02 mm
Z = 2	

Data collection

XtaLAB Synergy, Dualflex, HyPix diffractometer	14028 independent reflections
Radiation source: micro-focus sealed X-ray tube, PhotonJet (Cu) X-ray Source	8187 reflections with $I > 2.0\sigma(I)$
Mirror monochromator	R_{int} = 0.105
Detector resolution: 10.0000 pixels mm^{-1}	θ_{max} = 74.8°, θ_{min} = 3.0°
φ & ω scans	h = −11 14
Absorption correction: multi-scan CrysAlisPro 1.171.42.102a (Rigaku Oxford Diffraction, 2023)	k = −18 18
T_{min} = 0.63, T_{max} = 0.92	l = −26 27
43928 measured reflections	

Refinement

Refinement on F^2	
Least-squares matrix: full	Hydrogen site location: difference Fourier map
$R[F^2 > 2\sigma(F^2)]$ = 0.106	H-atom parameters not refined
$wR(F^2)$ = 0.313	Method = Modified Sheldrick $w = 1/[\sigma^2(F^2) + (0.19P)^2 + 81.22P]$, where $P = (\max(F_o^2,0) + 2F_c^2)/3$
S = 0.79	$(\Delta/\sigma)_{max}$ = 0.0003
12287 reflections	$\Delta\rho_{max}$ = 4.68 e Å^{-3}
848 parameters	$\Delta\rho_{min}$ = −2.10 e Å^{-3}
14 restraints	Extinction correction: None

5. Electrochemistry

Voltammetric measurements were carried out with a potentiostat Autolab PGSTAT100. Experiments were performed at room temperature in a homemade airtight three–electrode cell connected to a vacuum/argon line. The reference electrode was a saturated calomel electrode (SCE) separated from the solution by a bridge compartment. The counter electrode was a platinum wire of 1 cm^2 apparent surface. The working electrode was a glassy carbon disk (1 mm diameter). The supporting electrolyte ($nBu_4N)[PF_6]$ (Supelco, 99% puriss electrochemical grade) was dried and degassed under argon prior to use. THF (HPLC grade) was dried by passing through an activated alumina column under argon prior to use. The solutions used during the electrochemical studies were typically 0.1 M in supporting electrolyte and 10^{-3} $mol{\cdot}L^{-1}$ in analyte. Parameters for square wave voltammetry: modulation amplitude 20 mV, frequency 20 Hz, step potential 5 mV or 0.1 V/s. Before each measurement, the solutions were degassed by bubbling Ar and the working electrode was polished with a polishing machine (Presi P230). In these conditions, the half-wave potential of ferrocene is : $E_{1/2}(Fc^+/Fc)$ = 0.550 V *vs*. SCE.

5.1. Ligand L^{CF_3}

5.1.1. Cyclic Voltammetry

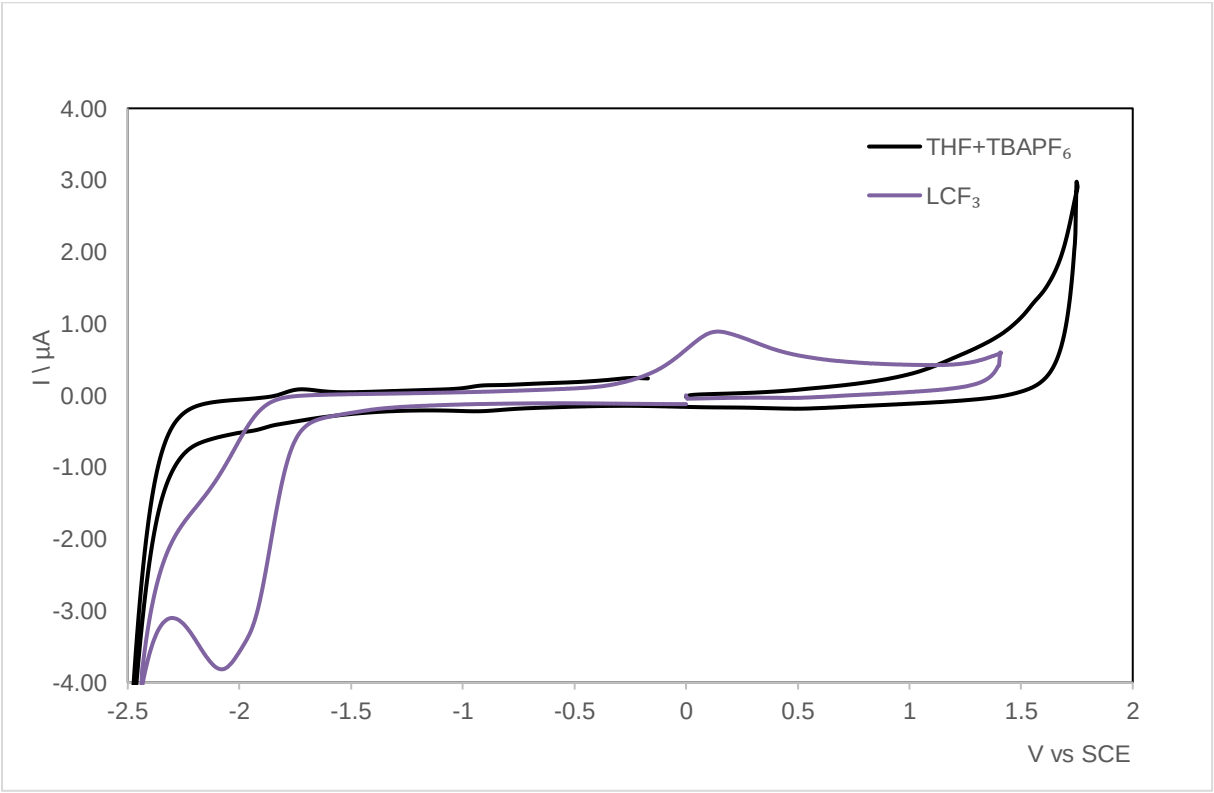

Figure S63. Cyclic voltammogram of $\mathbf{L^{CF_3}}$ in THF (0.10 M $TBAPF_6$, GC working electrode), scan rate 0.2 V/s, room temperature, initial scan: OCP going from about cathodic potential.

5.1.2. Square wave Voltammetry

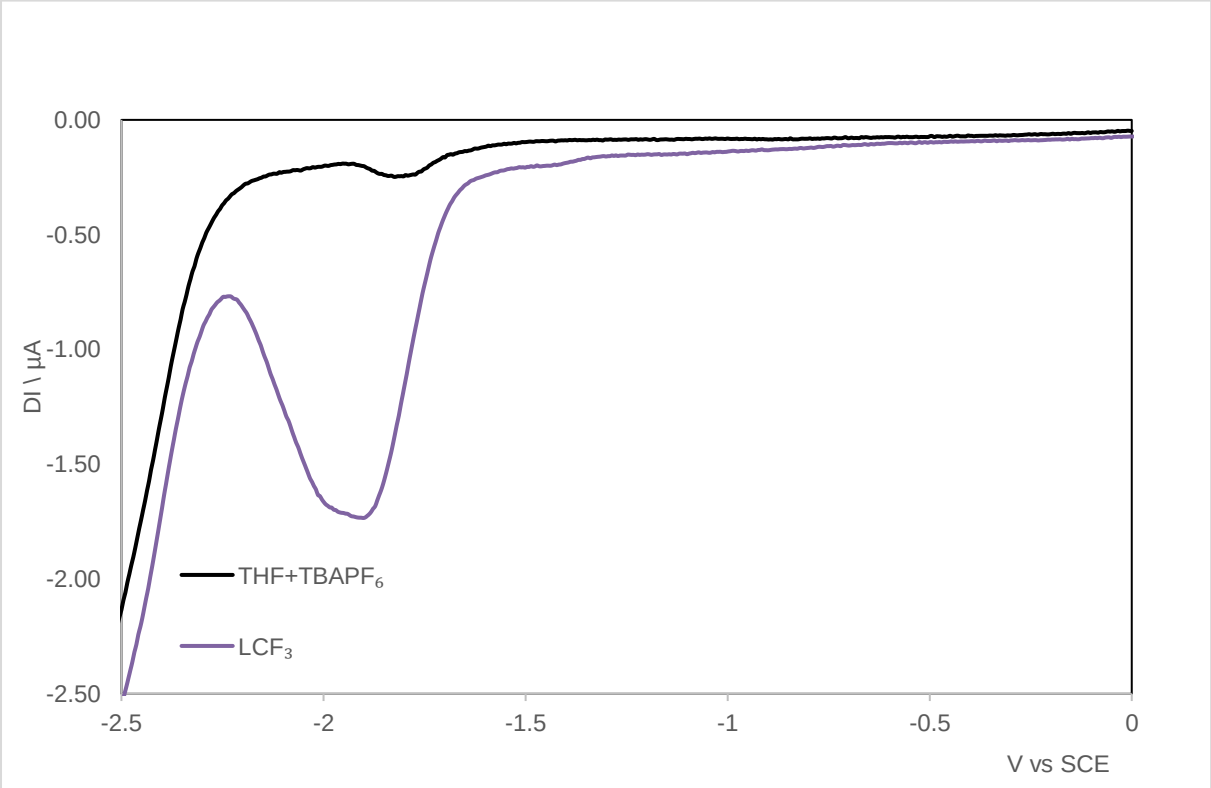

Figure S64. Cathodic square wave voltammogram (0.1 M TBA[PF_6] / THF, *v* = 0.1 V/s, r.t.) of $\mathbf{L^{CF_3}}$.

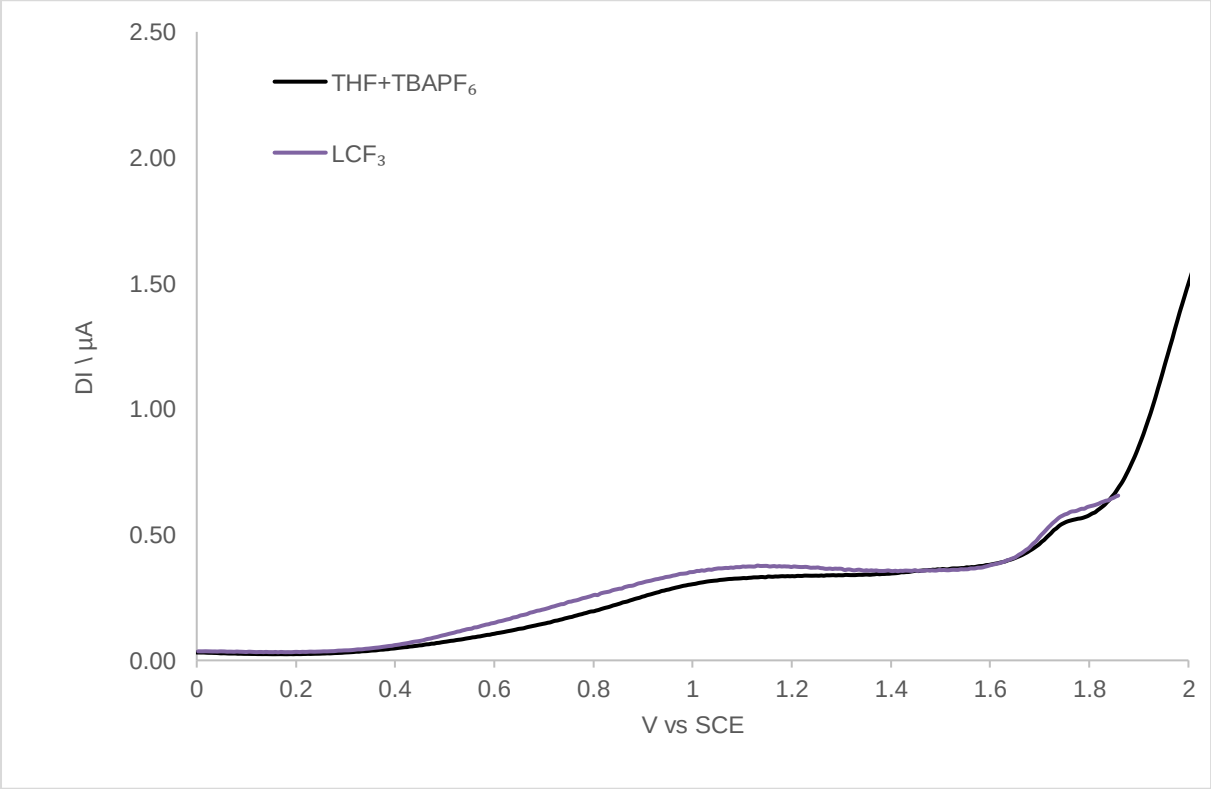

Figure S65. Anodic square wave voltammogram (0.1 M TBA[PF_6] / THF, *v* = 0.1 V/s, r.t.) of $\mathbf{L^{CF_3}}$.

5.2. Ligand L^{tBu}

5.2.1. Cyclic voltammetry

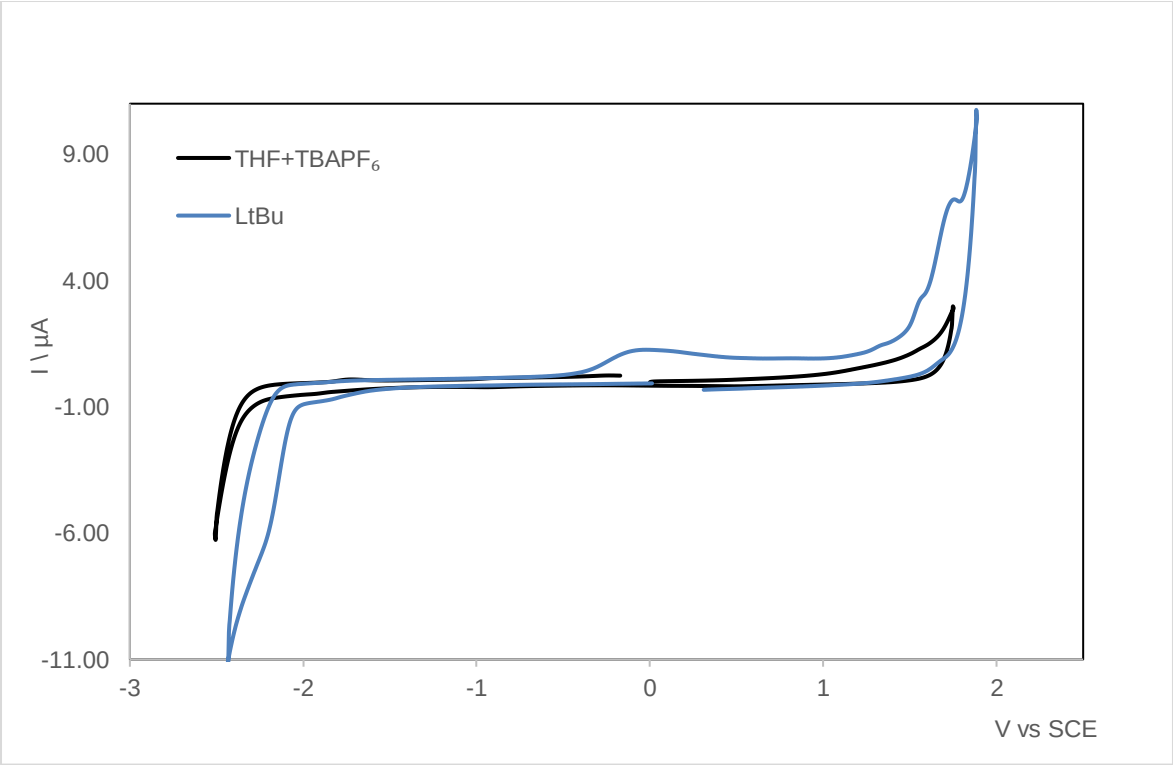

Figure S66. Cyclic voltammogram of L^{tBu} in THF (0.10 M TBA[PF_6], GC working electrode), scan rate 0.2 V/s, room temperature, initial scan: OCP going from about cathodic potential..

5.2.2. Square wave voltammetry

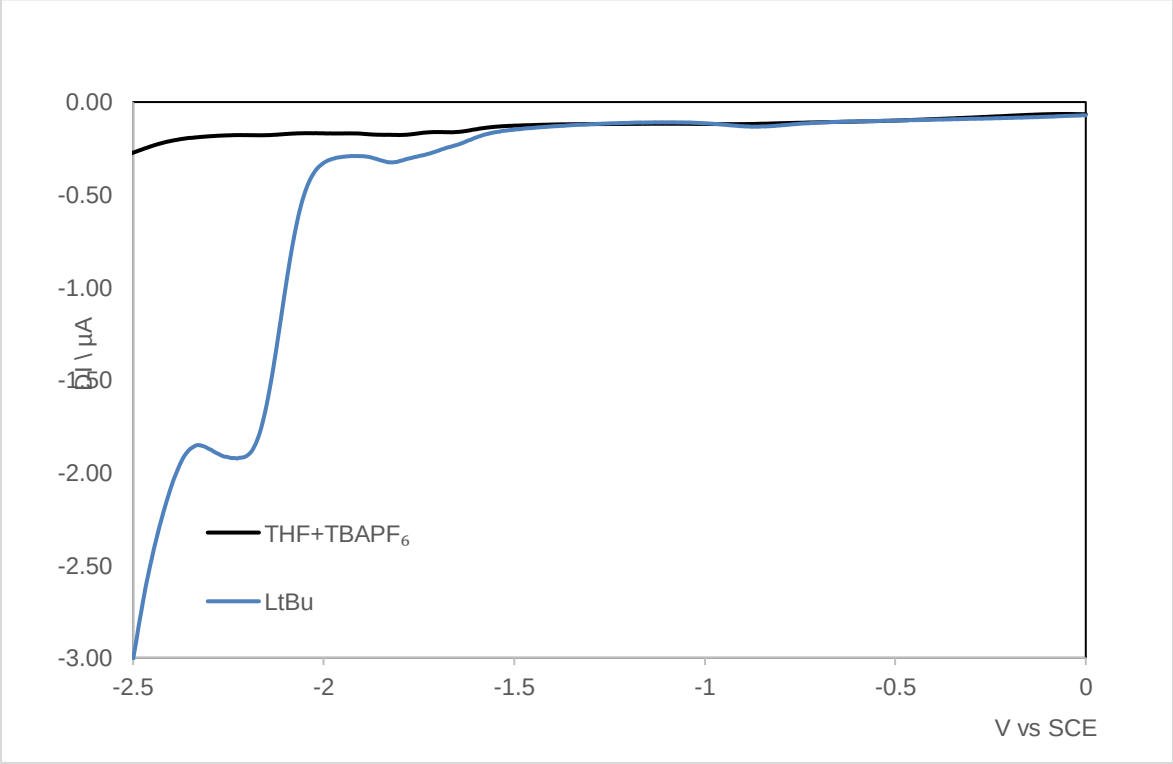

Figure S67. Cathodic square wave voltammogram (0.1 M TBA[PF_6] / THF, *v* = 0.1 V/s, r.t.) of L^{tBu}.

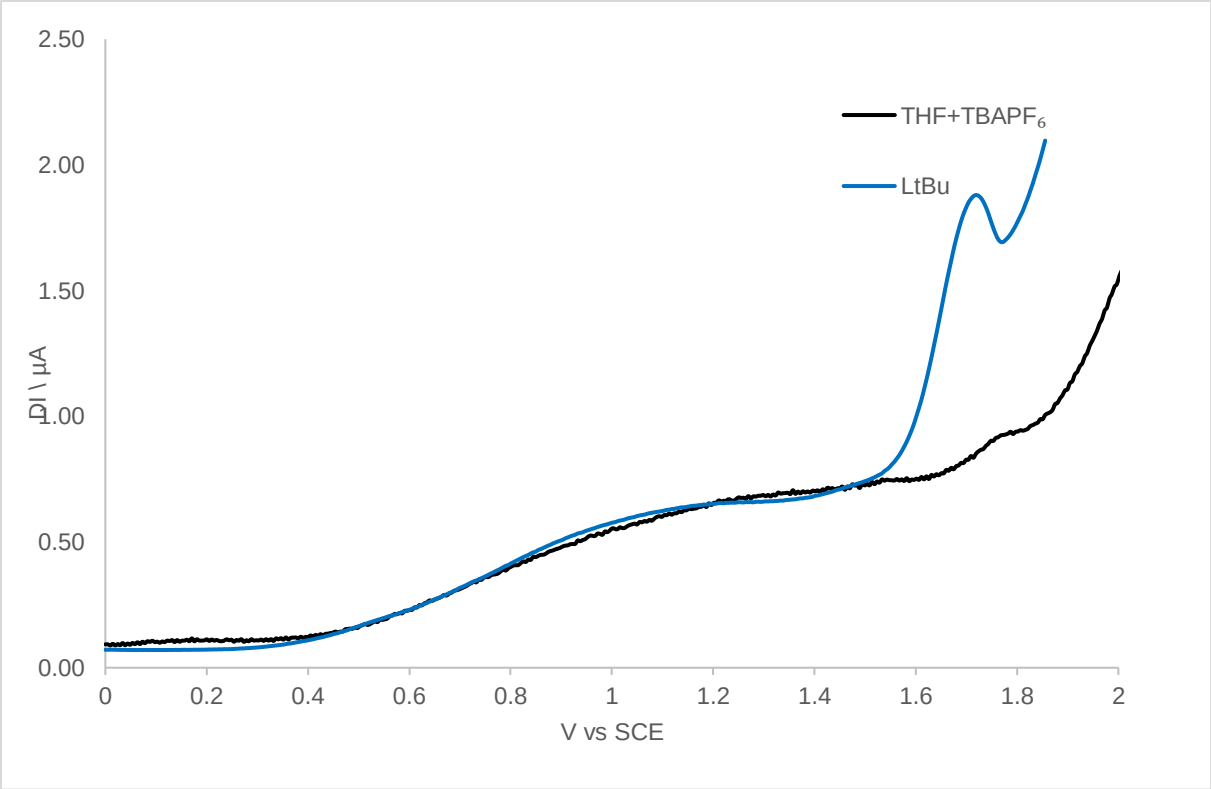

Figure S68. Anodic square wave voltammogram (0.1 M TBA[PF_6] / THF, *v* = 0.1 V/s, r.t.) of **L^{tBu}**.

5.3. Compound 4a

5.3.1. Cyclic Voltammetry

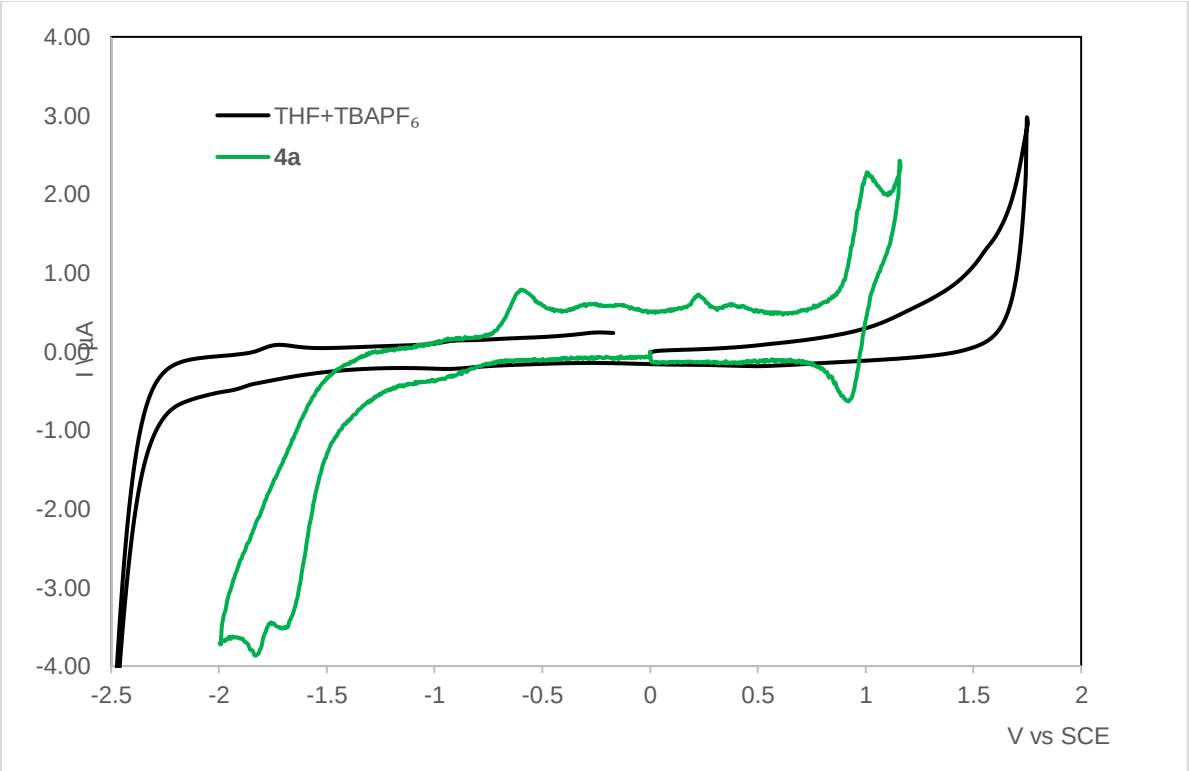

Figure S69. Cyclic voltammogram of **4a** in THF (0.10 M $TBAPF_6$, GC working electrode), scan rate 0.2 V/s, room temperature, initial scan: OCP going from about cathodic potential.

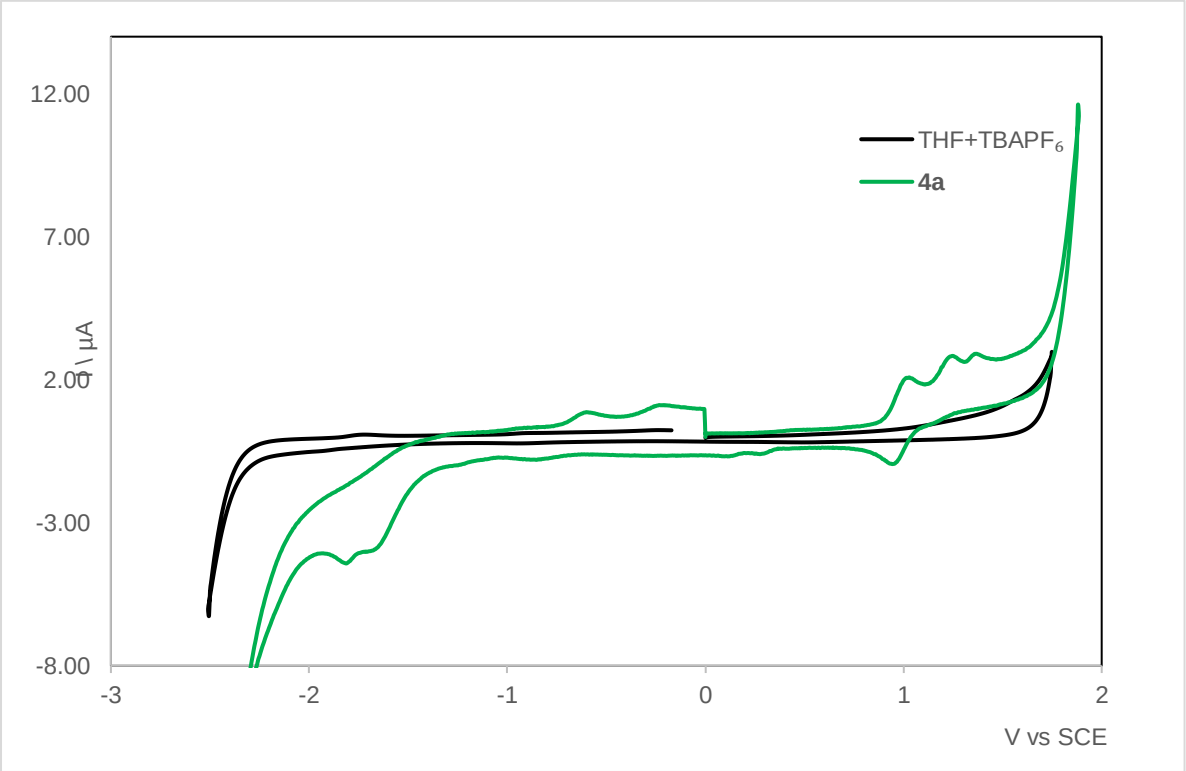

Figure S70. Cyclic voltammogram of **4a** in THF (0.10 M $TBAPF_6$, GC working electrode), scan rate 0.2 V/s, room temperature, initial scan: OCP going from about anodic potential.

5.3.2. *Square wave voltammetry*

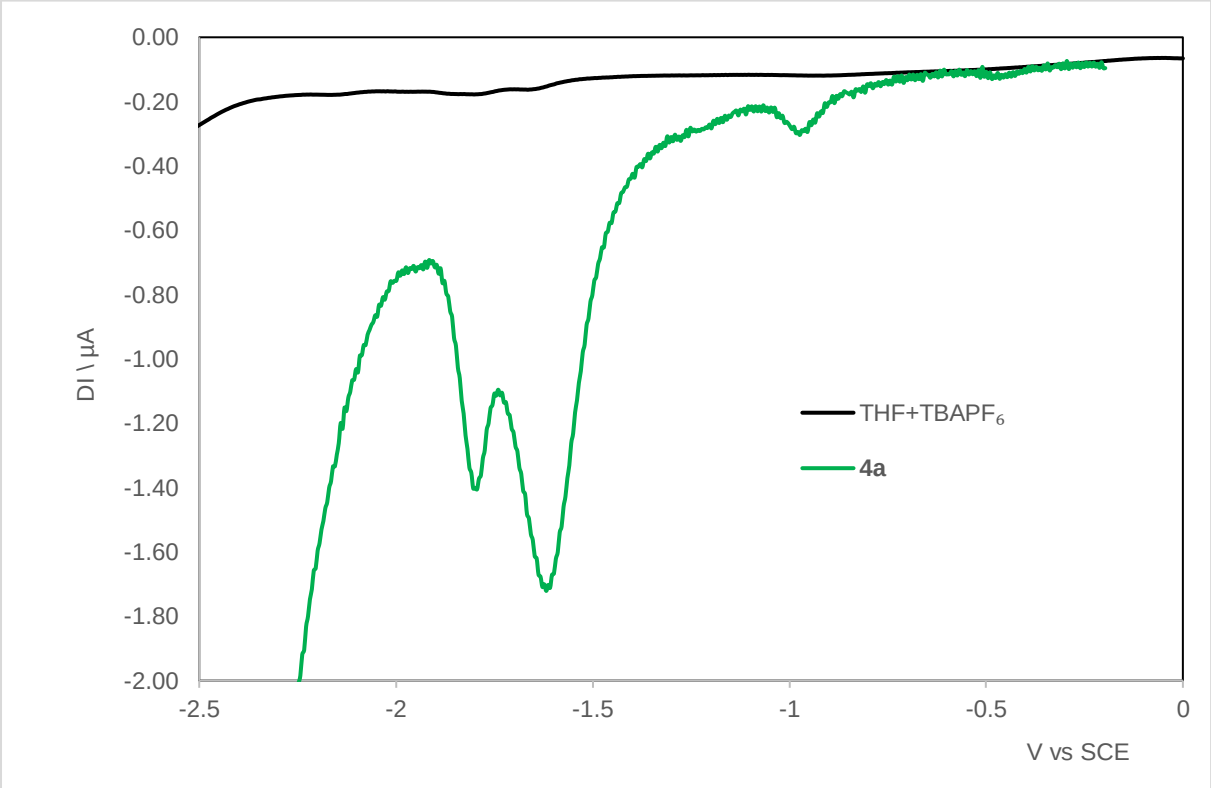

Figure S71. Cathodic square wave voltammogram (0.1 M TBA[PF_6] / THF, *v* = 0.1 V/s, r.t.) of **4a**.

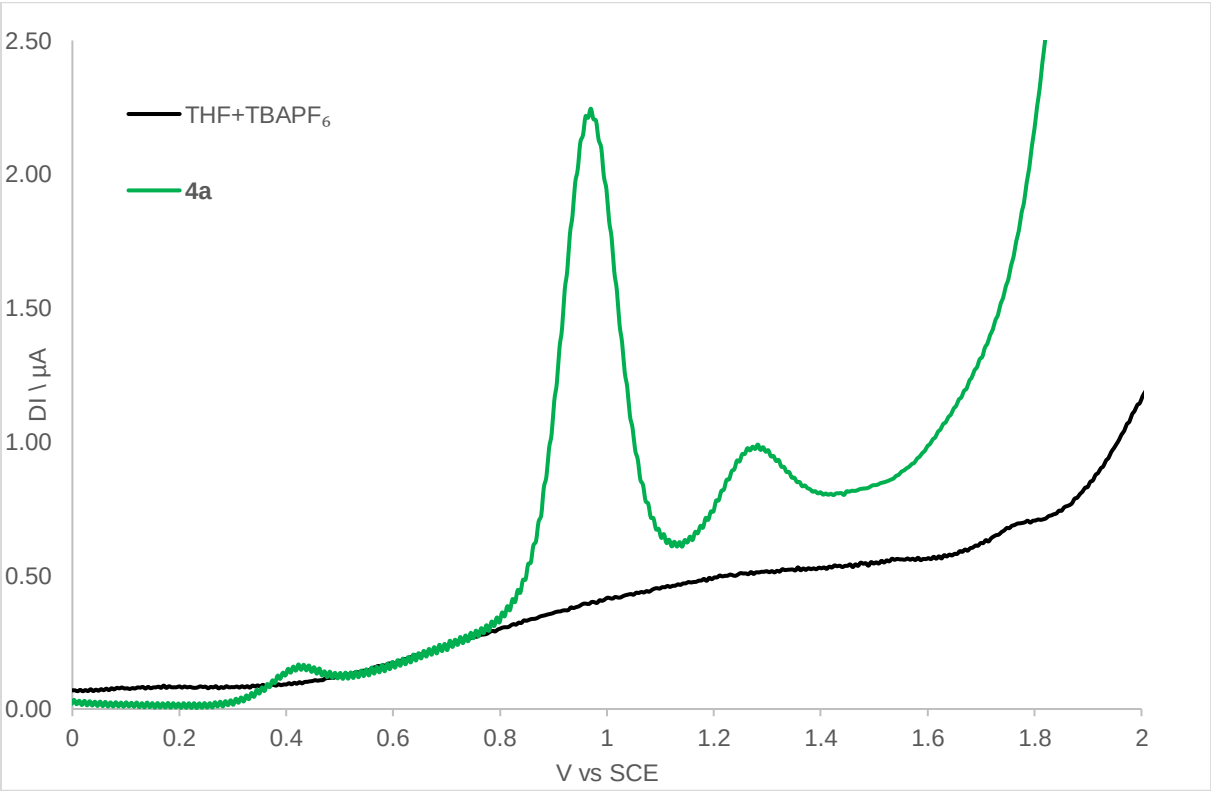

Figure S72. Anodic square wave voltammogram (0.1 M TBA[PF_6] / THF, *v* = 0.1 V/s, r.t.) of **4a**.

5.4. Compound 4b

5.4.1. Cyclic Voltammetry

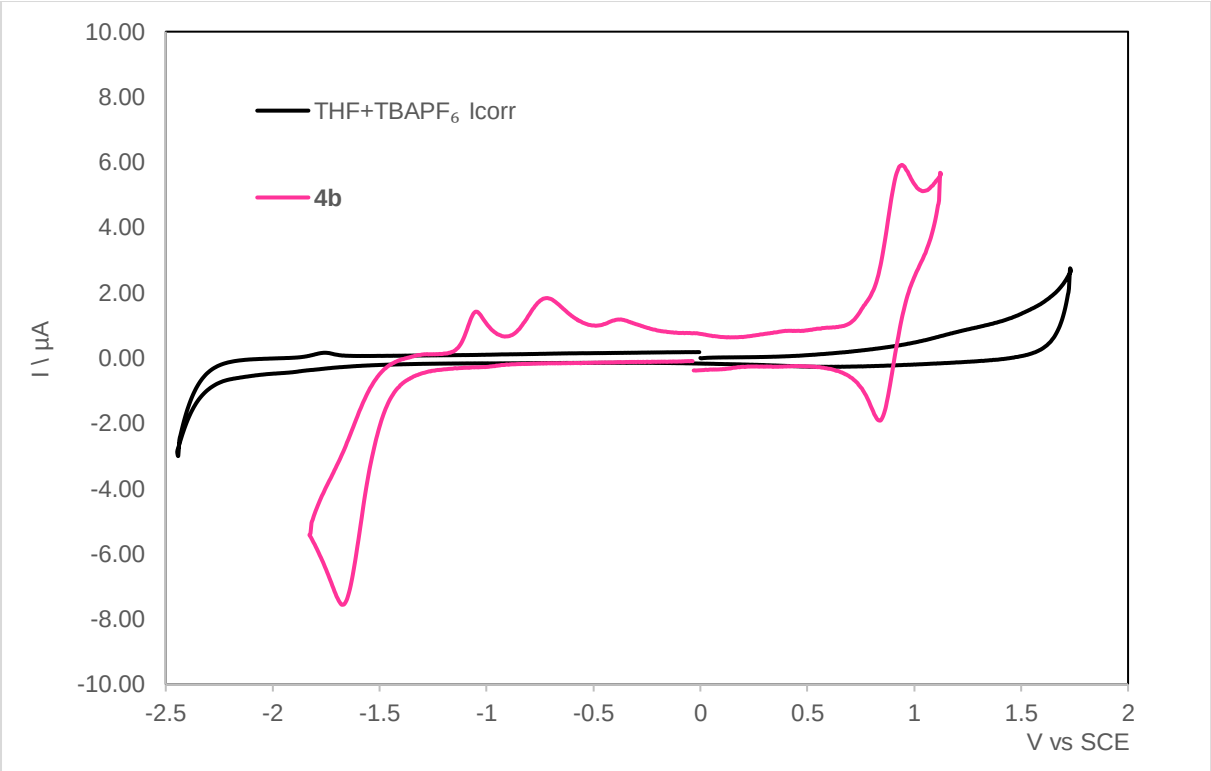

Figure S73. Cyclic voltammogram of **4b** in THF (0.10 M $TBAPF_6$, GC working electrode), scan rate 0.2 V/s, room temperature, initial scan: OCP going from about cathodic potential.

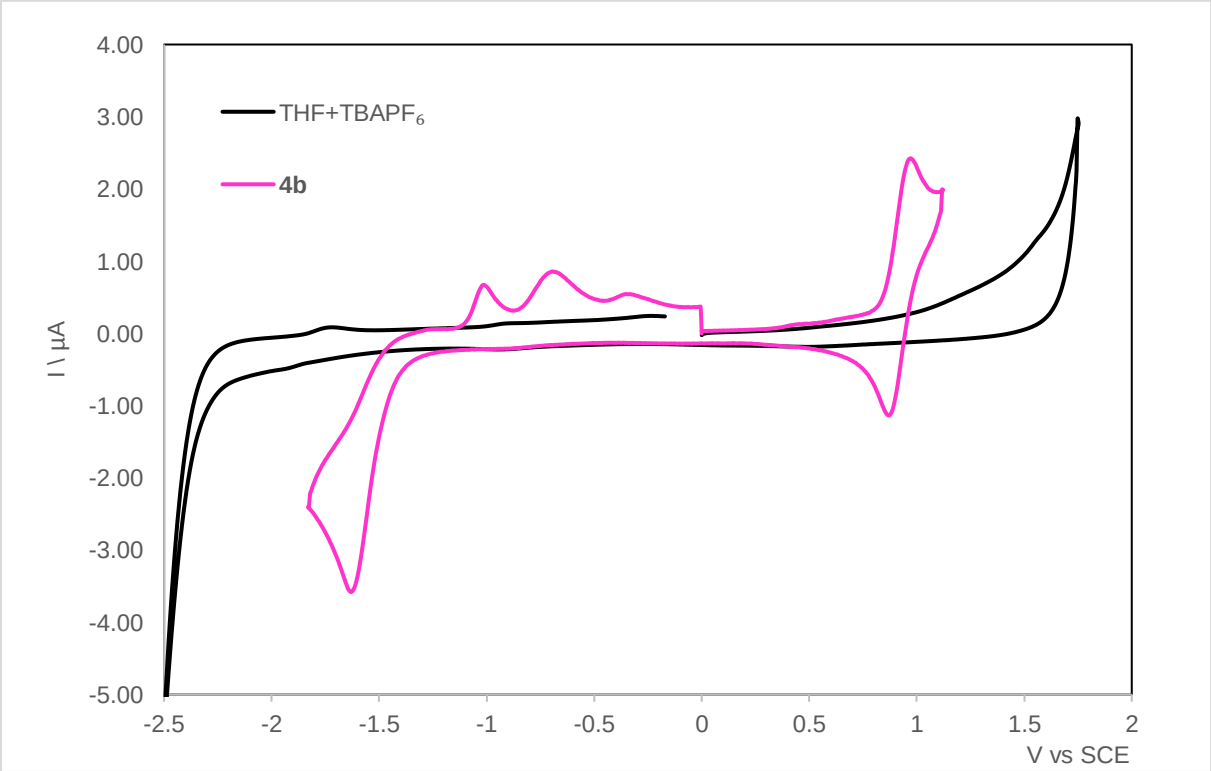

Figure S74. Cyclic voltammogram of **4b** in THF (0.10 M $TBAPF_6$, GC working electrode), scan rate 0.2 V/s, room temperature, initial scan: OCP going from about anodic potential.

5.4.2. *Square wave voltammetry*

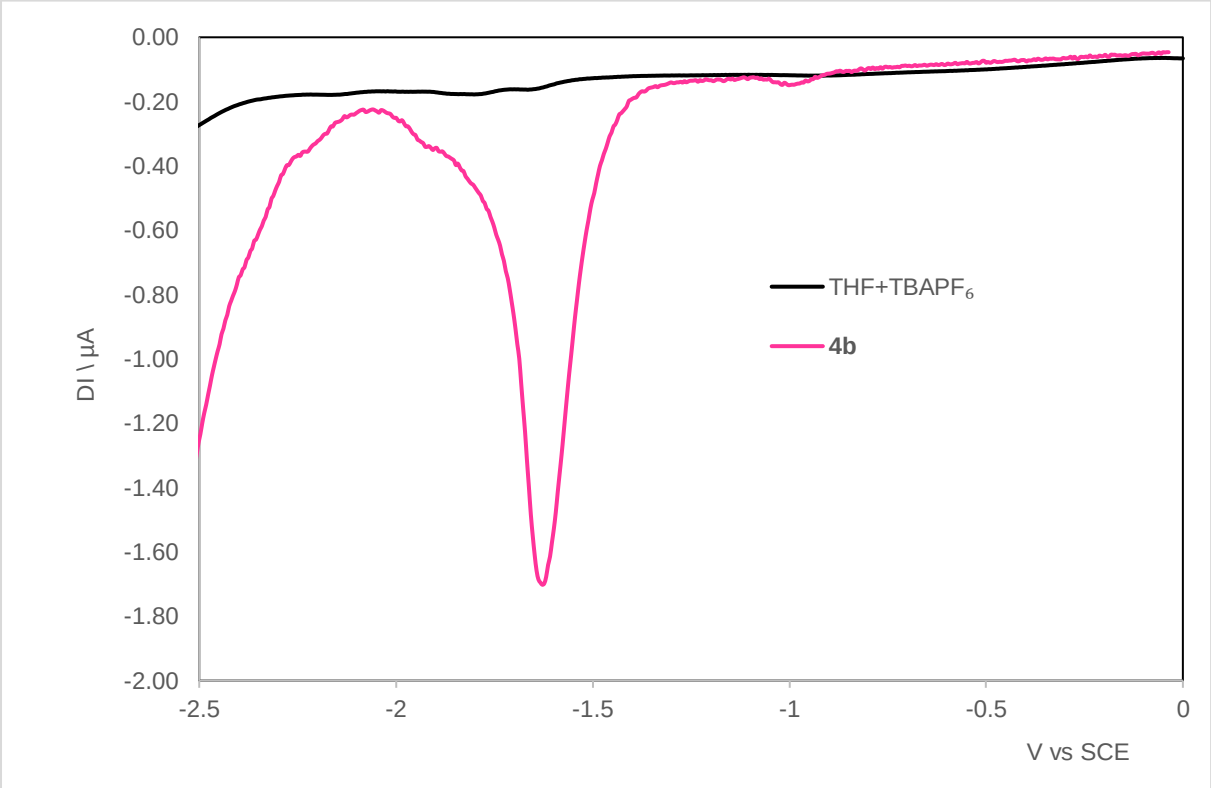

Figure S75. Cathodic square wave voltammogram (0.1 M TBA[PF_6] / THF, *v* = 0.1 V/s, r.t.) of **4b**.

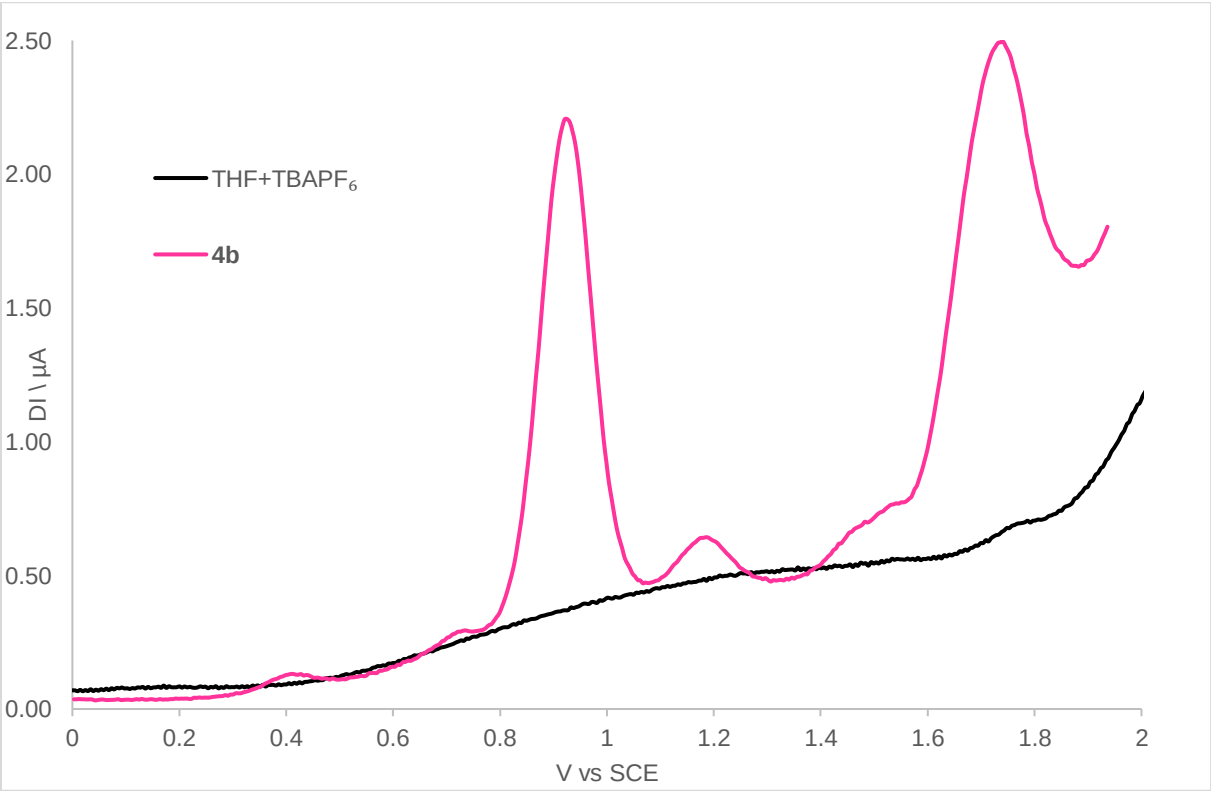

Figure S76. Anodic square wave voltammogram (0.1 M TBA[PF_6] / THF, *v* = 0.1 V/s, r.t.) of **4b**.

5.5. Compound 5b

5.5.1. Cyclic voltammetry

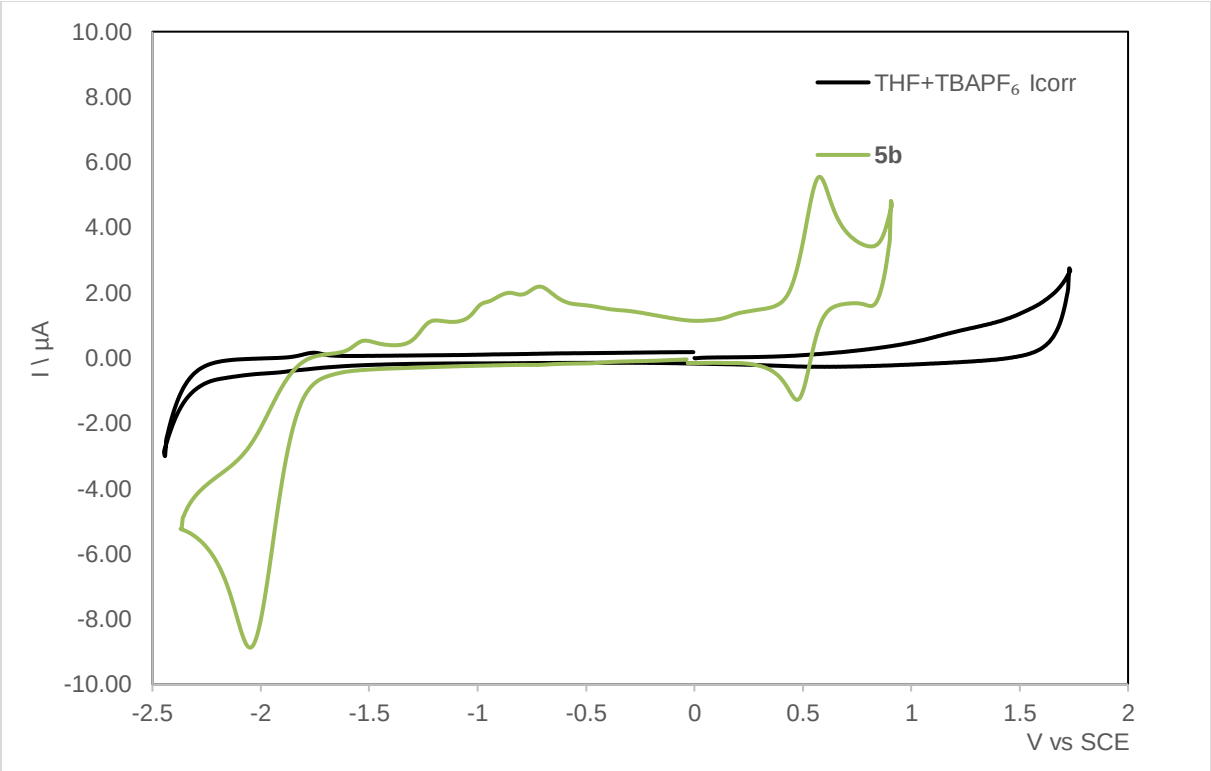

Figure S77. Cyclic voltammogram of **5b** in THF (0.10 M $TBAPF_6$, GC working electrode), scan rate 0.2 V/s, room temperature, initial scan: OCP going from about cathodic potential.

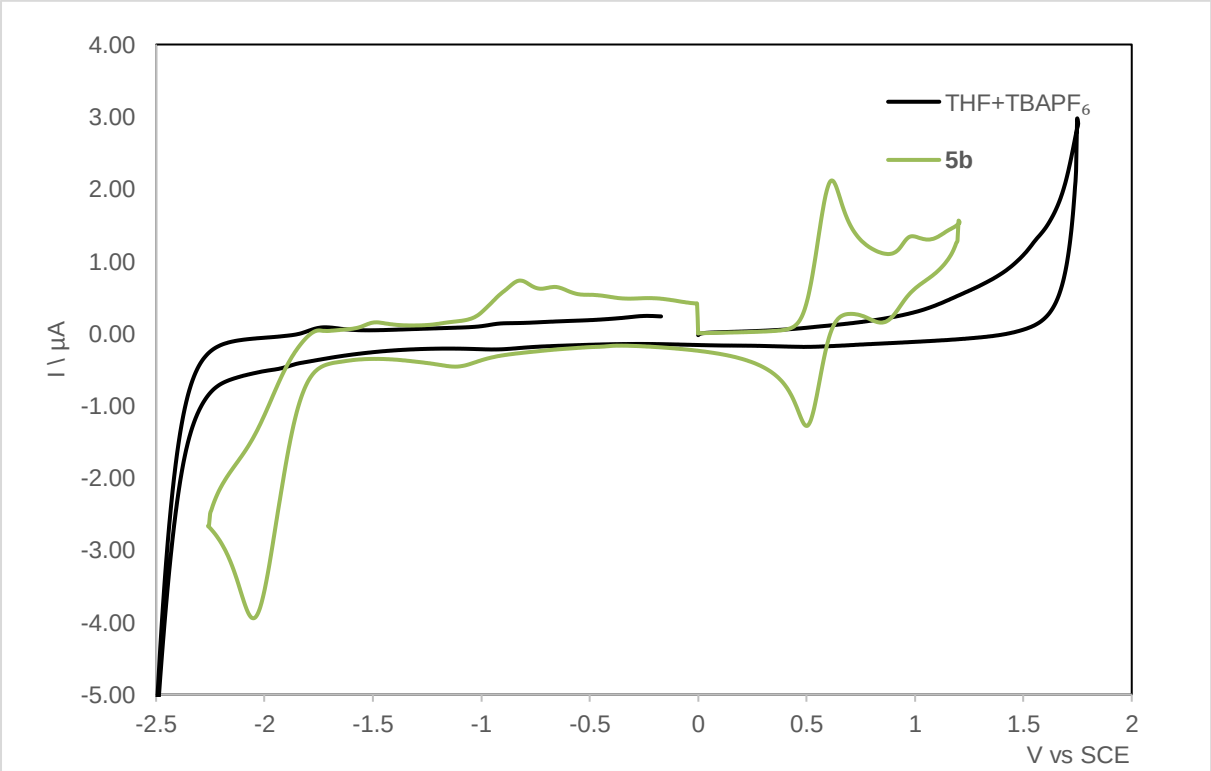

Figure S78. Cyclic voltammogram of **5b** in THF (0.10 M $TBAPF_6$, GC working electrode), scan rate 0.2 V/s, room temperature, initial scan: OCP going from about anodic potential.

5.5.2. *Square wave voltammetry*

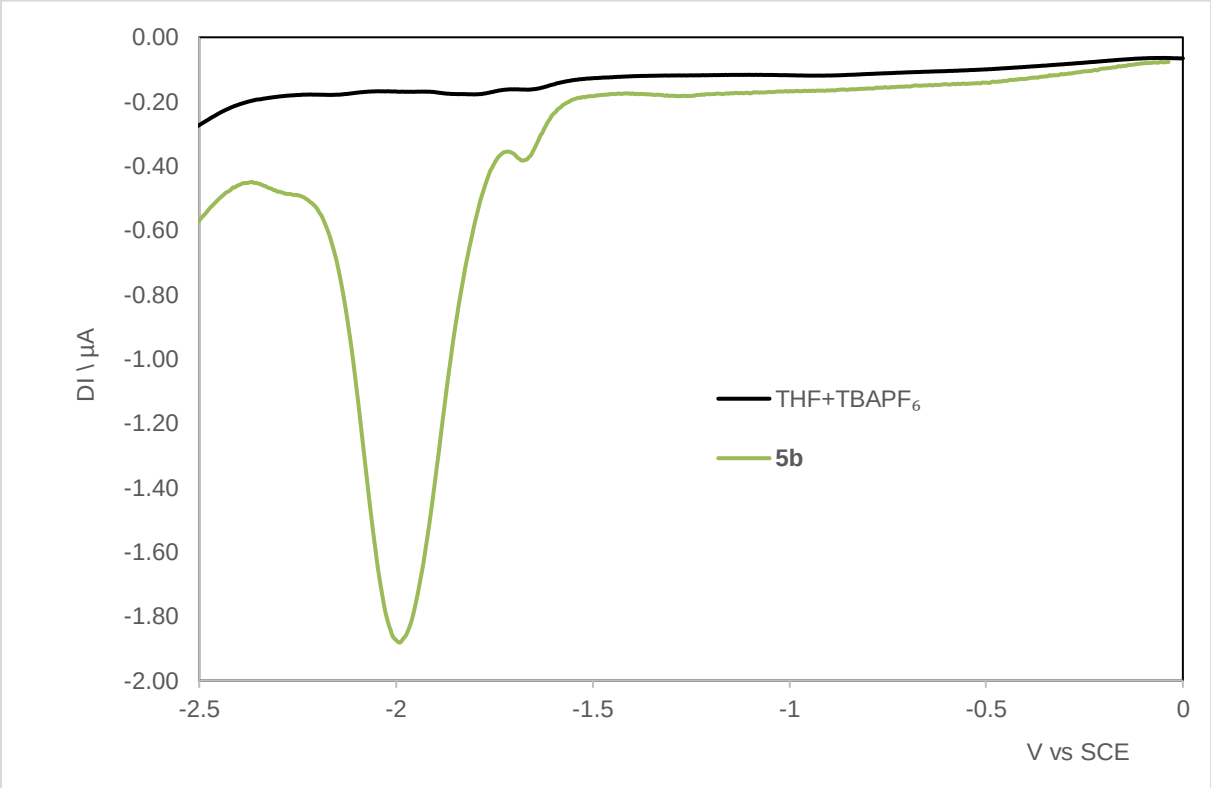

Figure S79. Cathodic square wave voltammogram (0.1 M TBA[PF_6] / THF, *v* = 0.1 V/s, r.t.) of **5b**.

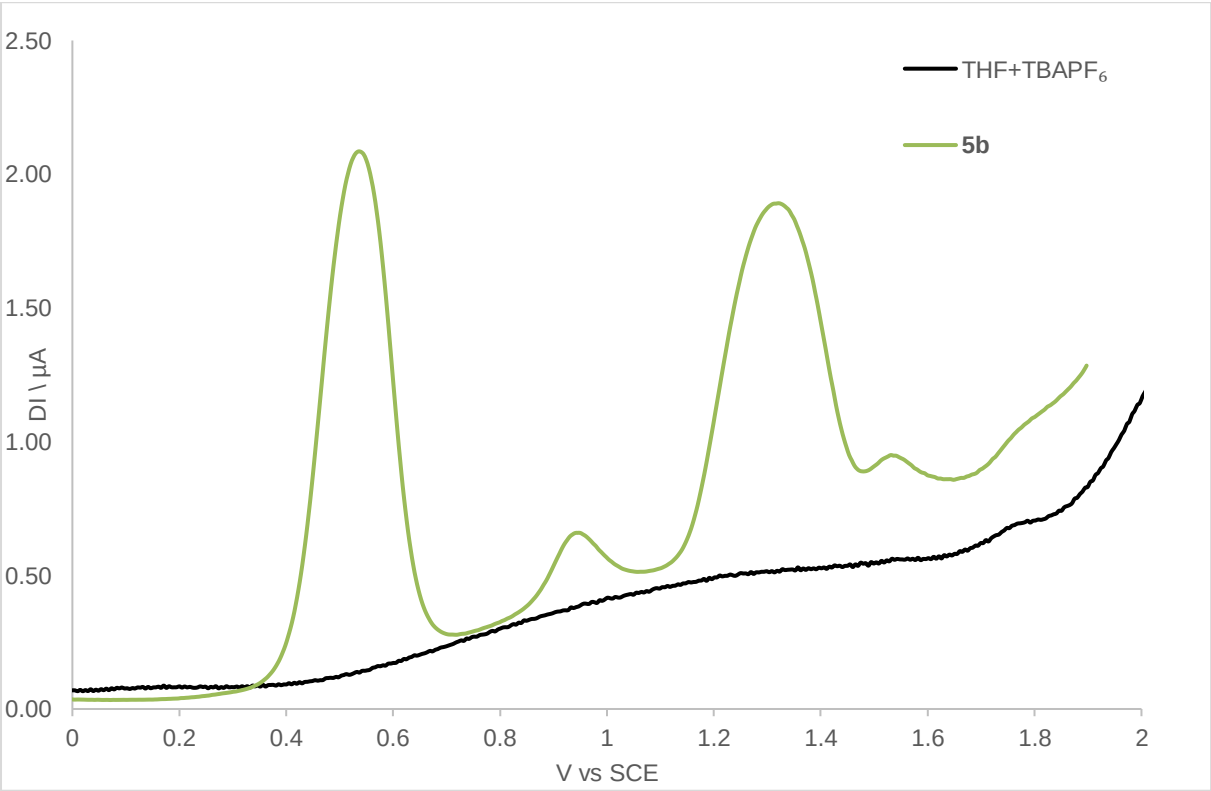

Figure S80. Anodic square wave voltammogram (0.1 M TBA[PF_6] / THF, *v* = 0.1 V/s, r.t.) of **5b**.

5.6. Compound 6b

5.6.1. Cyclic voltammetry

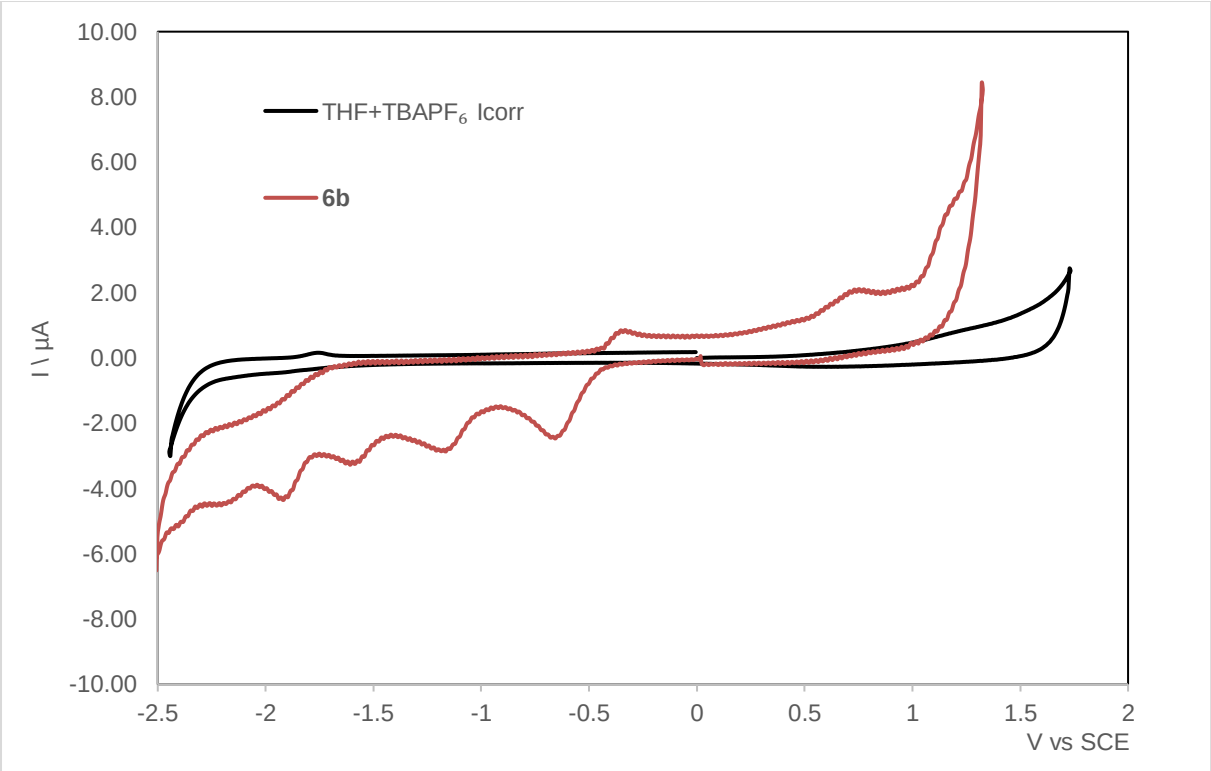

Figure S81. Cyclic voltammogram of **6b** in THF (0.10 M $TBAPF_6$, GC working electrode), scan rate 0.2 V/s, room temperature, initial scan: OCP going from about cathodic potential.

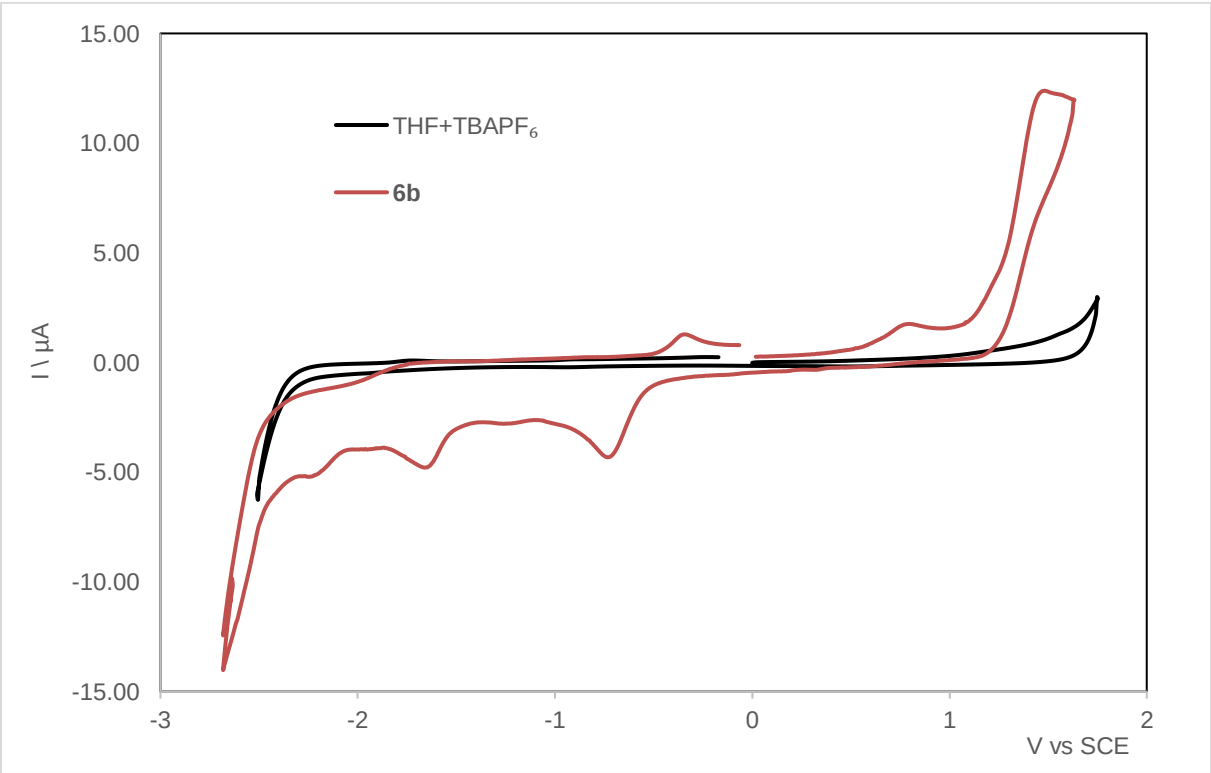

Figure S82. Cyclic voltammogram of **6b** in THF (0.10 M $TBAPF_6$, GC working electrode), scan rate 0.2 V/s, room temperature, initial scan: OCP going from about anodic potential.

5.6.2. *Square wave voltammetry*

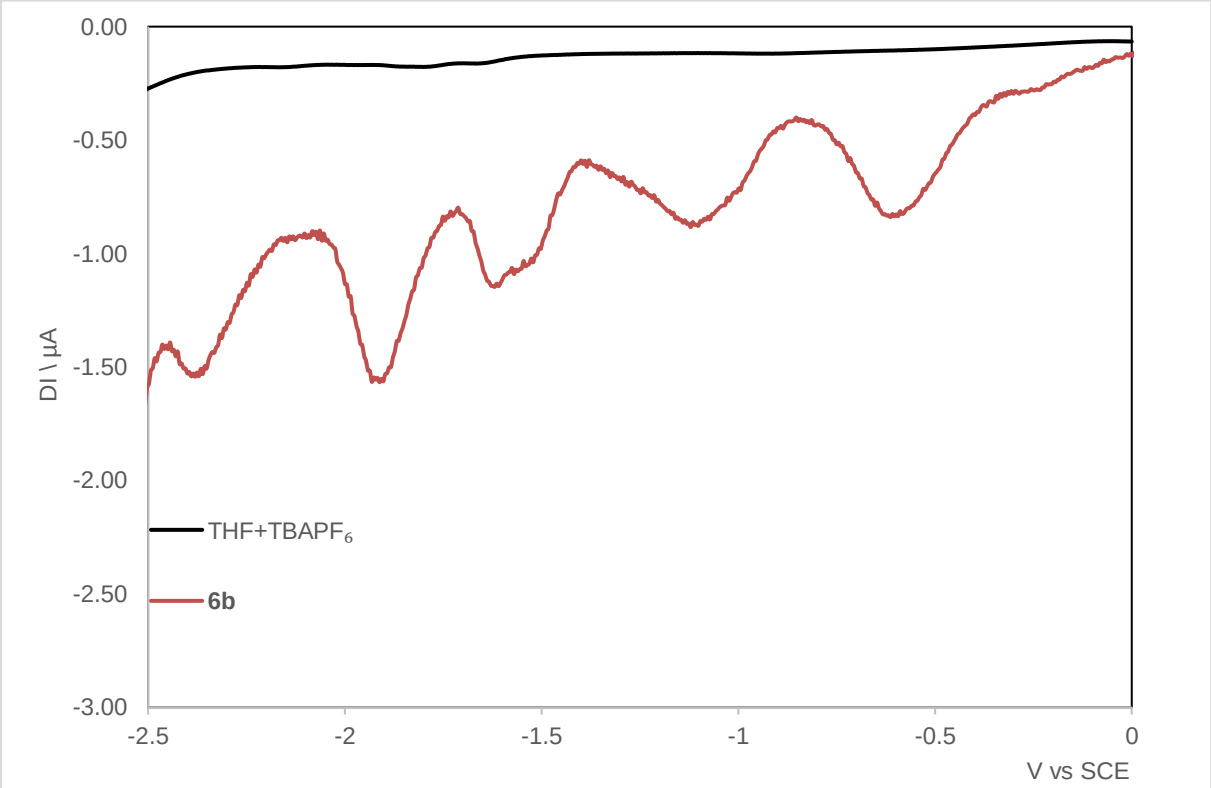

Figure S83. Square wave voltammetry of **6b**, sweeping cathodic potentials.

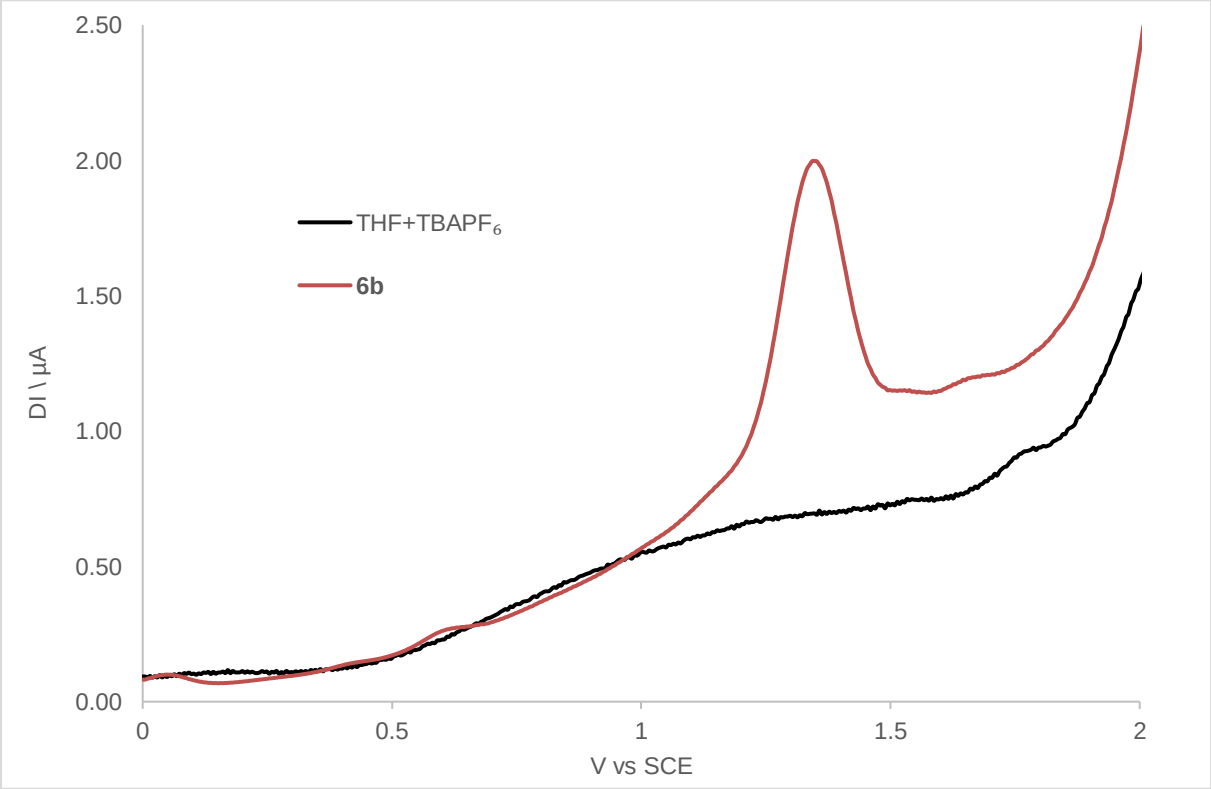

Figure S84. Square wave voltammetry of **6b**, sweeping anodic potentials.

5.7. Table S1 – Compilation of redox potentials (V *vs*. SCE) determined by cyclic voltammetry.

	Oxidation				Reduction							
	I	**II**	**III**	**$L^{+/0}$**	**I**	**II**	**III**	**IV**	**V**	**VI**	**$L^{0/-}$**	**$L^{-/2-}$**
L^{CF_3}											-1.87[a]	-2.00[a]
L^{tBu}				1.73[a]							-2.16[a]	
4a	0.97[b] (64[c])	1.27[a]	1.39[a]	-				–1.61[a]	–1.80[a]			
4b	0.92[b] (78[c])	1.19[a]	1.49[a]	1.83[a]				–1.59[a]				
5b	0.56[b] (107[c])	0.94[b]	1.44[a]				–1.64[a]	–2.00[a]				
6b			1.45[a]		–0.68[a]	–1.17[a]	–1.56[a]	-1.91[a]		–2.38		

[a] irreversible waves, E_p. [b] quasi-reversible waves, $E_{1/2}$. [c] peak-to-peak separation, ΔE_p in mV.

5.8. Table S2 – Compilation of redox potentials (V *vs*. SCE) determined by square wave voltammetry.

	Oxidation				Reduction							
	I	**II**	**III**	**$L^{+/0}$**	**I**	**II**	**III**	**IV**	**V**	**VI**	**$L^{0/-}$**	**$L^{-/2-}$**
L^{CF_3}											–1.88	–2.00
L^{tBu}				1.72							–2.18	
4a	0.97	1.28	1.88	-				–1.61	–1.81			
4b	0.92	1.18	1.73	1.73				–1.59				
5b	0.54	0.94	1.31				–1.64	–1.99				
6b			1.36		–0.68	–1.17	–1.56	–1.91		–2.38		

6. References

(1) Sheldrick, G. M. Crystal Structure Refinement with SHELXL. *Acta Cryst C* **2015**, *71* (1), 3–8. https://doi.org/10.1107/S2053229614024218.

(2) Farrugia, L. J. *WinGX* Suite for Small-Molecule Single-Crystal Crystallography. *J Appl Crystallogr* **1999**, *32* (4), 837–838. https://doi.org/10.1107/S0021889899006020.

(3) Betteridge, P. W.; Carruthers, J. R.; Cooper, R. I.; Prout, K.; Watkin, D. J. *CRYSTALS* Version 12: Software for Guided Crystal Structure Analysis. *J Appl Crystallogr* **2003**, *36* (6), 1487–1487. https://doi.org/10.1107/S0021889803021800.

(4) Schmitz, W. International Tables for X-Ray Crystallography, Vol. IV (Ergänzungsband). Herausgegeben von Der International Union of Crystallography. The Kynoch Press, Birmingham, England, 1974, 366 Seiten Einschließlich Tabellen Und Sachwortverzeichnis. *Kristall und Technik* **1975**, *10* (11), K120–K120. https://doi.org/10.1002/crat.19750101116.

(5) Van Der Sluis, P.; Spek, A. L. BYPASS: An Effective Method for the Refinement of Crystal Structures Containing Disordered Solvent Regions. *Acta Crystallographica Section A* **1990**, *46* (3), 194–201. https://doi.org/10.1107/S0108767389011189.

(6) Macrae, C. F.; Sovago, I.; Cottrell, S. J.; Galek, P. T. A.; McCabe, P.; Pidcock, E.; Platings, M.; Shields, G. P.; Stevens, J. S.; Towler, M.; Wood, P. A. Mercury 4.0: From Visualization to Analysis, Design 72 and Prediction. *J Appl Crystallogr* **2020**, *53* (Pt 1), 226235. https://doi.org/10.1107/S1600576719014092.